Fakultät für Medizin

Comparison of T Cells Engineered With CRISPR/Cas9 or Retroviral Gene Transfer In Immunotherapy of Ewing Sarcoma

Busheng Xue

Vollständiger Abdruck der von der Fakultät für Medizin der Technischen Universität München zur Erlangung eines Doktors der Medizin genehmigten Dissertation.

Vorsitz: Prof. Dr. Florian Eyer

Prüfer*innen der Dissertation:

1. Prof. Dr. Stefan Burdach
2. Priv.-Doz. Dr. Josef Mautner
3. Prof. Dr. Gabriele Multhoff

Die Dissertation wurde am 28.04.2022 bei der Technischen Universität München eingereicht und durch die Fakultät für Medizin am 08.11.2022 angenommen.

For patients suffering from Ewing sarcoma

Contents

1 ABBREVIATIONS

ACT	Adoptive T cell therapy
AES	Advanced Ewing sarcoma
ALL	Acute lymphoblastic leukemia
allo-SCT	allogeneic stem cell transplantation
BM	Bone Marrow
BSA	Bovine serum albumin
CAR	Chimeric antigen receptor
CCLE	Cancer Cell Line Encyclopedia
cDNA	Complementary DNA
CHM1	Chondromodulin-1
CM	Central memory
CRISPR/Cas9	Clustered regularly interspaced palindromic repeats/Cas9
DEPC	Diethypyrocarbonat
DMEM	Dulbecco's modified eagle's medium
DMF	Dimethylformamide
DMSO	Dimethyl sulfoxide
EwS	Ewing sarcoma
GEO	Gene Expression Omnibus
GvHD	Graft versus host disease
GVT	Graft versus tumor effect
HDR	Homology-directed repair
HLA	Human leukocyte antigen
IGV	Integrative Genomics View
mRNA	Messenger ribonucleic acid
NHEJ	Non-homologous end joining
NuRD	Nucleosome remodeling and deacetylase
PBMC	Peripheral blood mononuclear cell
PAPPA	Pregnancy-associated plasma protein-A
RT-PCR	Real-time polymerase chain reaction
STEAP1	Six-transmembrane epithelial antigen of the prostate 1
TAA	Tumor-associated antigen
TCR	T cell receptor
TIL	Tumor-infiltrating lymphocyte
TreoMel-HDT	treosulfan/melphalan high-dose chemotherapy
TSA	Tumor-specific antigen
VAC	Vincristine, actinomycin D and cyclophosphamide
VAI	Vincristine, actinomycin D and ifosfamide
VCN	Vector Copy Number
VIDE	Vincristine, ifosfamide, doxorubicin and etoposide
β-Me	2-Mercaptoethanol

2 INTRODUCTION

2.1 EWING SARCOMA

2.1.1 BASICS

Ewing sarcoma (EwS) is a highly malignant bone and soft-tissue cancer that arises predominantly in children and adolescents (Grunewald et al., 2018; Riggi et al., 2021). The incidence is one case per 1.5 million population, with a higher frequency among Caucasians and a slight tendency for males (case ratio of male to female is 1.6: 1.0) (Bernstein et al., 2006; Burchill, 2003; Grunewald et al., 2018). EwS is molecularly characterized by the expression of EWS-ETS chimeric protein (Delattre et al., 1992; Sorensen et al., 1994) with a quiet genomic background (Grobner et al., 2018). Diagnosis of EwS relies on the histologic and molecular analysis of the tumor biopsy.

2.1.2 HISTOLOGY AND ORIGIN

Histologically, EwS consists of small, round, blue cells with a prominent nucleus and scant cytoplasm (Riggi et al., 2021). Immunohistochemical staining of EwS presents with a high level of CD99 (also named MIC2) expression on the plasma membrane (Martinelli et al., 2016; Perlman et al., 1994), which serves as a relevant diagnostic marker for EwS (positive in 95% of EwS patients) (Ambros et al., 1991; Grunewald et al., 2018). CD56 and synaptophysin (positive in 66.7% of EwS patients) are also frequently expressed on the cell membrane of EwS (Dierick et al., 1993; Gardner et al., 1998).

EwS was first described as “diffuse endothelioma of bone” in 1921 by James Ewing (Ewing, 1972) during the New York Pathology Society meeting. In the last four decades, our group contributed to the debate about the histogenetic origin of EwS in neural-crest-derived stem cells (Schmidt et al., 1985; Staege et al., 2004), endothelial cells (Schmidt et al., 1985; Staege et al., 2004) or bone marrow-derived mesenchymal stem cells (Castillero-Trejo et al., 2005; Richter et al., 2009; Riggi et al., 2005; von Levetzow et al., 2011).

EwS can occur in any part of the body, including orbit (Kaliki et al., 2018) and kidney (Cheng et al., 2020), but predominantly in the axial skeleton (45%) and distal skeleton (35%) (Riggi et al., 2021). Extraosseous tumors account for approximately 20% of patients, with a tendency to occur more frequently in adults (Jahanseir et al., 2020).

2.1.3 GENETIC AND PATHOMECHANISMS

Balanced chromosomal translocation t (11; 22) (q24; q12), which leads to EWS-FLI1 chimeric protein (Delattre et al., 1992), was first discovered to participate in the malignancy of EwS in 1992, 70 years after the first description. Gradually, the defining genetic alterations were found to be the fusion between EwS breakpoint region 1 (EWSR1) and a gene coding a member of the E-twenty six (ETS) family of transcription factors (FLI1, ERG, ETV1, ETV5, FEV) (Riggi & Stamenkovic, 2007). EWS-FLI1 accounts for 85%-90% of the arrangements (Grunewald et al., 2018; Kovar et al., 1996), followed by EWS-ERG, which accounts for 10% (Sorensen et al., 1994), and a growing consensus that EWS-ETS is the primary initiating factor in Ewing sarcoma.

As an aberrant transcription factor, EWS-FLI1 participates in the genomic reprogram to deregulate the proliferation, cell-cycle regulation and metastasis by binding to DNA at GGAA motif or GGAA microsatellites (Gangwal et al., 2010; Gangwal et al., 2008; Guillon et al., 2009) via the conserved ETS domain. EWSR1 drafts multiple proteins through the prion-like domains to tumor-specific enhancers to recruit acetyltransferases and establish de novo enhancers by generating H3K27ac. Thereby it opens the chromosome architecture, which contributes to the activation of the target genes (Boulay et al., 2017; Gangwal et al., 2008; Guillon et al., 2009; Riggi et al., 2014). The protein complex mainly include RNA polymerase II (Ahmed et al., 2021; Yang et al., 2000), and core subunit hsRBP7 (Petermann et al., 1998; Zhou & Lee, 2001), E2F3 (Bilke et al., 2013; Schwentner et al., 2015), EWSR1 (Mertens et

al., 2016), CBP/p300 (Ramakrishnan et al., 2004), WDR5, ASH2, MLL (Riggi et al., 2014), and BAF complex (mammalian SWI/SNF complex) (Boulay et al., 2017; Harlow et al., 2019). Of interest, the threshold of the GGAA motifs arranges from 20 to 26 (Monument et al., 2014), which is different from wild-type FLI1. Super-enhancer-associated MEIS1 and RING1B also contribute to the chromatin reprogram through co-localization with EWS-FLI1 at the active enhancers (Sanchez-Molina et al., 2020). As a result of this specific binding, quantities of genes are activated to drive the malignancy of EwS, such as NKX2.2 (Smith et al., 2006), NROB1 (Boro et al., 2012; Kinsey et al., 2006), IGF1R (Cironi et al., 2008), BCL11B (Wiles et al., 2013), EZH2 (Richter et al., 2009), VRK1 (Riggi et al., 2014), GLI1 (Beauchamp et al., 2009), PTPL1 (Abaan et al., 2005), PPPR1A (Luo et al., 2018), ERG2 (Grunewald et al., 2015), GSTM4 (Luo et al., 2009), PAX7 (Charville et al., 2017), CHM1 (von Heyking et al., 2017), REST (Zhou et al., 2014), PHF19 (Gollavilli et al., 2018), STEAP1 (Grunewald et al., 2012), SLFN11 (Tang et al., 2015), HDAC3 (Ma et al., 2019), TNC (He et al., 2019), APCDD1 (Lin et al., 2019), IL1RAP (Grohar et al., 2011; Zhang et al., 2021), and PRC1 (Li et al., 2021) (Figure 1).

EWS-FLI1 also participates in transcriptional repression of tumor suppressors to drive the oncogenic transformation (Sankar et al., 2013; Sankar et al., 2014), such as IGFBP3 (Prieur et al., 2004) and PHLDA1 (Boro et al., 2012). The nucleosome remodeling and deacetylase (NuRD) complex is a typical ATP-dependent chromatin remodeling complex (Clapier & Cairns, 2009), which plays a critical role in transcription and determines the differentiation and development (Lai & Wade, 2011). EWS-FLI1 recruits the NuRD-LSD1 complex to repress LOX and TGFBR2 (Agra et al., 2013; Sankar et al., 2013). EWS-FLI1 perturbs transcriptional activation of AP-1 (Tomazou et al., 2015) and MRTFB (Katschnig et al., 2017), thereby participating in transcription repression. EWS-FLI1 binds to the promotor of FOXO1 to repress its expression (Niedan et al., 2014). Meanwhile, EWS-FLI1 promotes the

phosphorylation of cyclin/dependent kinase2- and AKT to inhibit the activity of FOXO1, which further rewires the transcription repression (Niedan et al., 2014). EWS-FLI1 also participates in miRNA regulation (Dylla et al., 2013). EWS-FLI1 downregulates miRNA145 to initiate mesenchymal stem cell reprogramming toward EwS stem cells (Riggi et al., 2010). EWS-FLI1 also represses miR-708, which further induces the overexpression of EYA3, and contributes to the chemoresistance of etoposide and doxorubicin (Robin et al., 2012).

Protein partners of EWS-FLI1 are identified to participate in mRNA alternative splicing (Knoop & Baker, 2000; Neckles et al., 2019; Paronetto et al., 2011; Selvanathan et al., 2019), R-loops formation (Gorthi et al., 2018), DNA damage response (Gorthi & Bishop, 2018) and epigenetic regulations (Pishas et al., 2018; Theisen et al., 2016).

Expression of EWS-FLI1 also induces senescence or apoptosis in most cells (Deneen & Denny, 2001; Lessnick et al., 2002), indicating EWS-FLI1 driving the malignancy is dependent on the genomic background, although EwS suffers a low mutation burden (Grobner et al., 2018).

2.1.4 CLINICAL PRESENTATION AND RISK FACTORS

Initial symptoms and clinical features are largely nonspecific in EwS patients, including pain accompanied by fever, night sweats, and weight loss (Widhe & Widhe, 2000). Bone remodeling factors, such as alkaline phosphatase, might be elevated (Biswas et al., 2014), and pathological fracture is observed in 10-15% of cases. The prognosis of patients only with local disease has a 5-year survival rate of more than 70%. In contrast, advanced-EwS (AES) patients with metastasis or recurrence remain dismal, especially those with metastasis to bone or bone marrow (Burdach, 2004; Burdach & Jurgens, 2002; Burdach et al., 2003; Ladenstein et al., 2010; Paulussen et al., 1993; Thiel et al., 2016). The overall survival of patients with metastasis at diagnosis is less than 30% (Burdach et al., 2010). Patients with lung metastasis have a better prognosis

than those with bone metastasis based on the analysis of 975 patients from the European Intergroup Cooperative Ewing's Study Group (Cotterill et al., 2000). Elevated serum lactate dehydrogenase (LDH) and IL-6 also correlate with the tumor burden and poor prognosis (Bacci et al., 1999; Biswas et al., 2014; Lissat et al., 2015). Besides, tumor size is another independent risk factor, tumor volume＞200 ml confers a poor prognosis (MÜNCHEN, 2017; Pappo & Dirksen, 2018).

2.1.5 THERAPY

2.1.5.1 TREATMENT OF THE PRIMARY DISEASE

Several international groups have developed excellent cooperation to establish curative therapy of EwS (Biswas et al., 2014; Cotterill et al., 2000; Paulussen et al., 1998; Worch et al., 2018), but international standard pharmacological treatments are still in discussion (Anderton et al., 2020). Primary EwS is treated mainly by a combination of chemotherapy and local control (surgery or irradiation) (Thacker et al., 2005). Marginal or wide resection is performed whenever possible because surgical resection appears superior to radical irradiation in local control (Bacci et al., 2004; Schuck et al., 2003; Schuck et al., 2002). Evidence from the EURO-E.W.N.G 99 (European Ewing tumor working initiative of national groups) leads to the employment of induction combination chemotherapy, including six cycles of vincristine, ifosfamide, doxorubicin, and etoposide (VIDE) every three weeks prior to local therapy, with additional VAI (vincristine, actinomycin D and ifosfamide) or VAC (vincristine, actinomycin D and cyclophosphamide) (Juergens et al., 2006). The Children's Oncology Group AEWS0031 trial applied alternating cycles of vincristine, doxorubicin-cyclophosphamide, and ifosfamide-etoposide (VDC/IE) as induction chemotherapy with additional consolidation chemotherapy by alternating cycles of ifosfamide-etoposide and vincristine-cyclophosphamide (IE/VC) (Womer et al., 2012). Both strategies showed positive results. VIDE induction in localized

EwS with additional randomization between busulfan and melphalan (BuMel) also benefits the patients with predefined high-risk factors (Whelan et al., 2018).

2.1.5.2 THERAPY FOR METASTATIC AND REFRACTORY DISEASE

The majority of EwS recurrences (47-73%) occur within two years after the first diagnosis. Patients with metastatic and refractory disease were treated with high-dose chemotherapy and myeloablation (Burdach & Jurgens, 2002; Burdach et al., 1993; Burdach et al., 2010), with additional allogeneic stem cell transplantation (Burdach et al., 2010; Burdach et al., 2000; Koscielniak et al., 2005). Chemotherapy regimens may utilize a combination of agents that were included in front-line therapy with additional novel agents (Ferrari et al., 2009). Additional high-dose chemotherapy also evidently reduces the risk of further events in EwS patients who respond to conventional second-line chemotherapy.

2.1.5.3 GENETIC THERAPY

As the master regulator and the driver of EwS (Erkizan et al., 2010), targeting EWS-ETS should be a promising strategy. However, the lack of enzymatic activity and disordered structure hindered the efforts for further drug prediction and design. The alternative solution relies on the genomic architecture driven by EWS-ETS or targeting EWS-ETS such as the molecules and signaling pathways, including the receptor tyrosine kinase insulin-like growth factor (IGF-1R) (Juergens et al., 2011; Olmos et al., 2010). YK-4-279 in the dislocation of EWS/ETS and RNA helicase A (Erkizan et al., 2009) also offers another strategy, but the drug resistance hindered the clinical application (Hong et al., 2014; Lamhamedi-Cherradi et al., 2015). EwS was first found to be sensitive to radiation therapy and gradually found to the sensitivity of PARP inhibitor (Garnett et al., 2012) due to the advantage of EWS-FLI1 (Gorthi et al., 2018), although the clinical trial was disappointing (Choy et al., 2014). A clinical trial (NCT01858168) of combined Olaparib in adults with recurrent/metastatic Ewing's Sarcoma is ongoing. Chemical genomics screening performed by

Iniguez et al. (Iniguez et al., 2018) identified that CDK12/13 inhibitor THZ531 impairs DNA damage repair in an EWS-FLI1 dependent manner and leads to Synthetic Lethality with PARP inhibitors.

2.1.5.5 T CELL THERAPY

Current therapies are associated with acute and chronic adverse effects that may compromise the quality of life in survivors (Grunewald et al., 2018), such as chemotherapy-associated myeloid dysplastic syndrome, leukemia, and radiation-associated sarcoma. Besides, only minor improvements in prognosis have been achieved during the past two decades by multiple treatments. The overall survival remains dismal, especially the patients suffering metastasis have a 5-year overall survival <30% (Gaspar et al., 2015), demonstrating that additional therapeutic approaches are in need. Immunotherapies developed by our group and others, targeting downstream targets of EWS-FLI1, such as adoptive transfer of T cells targeting the CHM1 derived peptide VIMPCSWWV (Blaeschke et al., 2016; Thiel, Pirson, et al., 2011), showed pre-clinical and clinical tumor regressions (Thiel et al., 2017). T cell targeting LIPI-derived peptides LDYTDAKFV and NLLKHGASL (Mahlendorf & Staege, 2013) , STEAP1 derived YLPGVIAAI (Schirmer et al., 2016; Schober et al., 2020) and MIAVFLPIV (Rodeberg et al., 2005), PAPPA derived IILPMNVTV (Kirschner et al., 2017), EZH2 derived YMCSFLFNL (Thiel, Pirson, et al., 2011) , PAX3 derived QLMAFNHLI and modified version, QLMAFNHLV (Rodeberg et al., 2006), showed effective cytotoxicity of HLA-A*02:01+ EwS cell lines.

CAR-T targeting of GPR64, ROR1, IGF1R, and G_{D2}, which are highly expressed in EwS (Huang et al., 2015; Kailayangiri et al., 2019; Richter et al., 2013), also leads to selective cytotoxicity of EwS *in vivo* (Schirmer et al., 2018) . IL1RAP is a direct target of EWS-FLI1 and is highly expressed in EwS but minimally expressed in normal tissues, which serves as a new surface target of EwS (Zhang et al., 2021) and is worth advanced CAR-based T-cell therapy. Besides a TCR-based target, STEAP1 is also a potential CAR target (Challita-

Eid et al., 2007).

Patients suffering from EwS may thus benefit from adoptive T cell therapy (Kailayangiri et al., 2019; Thiel et al., 2017). Further research to optimize the method for T cell engineering is warranted.

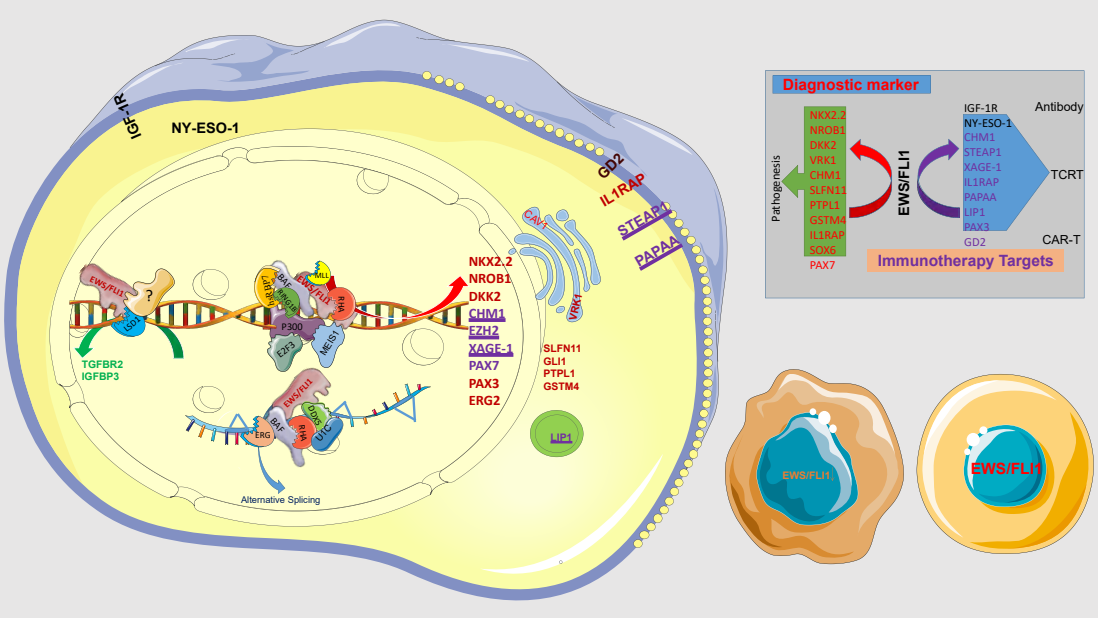

Figure 1. EWS-FLI1 protein complex and downstream targets are potential targets for chemotherapy and immunotherapy

Graphical abstract of EWS-FLI1 protein complex in Ewing sarcoma. The downstream of EWS-FLI1 could be used for chemotherapy and immunotherapy. EWS-FLI1 knockdown also drives the metastasis of Ewing sarcoma.

2.2 ADOPTIVE IMMUNOTHERAPY

Adoptive T-cell therapy mainly comprises tumor-infiltrating lymphocyte therapy (TIL) (Rosenberg et al., 1986), engineered T cell receptor (TCR) therapy (Schreiber et al., 2011), chimeric antigen receptor (CAR) T cell (CAR-T) therapy (Hanssens et al., 2022; Jena et al., 2010), and natural killer (NK) (Liu et al., 2021; Smyth et al., 2002) cell therapy.

Allogeneic stem cell transplantation (allo-SCT) represents an effective adoptive

therapy targeting cancers based on graft versus tumor effect (GvT) (Horowitz et al., 1990; Nicholson et al., 2012). Such allogenic hematopoietic stem cell transplantations are curative immunotherapeutic treatments for high-risk hematological malignancies (Cieri et al., 2014; Kolb, 2008), but their efficacy in solid tumors is limited. Besides GvT, allo-SCT also leads to graft versus host disease (GvHD), which is observed in 60% of all cases (Ito et al., 2019) based on 2014 National Institutes of Health criteria and might be life-threatening (Marmont et al., 1991; McDonald et al., 2015).

The application of TIL-derived T cells has been a promising strategy for cancer therapy in the past three decades (Jones et al., 2020) and showed clinical success, but the heterogeneous cell mixture and therapeutic outcome varies in patients and is hard to predict (Hinrichs & Rosenberg, 2014; Yee, 2018). Technical difficulties (Tran et al., 2008) and early cost-effectiveness (Retel et al., 2018) hindered the further clinical application of TIL.

CAR-T cell therapy revolutionized therapeutic strategies (Chandran & Klebanoff, 2019; Larson & Maus, 2021). Several adoptive T-cell transfer (ACT)-based therapies have already achieved regulatory clinical applicants for B-cell malignancies (Kochenderfer et al., 2010; Myers et al., 2022), melanoma (Dafni et al., 2019; Effern et al., 2020). Clinical results demonstrate that CAR-T cell products have great advantages in treating hematological malignancies (Baird et al., 2021) but are also accompanied by clinical toxicities, including cytokine release syndrome and neurotoxicity. CAR-T therapy is unpredictable in animal experiments (Larson & Maus, 2021).

TCRs can recognize the peptide antigens presented on the cell membrane of the host cells via the histocompatibility complex (MHC)/human leukocyte antigen (HLA) system (Burdach & Kolb, 2013). TCR is a heterodimer comprised mostly commonly of an α and a β chain (Rudolph et al., 2006) alternatively of a γ and a δ chain (Davis & Bjorkman, 1988). TCR-based ACT allows the genetic

redirection of the T-cell specificity.

Transduction with viral vectors is the conventional method of antigen-specific TCR insertion by either retro- or the lentivirus particles. However, following the viral transfer of exogenous TCR genes, the exogenous could mix with the endogenous TCR forming mispaired heterodimers (Figure 2). Thus, mispaired heterodimers may recognize auto-antigens and constitute neoantigens. This may lead to lethal graft versus host disease (GvHD) following adoptive transfer (Bendle et al., 2010). Random insertion of viruses into the genome also raises safety concerns, such as insertional mutations and tumorigenesis (Howe et al., 2008).

CRISPR/Cas9 engineered orthotopic TCR replacement leads to accurate α and β chain pairing, and the TCR regulation is similar to that of physiological T cells (Schober et al., 2019).

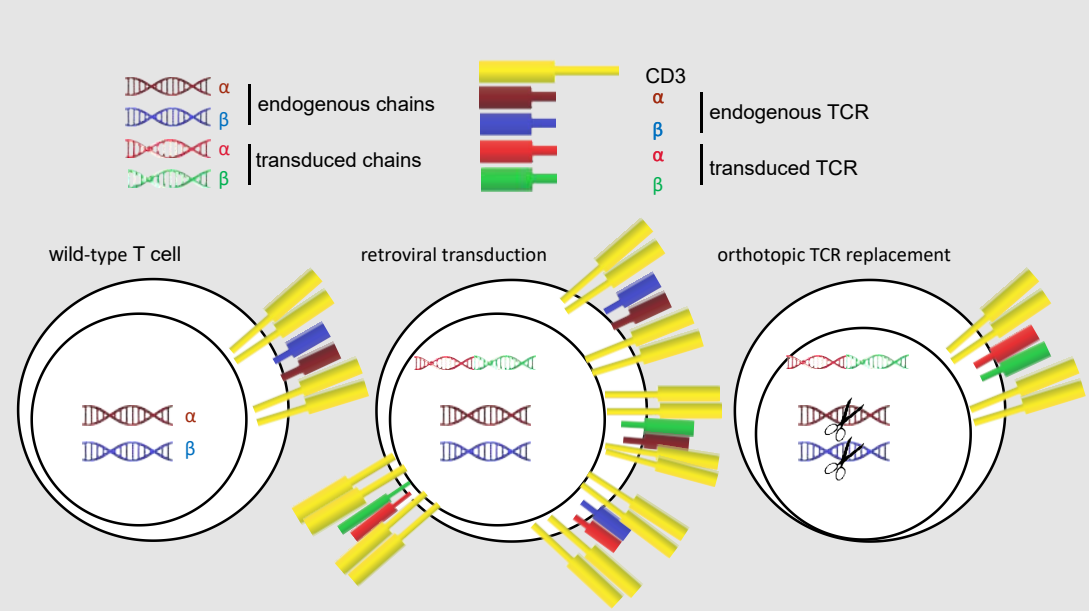

Figure 2. Advancement of T-cell engineering with targeted TCR knock-in (KI) into endogenous TCR-α constant (TRAC) gene locus with concomitant knock-out (KO) of endogenous α and β chains.

Retrovirus transduction of TCRs leads to the mispairing between the transgenic and endogenous TCRs, which can diminish the function of the T cells. CRISPR/Cas9 engineered T cells could avoid the potential mispairing and the T cell product is physiological to the wild type T cells.

3 RESEARCH OBJECTIVES

The canonical methods of TCR gene delivery in pre-clinical and clinical applications are based on the viral transduction of full-coding sequences, including α- and the β-chain of the tumor-specific antigen (TSA) and tumor-associated antigen (TAA) (Coulie et al., 2001; Sarukhan et al., 1998). As the transduced α- and β-chain may mispair with the endogenous α- and β-chain, the resultant new antigen specificities may cause auto-reactivity, potentially leading to graft-versus-host disease (GvHD). The mispaired TCR chains may also lose their function. Fortunately, there is no documented GvHD in patients up to now in our work, but the patient number is low (Thiel et al., 2017), and related mechanisms are not fully understood.

Schober et al. (Schober et al., 2019) at our institution, established a non-viral TRBC knock-out/TRAC knock-in model, which showed a TCR regulation pattern very similar to that of a physiological T cell population.

Incompletely differentiated, including naïve and central memorial phenotypes of T cells, are associated with prolonged peripheral persistence and lead to better survival of patients when treated with them ((Buchholz et al., 2013; Graef et al., 2014; Kaneko et al., 2009). Our study was initiated to compare T cells against a metastatic driver engineered with CRISPR/Cas9 vs. retroviral gene transfer for immunotherapy of Ewing sarcoma.

4 HYPOTHESIS

CRISPR/Cas9 engineered T-cell receptor insertion to the TRAC locus of $CD3^+$ T cells preserves physiological properties and yields a therapeutic product that is at least as efficacious in immunotherapy of Ewing sarcoma as the product generated by retroviral gene transfer.

5 MATERIALS

5.1 TECHNICAL EQUIPMENT

Manufacturers	**Locations**
Bacteria shaker Certomat BS-T	Sartorius, Göttingen, Germany
Cell counting chamber Neubauer	Brand, Wertheim, Germany
Electrophoresis chamber Easy cast	Thermal Fisher Scientific, Ulm, Germany
Electroporator Gene Pulser Xcell™	BioRad, Richmond, CA，USA
ELISpot reader AID iSpot Reader Unit	AID GmbH, Straßberg, Germany
Flow cytometer FACS Calibur™	Becton Dicknson and Compang, New Jersey, USA
Fridge(+4°C) cool varia	Siemens, Munich, Germany
Freezer (-20°C) cool vario	Siemens, Munich, Germany
Freezer(-80°C) Hera freeze	Heraeus Holding, Hanau, Germany
Gel Logic 1500 imaging system	Cole-Parmer,USA
Heating block Thermomixer Comfort	Eppendorf, Hamburg, Germany
Ice machine AF100	Scotsman Ice System, Vernon Hills, IL,USA
Incubator BBD 6220	Heraeus, Hanau, Germany
Liquid nitrogen tank L-240K series	Taylor-Wharton, Theodore, USA
Micropipets	Eppendorf, Hamburg, Germany
Microwave oven	Siemens, Munich, Germany

NanoPhotometer	Implen, Munich, Germany
Lonza 4D Nucleofector	Lonza, Swiss
Step One Plus Real-Time PCR	Thermo Fisher Scientific, USA
Sterile Bench	Heraeus, Hanau, Germany
Thermal cycler iCycler	BioRad, Richmond, CA, USA
Thermocycler	Eppendorf, Hamburg, Germany
UV transilluminator Gene Genius	Syngene, Cambridge, UK
Water bath	GFL, Burgwedel, Germany

5.2 CONSUMABLE SUPPLIES

Materials	**Manufacturers and Locations**
Cell culture flasks	TPP, Trasadingen, Switzerland
Cell strainer	Becton Dickinson and Company, New Jersey, USA
Cyto tubes	Greiner-bio One GnbH, Frickemhausen, Germany
Falcons	Greiner-bio One GnbH, Frickemhausen, Germany
Fliters (sterile) Minisart	Sartorius, Göttingen, Germany
Gloves nitrile	Sempermed, Vienna, Austria
Paraflim	Brans, Wertheim, Germany
Plates for cell culture	Becton Dicknson and Company, New Jersey, USA

Tubes(200ul, 1.5ml and 2ml)	Eppendorf, Hamburg, Germany
Real-time PCR plates	Eppendorf, Hamburg, Germany

5.3 CHEMICALS AND REAGENTS

Materials	**Manufacturers and Locations**
100mM dNTP Set	Invitrogen, Life Technologies, Darmstadt, Germany
1-Bromo-3-Chloro_Propan (BCP)	Sigma-Aldrich, St. Louis, Missouri, USA
1 Kb plus DNA ladder	Invitrogen, Life Technologies, Darmstadt, Germany
2-Propanol	Roth, Karlsruhe, Germany
5% trypsine	Gibco, Life Technologies, Darmstadt, Germany
6×DNA loading dye	Fermentas, St. Leon-Rot, Germany
SfiI	NEB, United Kingdom
NEB 5-alpha Competent E. coli	NEB, United Kingdom
DH10B Competent Cells	Invitrogen, Life Technologies, Darmstadt, Germany
MEM NEAA 100×	Gibco, Life Technologies, Darmstadt, Germany
ACK lysis buffer	Gibco, Life Technologies, Darmstadt, Germany
Agar	Sigma-Aldrich, St. Louis, Missouri, USA
Agarose	Invitrogen, Life Technologies, Darmstadt, Germany
AIM V medium	Gibco, Life Technologies, Darmstadt, Germany

Albumin Standard	Thermal Fisher Scientific, Ulm, Germany
Ampicillin	Merck, Darmstadt, Germany
Anti-PE Microbeads	Miltenyi Biotech, Bergisch-Gladbach, Germany
AutoMACS™ Ringsing Solution	Miltenyi Biotech, Bergisch-Gladbach, Germany
DEPC Water	Ambion, Darmstadt, Germany
DMSO	Sigma-Aldrich, St. Louis, Missouri, USA
Duplex Buffer	Integrated DNA Technologies, Coralville, USA
DPBS (10×)	Gibco, Life Technologies, Darmstadt, Germany
Enhancer (10nmol)	Integrated DNA Technologies, Coralville, USA
Erythrocyte Lysis Buffer	Pharmacy of Klinikum Rechts der Isar
Ethanol	Roth, Karlsruhe, Germany
Ethidium Bromide	Sigma-Aldrich, St. Louis, Missouri, USA
FACS™ Clean	Becton Dicknson and Company, New Jersey, USA
FACS™ Flow	Becton Dicknson and Company, New Jersey, USA
FACS™ Rinse	Becton Dicknson and Company, New Jersey, USA
Fetal bovine Serum (FBS)	Biochrom, Berlin, Germany/ Life Technologies Limited, Paisley, UK
Ficoll-Paque	GE Heathcare, Uppsala, Sweden
Glycerol	Sigma-Aldrich, St. Louis, Missouri, USA
HBSS (1×)	Gibco, Life Technologies, Darmstadt, Germany

HEPES	Sigma-Aldrich, St. Louis, Missouri, USA
HEPES Buffer (1M)	Biochrom, Berlin, Germany
Human Serum Type AB	Sigma-Aldrich, St. Louis, Missouri, USA
Hydrogene peroxide solution	Sigma-Aldrich, St. Louis, Missouri, USA
IFNγ	R&D Systems, Minneapolis, Minnesota, USA
IL-2	R&D Systems, Minneapolis, Minnesota, USA
IL-15	ImmunoTools, Friesoythe, Germany
Isopropanol	Sigma-Aldrich, St. Louis, Missouri, USA
L-glutamine	Miltenyi Biotech, Bergisch-Gladbach, Germany
MACS®BSA Stock Solution	Miltenyi Biotech, Bergisch-Gladbach, Germany
N,N-Dimethylformamide	Agilent Technologies, Böblingen, Germany
Peptide $CHM1^{319}$	Thermal Fisher Scientific, Ulm, Germany
Penicillin-Streptomycin	Gibco, Life Technologies, Darmstadt, Germany Life Technologies Limited, NY,USA
Pierce™ BCA Protein Assay	Thermal Fisher Scientific, Ulm, Germany
Propidium iodide staining solution	Becton Dicknson and Company, New Jersey, USA
RetroNectin	TaKaRa, Saint-Germain-en-Laye, France
PRMI 1640 medium	Gibco, Life Technologies, Darmstadt, Germany/ Life Technologies Limited, Paisley,UK
S.O.C medium	Invitrogen, Life Technologies, Darmstadt, Germany
Sodium Pyruvate	Gibco, Life Technologies, Darmstadt, Germany / Life Technologies Limited, Paisley,UK

TransIT®293	Mirus, Madison, WI, USA
Tri Reagent solution	Ambion, Darmstadt, Germany
Trypan blue	Gibco, Life Technologies, Darmstadt, Germany
Tween 20	Sigma-Aldrich, St. Louis, Missouri, USA
RIPA lysis buffer	Sigma-Aldrich, Germany
Bromophenol blue	Sigma-Aldrich, Germany
SDS	Sigma-Aldrich, Germany
Glycerol	Sigma-Aldrich, Germany
TRIS	Sigma-Aldrich, Germany
Glycine	Sigma-Aldrich, Germany
Methanol	Sigma-Aldrich, Germany
2-Mercaptoethanol (100X)	Sigma-Aldrich, Germany
PageRuler™ Prestained Protein Ladder	Thermal Fisher Scientific, Ulm, Germany
Anti-FLI1 antibody	Abcam, Cambridge, UK
Anti-GAPDH antibody	Santa Cruz Biotechnology,USA
Anti-CHM1	R&D Systems, Minneapolis, Minnesota, USA
Anti-PARP	Cell Signaling Technology, Massachusetts, USA
Anti-mouse	Santa Cruz Biotechnology, USA

Anti-Rabbit	Santa Cruz Biotechnology, USA

5.4 KITS

Materials	**Manufacturers and Locations**
EndoFree Plasmid Maxi Kit	Qiagen, Hilden, Germany
High Capacity Reverse Transcription Kit	Applied Biosystems, Life Technologies, Darmstadt, Germany
Pierce™ ECL Western Blotting Substrate	Applied Biosystems, Life Technologies, Darmstadt, Germany
RNeasy mini kit	Qiagen, Hilden, Germany
cDNA Reverse Transcription Kit	Applied Biosystems, Life Technologies, USA
GoTaq® Master Mix	Promega, Madison, USA
BCA	Thermal Fisher Scientific, Ulm, Germany

5.5 ELISPOT REAGENTS

Materials	**Working concentration**	**Manufacturer**
Anti-h-IFNγ mAb 1-D1K, purified (Capture antibody)	10ug/ml	mABTech, Nacka Strand, Sweden
Anti-h- IFNγ mAb 7-B6-1, biotinylated (Detection antibody)	2ug/ml	mABTech, Nacka Strand, Sweden
Streptavidin-Horse-Peroxidase		mABTech, Nacka Strand, Sweden
3-Amino-9-ethyl-carbazole (AEC)		Sigma-Aldrich, St. Louis, Missouri, USA

Acetate buffer: 37.5 ml H_2O +3.75ml 0.2N acetic acid+8.8 ml 0.2N sodium acetate

AEC solution: 1 piece of AEC tablet (20mg) + 2.5ml Dimethylformamide (DMF) + 47.5 ml acetate buffer

Development solution: 10ml AEC solution+ 30ul 30% H_2O_2 per plate

5.6 CRISPR/Cas9 REAGENTS

PBS	Thermo Fisher	14200067 (10x), 14190144 (1x)	no calcium, no magnesium
IL2	Proleucin		100000 Units
IL7	Peprotech oder R&D	#200-07-50UG oder 207-IL-025/CF	$1x10^4$ U/ml in 0,1% hAB Serum
IL15	Peprotech oder R&D	#200-15-50UG oder 247-IL-025/CF	5µg/ml in 0,15 hAB Serum
Anti-human CD3/28 dynabeads	Thermo Fisher	11131D	
crRNA TRAC (10nmol)	IDT		AGAGTCTCTCAGCTGGTACA
crRNA TRBC (10nmol)	IDT		GGAGAATGACGAGTGGACCC
tracrRNA (20nmol)	IDT	1072533	Alt-R CRISPR/Cas9 tracrRNA
crRNA negative control #1 (2nmol)	IDT	1072544	Alt-R® CRISPR/Cas9 Negative Control crRNA #1, 2 nmol
crRNA positive control #1 (2nmol) HPRT	IDT	1072541	Alt-R® CRISPR/Cas9 Positive Control crRNA, Human HPRT, 2 nmol
HiFi Cas9	IDT	1081060	Alt-R® S.p. HiFi Cas9 Nuclease V3, 100 µg
Enhancer (10nmol)	IDT	1075916	Alt-R® Cas9 Electroporation Enhancer
Duplex Buffer	IDT	11-01-03-01	Nuclease Free Duplex Buffer (10x2ml)
Ampure XP bead	Beckman Coulter	A63881	AMPure XP PCR Aufreinigungssystem
LoBind DNA 1,5 ml Eppis	Eppendorf	0030108051	
Herculase	Agilent	600675	Herculase II Fusion DNA Polymerase

5.7 FLOW CYTOMETRY ANTIBODIES

Specificity	Format	Clone	Manufacturer
CD3	APC		Becton Dicknson and Company, New Jersey, USA
CD3	FITC		Becton Dicknson and Company, New Jersey, USA
CD3	PE-Vio770		Miltenyibiotec,Germany
CD4	PE		Becton Dicknson and Company, New Jersey, USA
CD8	APC		Becton Dicknson and Company, New Jersey, USA
CD45RO	PE		Becton Dicknson and Company, New Jersey, USA
CD62L	APC		Becton Dicknson and Company, New Jersey, USA
mTCR	PE	H57-597	Biolegend, USA
hTCR	FITC	IP26	Biolegend, USA
Mouse IgG1	FITC/APC/PE		Becton Dicknson and Company, New Jersey, USA

5.8 VECTORS

The vectors for pMP71-GFP, was kind gifts of Prof. Angela Krackhardt, Medizinische Klinick III, Klinikum Rechts der Isar, Technical University of Munich. pMP-RQ-CHM1-TCR-KI were generated with the help of GeneArt, Life

Technologies, Regensburg and the related structure is shown as Figure 3.

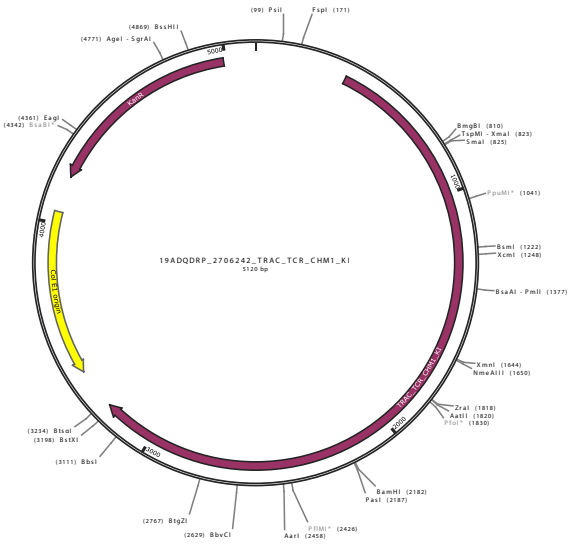

Figure 3. Vector map of CHM1 TCR plasmid for Knockin.

The vector map of the plasmid including TCR targeting CHM1 peptide.

6 METHODS

6.1 CELL CULTURE METHODS

6.1.1 FREEZING AND THAWING OF CELLS

For freezing, centrifuge the cells at 1500 rounds per minute (rpm) for 5 min. and re-suspend the cells in freezing medium according the corresponding medium, freeze in Mr. Frosty in -80°C at least for 24 hours.

For thawing, cells were rapidly transferred into 5ml medium, centrifuged once at 1500rpm for 5 min and re-suspend in the appropriate culture medium.

6.1.2 CULTURE OF CELL LINES

Split the suspension and adherent cell lines every 2 to 3 days according to their individual growth rate. Split suspension cells at a ratio of 1: 4. For adherent cells, washed once with 5ml of PBS, then washed with 1ml of 0.05% trypsin quickly, and incubated for 1-3 minutes at 37°C according to their property. After detachment, add medium and suspend the cells for further split or experiment.

6.1.3 CELL COUNTING

For the determination of the cell number, cells were diluted 1:4 or 1:10 with trypan blue and counted in four squares of the Neubauer counting chamber. Cell concentrations were determined using the following formula:

Concentration (cells/ml) = number of cells counted four square×10^4 (1:4)

2.5× number of cells counted four square×10^4 (1:10)

6.1.4 ISOLATION OF BLOOD CELLS

Peripheral blood mononuclear cells (PBMCs) were isolated from concentrates (Buffy coats) provided by the DRK-Blutspendedienst Baden-Wuerttemberg/ Hessen in Ulm using Ficoll density gradient centrifugation. The blood cell was diluted in 1:2 with PBS, and centrifuged at 2200rpm for 30 minutes without brake. The buffy coat was aspirated and transferred to a fresh tube and added

with PBS to 50 ml, centrifuge at 700 rpm for 7 minutes to remove the platelets, ACK lysis buffer to lysis the red cells for 10 minutes and fill up to 50ml with PBS. Centrifuged at 1300 rpm for 5 minutes and wash twice, counted the cells for further culture or freeze.

6.1.5 EXPANSION OF T LYMPHOCYTES WITH ENDOGENOUS TCR

5×10^4 to 1×10^5 T-cell were expanded in 25 T-cell medium together with 5×10^6 irradiated LCL (100 Gy) and 2.5×10^7 irradiated PBMC (30 Gy) pooled from three different healthy donors. 50ng/ml anti-CD3 was added. The next day, and every other day, 100 IU/ml IL-2 and 2ng/ml IL-15 were pipetted into the suspension. Replaced the medium whenever necessary.

6.2 RETROVIRAL TRANSDUCTION OF TCR CONSTRUCTS

On day 1, split and seed the packaging cell line, 293Vec-RD114TM cells, in 6-well-plates (2 x 10^5 cells/well), for retrovirus production.

On day 2, Mix 9µl TransIT solution and 200µl Opti-MEM and incubate at room temperature. After 20 minutes, 1ug of plasmids were added (pMP71-GFP or pMP71-CHM1-TCR) and the solution was incubated for another 30 minutes at room temperature before it was pipetted into one well of the 6-well-plate (Figure 4). T cells were isolated the same day and stimulated with anti-CD3/CD28 dynabeads (6ul/ml/1×10^6 T cells) and 100 U/ml IL-2.

On day 4, coat 24-well plates with RetroNectin. (RetroNectin coating was performed by an over-night incubation with 5µg RetroNectin per well and a washing step with 2 ml HBSS per well containing 2.5% HEPES.) Collect virus-containing supernatant of 293T cells, centrifuged at 1300rpm for 5 minutes, and filter through a 45µm filter to exclude cells. 1x10^6 T cells 1 ml T cell medium were plated into each well of the 24-well plate and co-cultured with 1 ml virus supernatant and 4µg protamine sulfate. PBMC and T cells additionally required 1 % HEPES and the appropriate cytokines (100 U/ml IL-2 or 30 ng/ml IL-21 and 2 ng/ml IL-15). Centrifuge plates at 2200rpm for 90 minutes at 32 °C and then

incubated at 37 °C for 24 hours.

On day 5, split the transduced cells 1: 2 and repeat the procedure of day 4.

On day 7, wash plates renew cytokines.

On day 10, check the transduction rates by flow cytometry analysis.

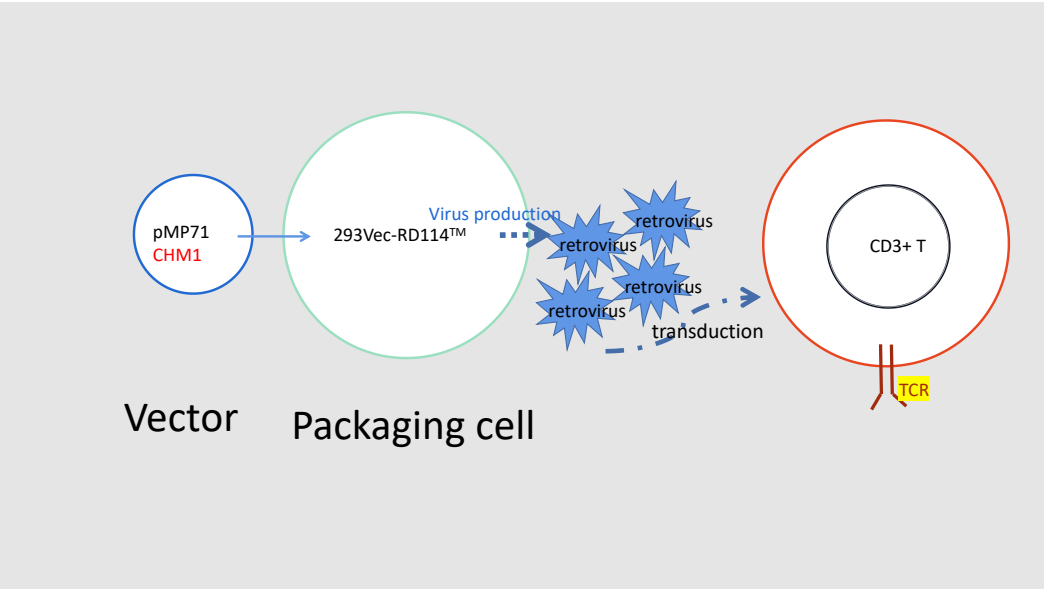

Figure 4. Principle of retroviral gene transfer.

293Vec-RD114 is a HEK 293-based packaging cell line that produces retroviral vectors pseudotyped by the cat RD114 virus envelope protein

6.3 CRISPR/CAS9 MEDIATED ORTHOTOPIC TCR REPLACEMENT

On day 1, activate T cells: 6µl anti-CD3/28 dynabeads + 300 IU/ml IL-2, 5ng/ml IL-7 and 5ng/ml IL-15 per 1×10^6 T cells.

On day 2 (or before), PCR for dsDNA PCR product

For the PCR reaction, use the Maxi Prep product of the delivered DNA KI Insert.

PCR: 100µl system

DNA (prediluted to have roughly 15-60ng/µl)	1µl
forward primer (10µM)	4µl

reverse primer (10µM)	4µl
dNTPs (10mM)	20µl
5x Herculase buffer	20µl
Herculase	1µl
PCR grade water	50µl
Total	100µl

Primer of KI fragment is as Supplementary Table 1

PCR-Program

•95°C for 3 min

95°C for 30 sec
62°C for 30 sec
72°C for 3min
} 34 cycles

•72°C for 3min final elongation

•Hold at 4°C

DNA Purification:

•Prepare Ampure XP bead at RT for at least 30 minutes.

•Mix beads thoroughly.

•Pool PCR samples (in this case 2x 5 samples with a total volume of 1000µl) in two LoBind DNA 1.5ml Eppendorf tubes and add Ampure XP beads in a 1:1 ratio.

•Mix by pipetting up and down and incubate 5min at RT.

•Place the tube on a magnetic stand for 3min until the solution is clear.

•Discard the supernatant carefully, without touching or disrupting the beads.

•Remove the tubes from the magnetic stand and wash with 200µl of 70% EtOH.

•Resuspend the beads and place tubes again on the stand for 3min.

•Discard the supernatant and repeat washing as before.

•Discard the rest of EtOH with a 10µl pipette (letting the tubes on the stand).

•Let samples dry for 5min, being careful not to over dry them.

•Remove the tubes from the magnetic stand and suspend beads in 20µl of 10mM Tris buffer pH 8.5.

•Place again the tubes on the magnetic stand and wait for 1min.

•Collect the supernatant containing the cleaned PCR product into a new tube.

Concentration measurement with Nanodrop (best 1µg/µl in 20µl).

On day 3, Electroporation

Remove dynabeads:

•Collect cells in 50ml falcon and centrifugate at 1300rpm 5-7min

•Completely discard the medium, resuspend cell pellet in 1ml T cell medium and transfer into 1,5ml tube

•Place the tube on a magnetic stand for 1min and collect the supernatant in a new 1,5ml tube (repeat this step)

•Wash cells once with T cell medium

•Count cells and resuspend cells at 1Mio cells/200µl T cell medium

•For each approach, pipette 200µl/well (1 Mio cells) in a 96 well V bottom plate (always 8 wells in a line)

•Incubate at 37°C 5% CO2 until the production of RNP

RNP production

•Thaw tracRNA and crRNA aliquots quickly

•Generate gRNA for each target as necessary. Prepare gRNA (tracrRNA + crRNA in a ratio of 1: 1) on ice! Important: first tracrRNA, then crRNA and resuspend carefully

•Heat at 95°C for 5min, then allow to cool to RT on bench top. (Store gRNA on

ice if you do not continue directly)

•Take 61µM Cas9 stock from -20°C quickly, store Cas9 on ice if you do not continue directly, otherwise bring Cas9 to RT for RNP assembly.

•Dilute 61µM Cas9 to 6µM with PBS. For 5µl of 6µM Cas9: add 4.51µl of 1x PBS + 0.49µl Hifi Cas9

•Allow gRNA to come to RT

•Add electroporation enhancer (carefully) to have at the end 20µM concentration in RNP mix (1:20 of 400uM stock of electroporation enhancer).

•Mix very, very slowly equal volumes of 6µM Cas9 protein and 40µM gRNA/enhancer (= tracRNA + crRNA + enhancer), move pipette tip in cycles while adding Cas9, always add Cas9 protein to gRNA solution, not the other way around. Final RNP concentration: 20µM.

•Check if RNP solution is clear and does not contain any precipitate; incubate RNPs for 15-20min at RT

•Subsequently put the RNPs on ice until you can proceed

•Nucleofection (Lonza 4D Nucleofector, P3 Primary Cell S-Kit)

•Allow RNPs to come to RT

•Prepare 96 well V bottom plate with RNPs and targeting construct. Pipette first targeting constructs (DNA 1µl/well (1µg)) and add then RNPs (3µl/well each RNP). Incubate at RT for at least 30 seconds. Plate in the same order as subset of cells will be ordered (always 8 wells in a line)

•Spin down T cells in 96 well v bottom plate (1500rpm, 3-5min), remove medium completely

•Prepare P3 buffer (for each sample 20µl: 16.4µl P3 solution + 3.6µl supplement)

and pipette 20µl in each well of a 96 well V bottom plate (same order as RNPs)

•Resuspend cells in 20µl supplemented P3 buffer (multichannel pipettes) and immediately transfer cells to V bottom plate with RNP and targeting constructs (minimize time the cells are resuspended in electroporation buffer)

•Mix carefully, transfer 20-24µl of cells to Nucleocuvette 16 well strip, tap the strips to remove air bubbles; put the strips in the nucleofector in the right direction (strips are marked at the side)

•Start nucleofection: Program EH-100 (custom program “CRISPR hum stim T cells”)

•Add 80µl pre-warmed T cell medium quickly to the cells after nucleofection and transfer to new 24 well flat bottom plate; add pre-warmed T cell medium without P/S and with IL-2 to have 1 Mio cells/ml and 180 IU/ml IL-2 (final concentration)

•Incubate at 37°C 5% CO2 for 24h (48h) and change the medium supplemented with 100 IU/ml IL-2

•Incubate at 37°C 5% CO2 for up to 72h

•Change medium every 1 - 2 days

On day 6, Analysis the transduction rate and phenotype by flow cytometry.

The methods was kindly provided by Dr.Kilian Schober from the Institute for Medical Microbiology, Immunology and Hygiene (Professor Dirk H. Busch), Technische Universität München, Munich, Germany

6.4 GENERATION OF POOL-PBMCs AS FEEDER CELLS

PBMCs were isolated from at least three different Buffy coats including HLA-A: 02 positive and HLA-A:02 negative. The amount of isolated PBMCs was determined after ACK lysis buffer and cell count from all Buffy coats was

adjusted equally. Pool-PBMCs were then frozen in 5 x 10^7 aliquots in 500 µl freezing medium (10% DMSO and 90% human AB serum) and stored in -80°C. For expansion of the T cells, the Pool-PBMC and LCL were irradiated (LCL: 100Gy, Pool-PBMC: 30Gy) and washed with T cell culture medium and further served as feeder cells.

6.5 ELISPOT ASSAY

On day 1, transferred 50ul of capture antibody solution to each well of the ELISpot plates, incubated the plates at 4°C overnight.

On day 2, Wash the ELISpot plates four times with cold PBS. Afterwards, replaced 150ul T cell medium in each well and incubate at 37°C for 1 hour to block the unspecific binding. During blocking, pulsed unspecific or $CHM1^{319}$ peptide to T2 cells for 2 hours in incubator, and mixed the every 15minutes. Afterwards, washed the T2 cells three times. Incubated other cell lines with 100IU/ml IFNγ for 48 hours before use.

After blocking, pipetted 50ul T-cell medium containing 10,000 T cells in the plates and incubated at least for 30 minutes. Carefully pipetted 50ul T-cell medium including 20000 target cells to over the suspension in each well and placed the plates at 37°C for 20 hours.

On day 3, Washed ELISpot plates six times with PBS containing 0.05% Tween and incubated with 100ul of detection antibody per well for 2 hours. Washed the plates another six times with PBS containing 0.05% Tween, pipetted 100ul Streptavidin-Horse Radish Peroxidase into each well and incubated at room temperature for 1 hour in dark room. Wash three times with PBS containing 0.05% Tween and another three times with normal PBS. Allocated 100ul development solution for 5 to 10 minutes and stopped by washing the plates with ddH_2O. After drying, analyzed ELISpot plates using the ELISpot reader.

6.6 RNA ISOLATION, cDNA SYNTHESIS, AND RT-PCR

After co-culture of T cells and EwS cells, remove the T cells and wash the EwS with cold PBS, and use trypsin to digest the EwS for 1-3 minutes, cultured medium is used again to stop digestion. Wash twice with cold PBS and then isolated with Trizol according to the protocol. cDNA synthesis and RT-PCR are performed according to the protocol.

6.7 SDS-PAGE AND WESTERN BLOT

After co-culture of T cells and EwS cells, remove the T cells and wash the EwS with cold PBS, and use trypsin to digest the EwS for 1-3 minutes, cultured medium is used again to stop digestion. Wash twice with cold PBS and then lysis the cells with protein lysis buffer on ice for 30 minutes. After 30 minutes concentrations were measured using BCA protein assay. Concentrations were adjusted in order to load 20-50 µg per well, complemented with 5×SDS loading buffer plus β-Me (Prepared as supplementary table). Denaturation by heating at 95°C for 5 min and separated on 8% or 12% Gel. Proteins were transferred to PVDF membrane using a Trans-Blot® Turbo™ (BioRad) set to the mix molecular weight program. Transferred-membranes were blocked with 5% BSA diluted in TBS with 0.1% Tween20 (TBST) for one hour at RT and incubated with the desired primary antibodies overnight at 4°C. The following day, membranes were washed 3 times in TBST for 10 min at RT and incubated with the respective HRP-coupled secondary antibodies for one hour at RT with rotation. Washing step was repeated 3 times prior to protein detectionwith ECL clarity for HRP-induced chemiluminescence inside a Gel Logic 1500 imaging system. Densitometric analyses of the bands were performed with Image J software, and arbitrary units were normalized to appropriate control (GAPDH).

6.8 *IN VIVO* EXPERIMENTS

To analyze local tumor growth *in vivo*, 3 x 10^6 A673 cells were re-suspended in

a final volume of 0.2 ml PBS/0.2% FCS. 3 x 106 A673 tumor cells were inoculated subcutaneously at the lower back of immunodeficient Rag2$^{-/-}\gamma c^{-/-}$ mice. Mice received a full body irradiation on day 3 with 3.5 Gy to facilitate engraftment of human T cells (Figure 5). 5 x 10^6 T cells together with 1.5 x 10^7 IL-15 secreting NSO cells were injected i.p. on day 3. 1.5 x 10^7 IL-15 secreting NSO cells (previously irradiated with 80 Gy) were injected i.p. twice per week after the first injection. Mice were sacrificed after 17 days of tumor bearing. Tumor size was determined. Also blood, bone marrow were collected to analyze the T cell homeostasis.

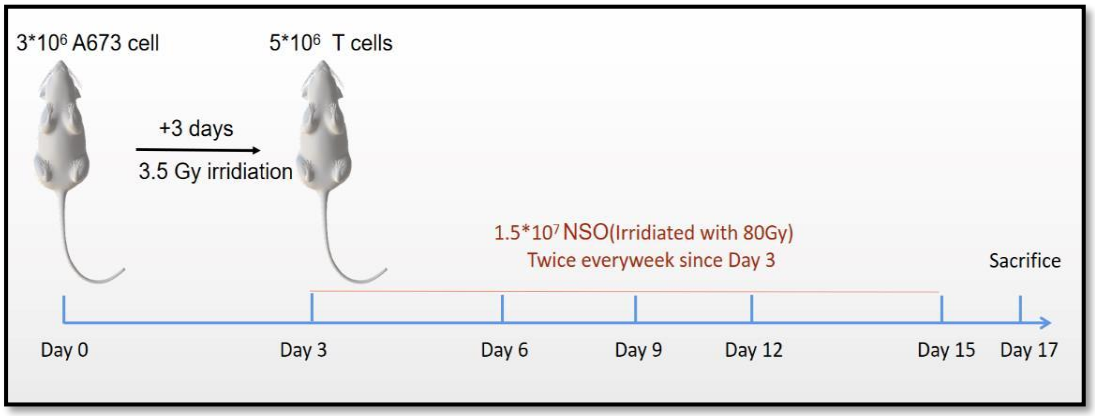

***Figure 5. Time scale for validation of transgenic TCR on HLA-A*02:01$^+$/CHM1$^+$ EwS* in vivo.**

Mice were inoculated with 3 x 10^6 s.c. HLA-A*02:01+/CHM1$^+$ A673 EwS cells at the lower back. On day 2, mice received a fully body irradiation with 3.5 Gy followed by the injection of T cells and NSO cells on day 3. NSO cells were injected twice per week until the sacrifice the mice.

6.9 ANALYSIS OF PUBLISHED CHIP-SEQUENCE DATA AND MICROARRAY

ChIP-sequence data (GSE61944: GSM1517546, GSM1517547, GSM1517555, GSM1517556, GSM1517569, GSM1517570, GSM15175472, GSM1517573, GSM1517577, GSM1517581) were downloaded from the GEO database, and processed and displayed in the IGV browser (Robinson et al., 2017).

Expression of CHM1 in EwS and bone marrow mesenchymal stem cell was mined from GEO database (GSE17618 and GSE6691), CCLE and ProteomicsDB database.

6.10 STATISTICAL ANALYSIS

All statistical analyses were performed using GraphPad Prism. Two-tailed T test was used for statistical analyses of ELISpot results. $p \leq 0.05$ was regarded as statistical significant (*), $p \leq 0.01$ was regarded as statistical very significant (**), $p \leq 0.001$ was regarded as statistical highly significant (***), $p \leq 0.0001$ was regarded as statistical highly significant (****). All data is presented as mean±standard error of the mean (SEM).

7 RESULTS

7.1 FEASIBILITY OF ORTHOTOPIC REPLACEMENT OF THE ENDOGENOUS T CELL RECEPTOR WITH A T CELL RECEPTOR CONTAINING A CHONDROMODULIN-1 TARGETING SEQUENCE

Based on our previous work (Thiel et al., 2017) on immunotherapy of EwS, we focus on targeting the Chondromodulin-1 peptide 319 (CHM1^{319}) peptide, VIMPCSWWV. For non-viral CRISPR/Cas9 engineered orthotopic TCR replacement, we refer to the established protocol kindly provided by Dr. Kilian Schober, Institute for Medical Microbiology, Immunology and Hygiene (Professor Dirk H. Busch), Technische Universität München, as shown in Figure 6 (Moosmann et al., 2022; Schober et al., 2019). The T cell receptor (TCR) DNA template containing the sequence targeting the CHM1^{319} peptide (Blaeschke et al., 2016) was established for homology-directed repair (HDR) (Figure 6 and Supplementary Table 2).

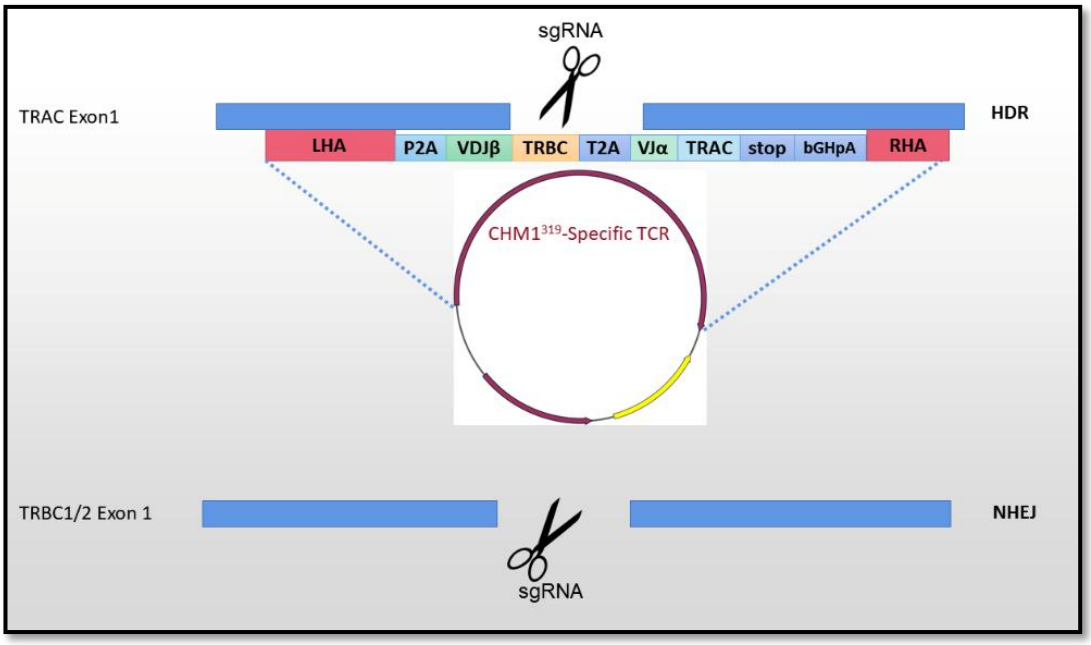

Figure 6. Schema of orthotopic TCR replacement by CRISPR/Cas9-engineered gene editing.

DNA template design for αβ-TCR integration via homology-directed repair (HDR, upper

panel) in TRAC exon1. Transgenic VDJ β-transcription is initiated with endogenous promoters. Endogenous TRAC (TRAC exon 1) and TRBC (TRBC1/2 exon1. Lower panel) are knocked out followed by transgene knock-in into the TRAC locus. TRBC knock-out leads to non-homologous end-joining (NHEJ) in the TRBC locus.
LHA, left homology arm; TRBC, TCR-β constant; TRAC, TCR-α constant; bGHpA, poly-A tail; stop, RHA, right homology arm; T2A and P2A, self-cleaving peptide inserts (The constant domain of the beta chain is murinized).

We performed PCR to amplify the knock-in (KI) fragment from the right homology arm to the left homology arm (Figure 7) according to the Schober protocol. SfiI enzyme was used to cut the plasmid and check the size of the KI fragment. The upper band (2482bp) served as the positive control; the lower band is the backbone of the plasmid. Here we identify that PCR using 15ng of original plasmid, 10ul of 20uM dNTP, 2ul of 10uM Primer, in a total of 50ul of reaction volume with DEPC water, could generate the most abundant PCR product.

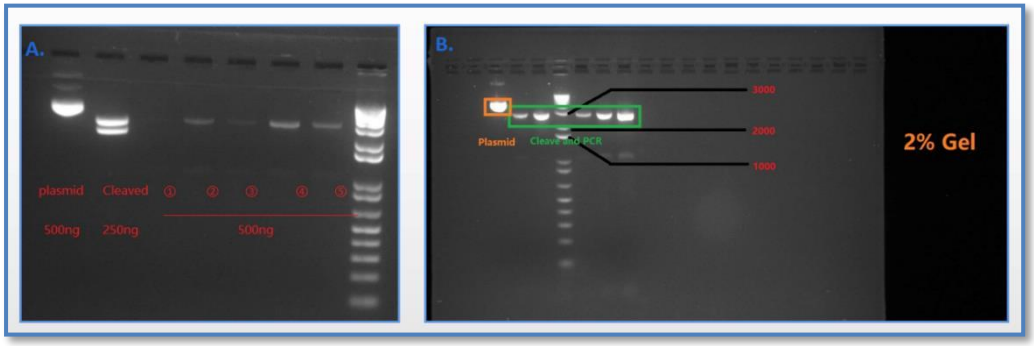

Figure 7. Detection of the CHM1^{319}-specific transgenic TCR fragments in the pMK-RQ-CHM1-TCR-KI plasmid by PCR. This plasmid was used to amplify the TCR sequence later used for CRISPR/Cas9 mediated KI.

After PCR of the knock-in fragment, products were loaded onto agarose gel. Restriction cleavage of the TCR was used as positive control.
Expected bands are shown for the backbone of the plasmid and the knock-in fragment (2842 bp) with different conditions: ①. Plasmid 7.5ng, dNTP 20uM 10ul, Primer 1ul, Total 50ul; ②. Plasmid 7.5ng, dNTP 20uM 10ul, Primer 2ul, Total 50ul; ③. Plasmid 15ng, dNTP 20uM 10ul, Primer 1ul, Total 50ul; ④. Plasmid 15ng, dNTP 20uM 10ul, Primer 2ul, Total 50ul; ⑤. Plasmid 25ng, dNTP 20uM 10ul, Primer 2ul, Total 50ul). The plasmid is 5120 bp.

7.1.1 CRISPR/CAS9 ENGINEERED TCR EXPRESSION

We performed CRISPR/Cas9 engineered knock-out (KO) of the endogenous T cell receptor (hTCR) combined with or without CHM1^{319}-TCR insertion into lymphocytes from peripheral blood mononuclear cells (PBMC). Single α- or β-stranded as well as double-stranded KO result in the loss of endogenous TCR surface expression (Figure 8A). Endogenous TCR KO combined with CHM1^{319}-TCR insertion leads to a T cell population containing a murinized TCR (mTCR), which are hTCR negative, indicating successful CRISPR/Cas9 engineered gene editing. The KO efficacy was approximately 98.5%. In contrast, the KI efficacy in T cells from thawed T cells ranged between 10%-23% (21% in Figure 8A), while the efficiency of KI in fresh T cells reached 45% (Figure 8B).

The CD3 complex is a heterodimeric glycoprotein cooperating with the TCR to convey signal transduction upon interaction with the antigenic peptides (Acuto & Reinherz, 1985). Upon combined TCR KO and KI, we see CD3 surface expression only in the population, where KI was successful (CHM1V β 23-PE, Figure 8C, right panel, Q2) while the KI negative population remains CD3 negative (Figure 8C, right panel, Q4). This indicates that CD3 expression is linked to TCR expression.

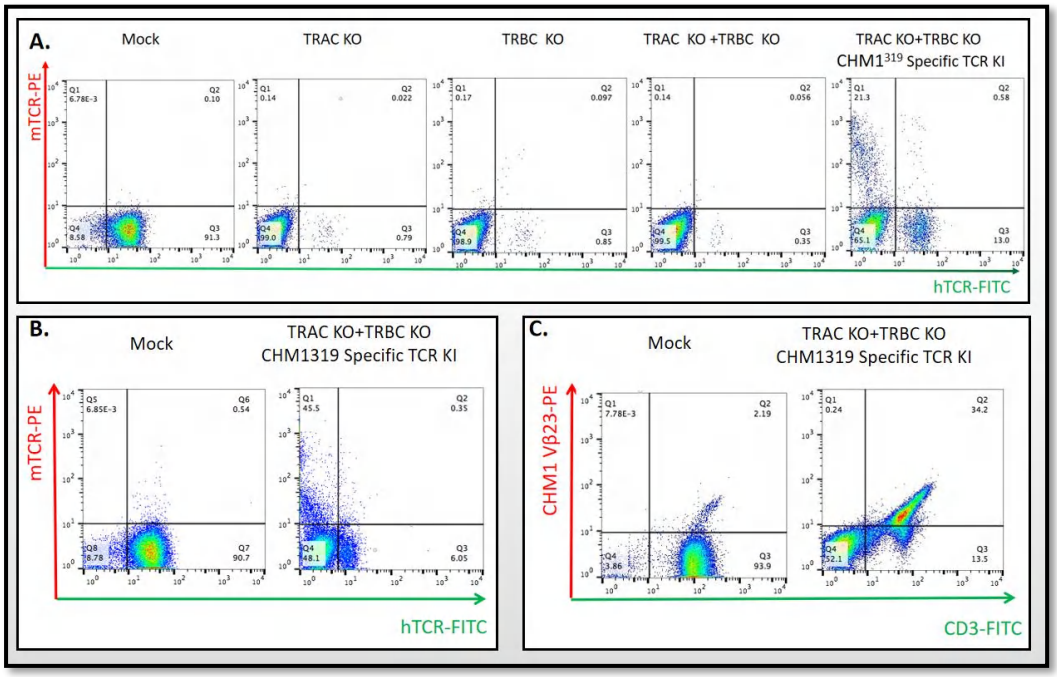

Figure 8. Assessment of transgenic TCR expression after CRISPR/Cas9 mediated orthotopic TCR replacement by FACS analysis.

(A) After knock-out of either α-chain (TRAC KO) or β-chain (TRBC KO) or of both chains, the endogenous TCR (hTCR) is undetectable by FACS analysis. After knock-out of both endogenous chains combined with Knock-in of the CHM1^{319}-specific TCR, mTCR is detectable (the TRBC constant chain of the CHM1^{319} specific TCR is murinized). Thawed T cells, knock-in efficiency: 21.3% (thawed T cells). Mock: electroporation of CRISPR/Cas9 but without guide RNA.
(B) knock-out of both chains combined with with transgenic TCR knock-in: mTCR positive T cells are hTCR negative. Fresh T cells, knock-in efficiency: 45.5%.
(C) Pentamer staining confirms transgenic TCR expression before enrichment.
T cells were double stained with either anti-mTCR (mTCR-PE) and anti-hTCR(hTCR-FITC), or anti-pentamer (CHM1 Vβ23-PE) and anti-CD3 (CD3-FITC).

7.1.2 TUMOR RECOGNITION AND CYTOTOXICITY BY CRISPR/CAS9 ENGINEERED T CELLS

For functional analysis of CRISPR/Cas9 engineered T cells, we assessed T cell activation by IFNγ-Elispot, tumor cell apoptosis (cleaved-PARP) by western blot, and T cell cytotoxicity against tumor cell by xCelligence detachment assays.

Selection of engineered T cells from six donors was initiated utilizing anti-murine TCR antibody coupled beads. Expression of the murinized TCR sequence (mTCR) was assessed by FACS analysis, yielding a 92.7 % homogenous transgenic products in a representative experiment. (Figure 9A, right panel, Q2). CHM1^{319} transgenic T cells specifically recognized T2 cells loaded with CHM1^{319} peptide, while T2 cells loaded with an HLA-A*02:01 binding influenza control peptide(FLU) were not recognized (Figure 9B). CRISPR/Cas9 engineered T cells secreted IFNγ when co-cultured with the HLA-A*02:01^{+} A673 and TC-71 EwS cell lines. In contrast, when co-cultured with HLA-A*02:01^{-} cell lines SB-KMS-KS or SK-N-MC, no IFNγ release was observed. These findings indicate that CRISPR/Cas9 engineered T cells caused specific HLA-restricted in vitro EwS cell line recognition.

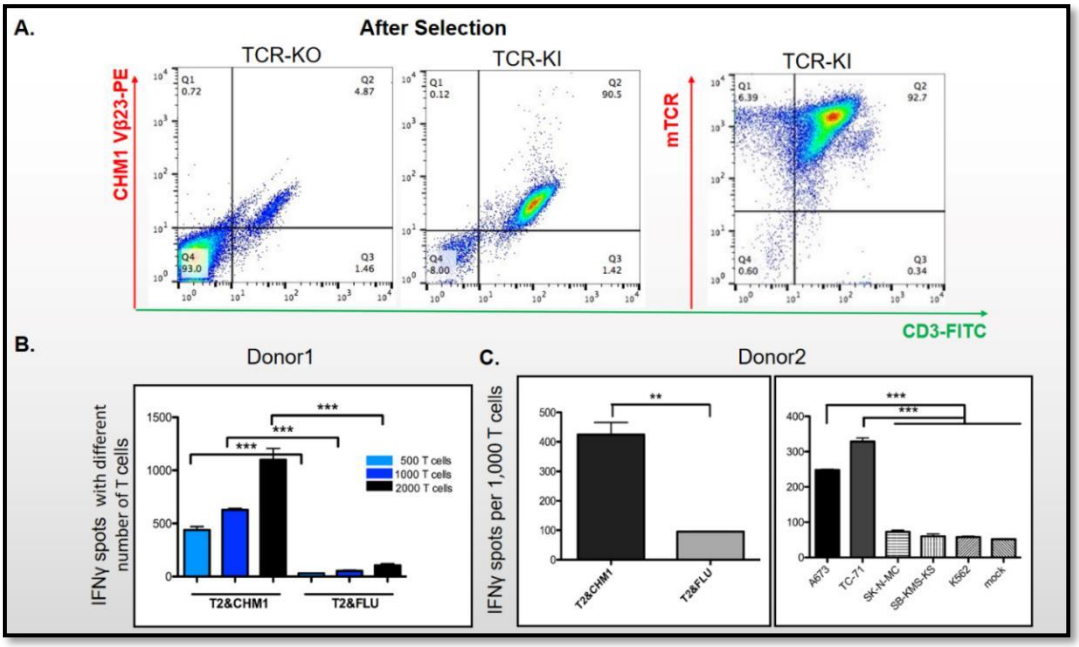

Figure 9. Assessment of functional activation of CRISPR/CAS9 engineered TRANSGENIC T CELLS after co-culture with tumor target cells by IFNγ-ELISpot.

(A) CHM1^{319}-TCR expression in the final product of CHM1^{319}-TCR insertion after enrichment. These cells were used for functional analysis. T cells were double stained with either anti-mTCR (mTCR-PE) or anti-pentamer (CHM1 Vβ23-PE) with anti-CD3 (CD3-FITC)

(B) IFNγ release with dose dependent manner of transgenic T cells after exposure to T2 cell loaded with either CHM1^{319}-peptide or with control-peptide (FLU) for 20 hours

in donor 1.
(C) IFNγ release to assess the specific reactivity against several tumor cell clines after co-culture with $CHM1^{319}$-TCR transgenic T cells in donor 2(A673 and TC-71: HLA-A*0201^{+} EwS, SK-N-MC and SB-KMS-KS: HLA-A*0201^{-} EwS, K562: MHC^{-} NK cell control). IFNγ release transgenic T cells after exposure to T2 cell loaded with either $CHM1^{319}$-peptide or with control-peptide (FLU) served as positive control. Error bars represent standard deviation of triplicates experiments. ** means P<0.01, *** means P<0.001.

We next asked whether these T cells also cause cytotoxicity of EwS tumor target cells and their apoptosis. Real-time analysis of EwS cytotoxicity (detachment from tissue culture tray) was assessed by xCelligence assay. After the addition of HLA-A*02:01/CHM1^{+} restricted TCR transgenic T cells, not only HLA-A*02:01^{+} A673 and TC-71 lines (Figure 10A, B), but also HLA-A*02:01^{-} SK-N-MC line (Figure 10C) detached. Of interest, TCR negative T cells (TCR KO) also caused a variable degree of detachment. These findings raised the possibility that the xCelligence assay may not represent solely HLA-TCR cognate specific cytotoxicity. To this end we asked, which T cells cause apoptosis, as a specific cell death modality induced by TCR-HLA recognition. Cl-PARP as a parameter of apoptosis was specifically induced by T cells with orthotopic TCR replacement in HLA-A*02:01^{+} A673 but not in HLA-A*02:01^{-} SK-N-MC lines (Figure 10D). Some marginal and variable cl-PARP was still seen after co-culture with TCR KO cells.

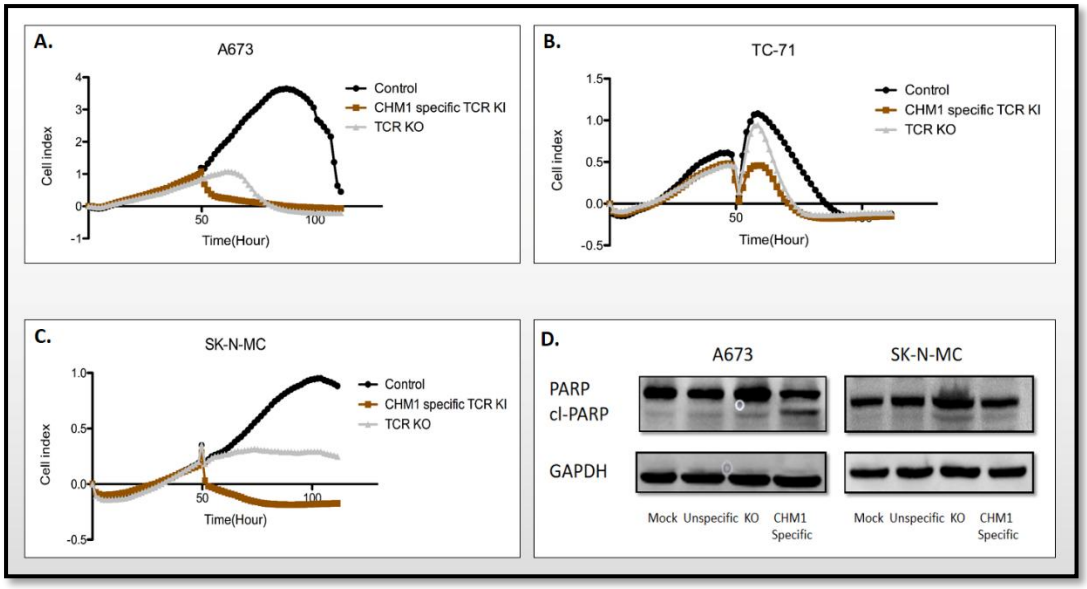

Figure 10. Assessment of apoptosis of CRISPR/CAS9 engineered TRANSGENIC T CELLS after co-culture with tumor target cells, by cleaved PARP (cl-PARP).

(A) xCelligence assay were performed to assess killing/detachment effect on of A673, TC-71, and SK-N-MC with the T cells with endogenous TCR knockout (TCR KO), or with orthotopic TCR replacement (CHM1 specific TCR KI), EwS cells without T cells co-culture is negative control.

(D) PARP cleavage (cl-PARP) analyzed by SDS-PAGE after co-culture of A673 (HLA-A*0201^{+}) or SK-N-MC (HLA-A*0201^{-}) with either no T cells (Mock), unspecific T cells (unspecific), T cells with TCR knock-out (KO) or T cells with orthotopic TCR replacement with CHM1^{319} TCR (CHM1 Specific).

7.2 COMPARISON OF TCR TRANSGENIC T CELLS ENGINEERED BY CRISPR/CAS9 VS. RETROVIRAL GENE TRANSDUCTION

The experimental design to compare the phenotype and cytotoxic effects of our transgenic T cells is shown in Figure 11. After isolating PBMC from buffy coat, we stimulated the T cells with CD3/CD28 dynabeads for two days. Meanwhile, we amplified the KI-DNA fragment for CRISPR/Cas9 transduction and transfected 293Vec-RD114 packaging cells with the pMP71-CHM1-TCR plasmid for retrovirus production. Subsequently, we purified the KI-DNA fragment for CRISPR/Cas9 or harvested the retrovirus for transduction. Next,

we isolated the transgenic T cells with anti-mTCR antibody and expanded the transgenic T cells for further functional analysis and *in vivo* experiments.

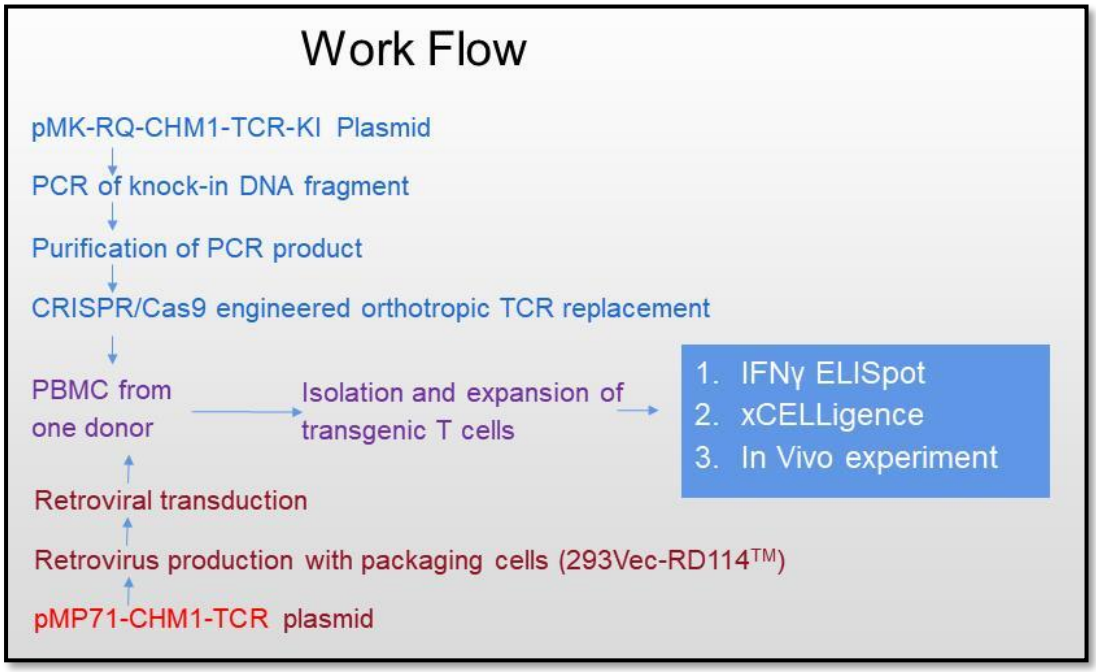

Figure 11. Procedures to compare transgenic T cells engineered by either CRISPR/Cas9 or retroviral gene transfer.

CRISPR/Cas9 engineered orthotopic TCR replacement or retrovirus transduced random TCR insertion into the T cell genome was performed on T cells from the same donor. Phenotype and endogenous TCR expression were evaluated by flow cytometry (FACS). Tumor cell cytotoxicity by xCELLigence (detachment) and cl-PARP by SDS-PAGE (apoptosis) as well as *in vivo* tumor growth were assessed in both groups to analyze the function of transgenic cells.

7.2.1 HIGHER EFFICIENCY OF RETROVIRAL TRANSDUCTION COMPARED TO GENE EDITING BY CRISPR/CAS9

We first assessed retroviral transduction efficacy. After transduction of T cells from two donors with GFP-containing control vector pMP71-GFP, we checked the GFP expression by fluorescence microscopy (Figure 12A) and by FACS analysis (Figure 12A). The cells from donor 1 were thawed, whereas cells from donor 2 were fresh. The transduction rate of thawed T cells was 78% (Figure 12B, upper panel), while fresh T cells reached 90% (Figure 12B, lower panel).

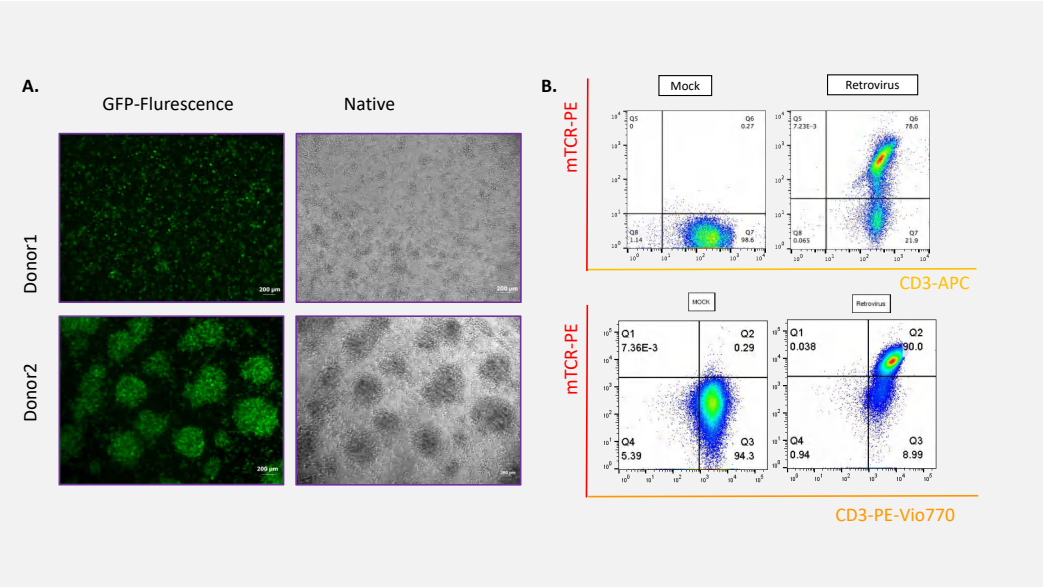

Figure 12. TRANSGENIC pMP71-GFP AND pMP71-CHM1-TCR EXPRESSION.

(A) A GFP sequence containing pMP71 vector was used to assess efficiency of T cells in general. Transduction is performed twice at day 1 and day 2 of culture. 4 days after the first transduction, representative fluorescence microscopy was performed to assess the transduction efficacy of GFP in T cells. Although the colony size is different between the two donors, transduction rates are comparable. Material from donor 1 was thawed, material from donor 2 was fresh.
(B) The CHM1-TCR sequence containing the pMP71-CHM1-TCR vector, was used to transfect T cells. 4 days after the first transduction, representative FACS analysis was performed to access the transduction rates. T cells were stained with murine anti-TCR antibody (mTCR-PE) and anti-CD3-APC (anti-CD3-APC) or anti-CD3-Vio770 (the constant domain of the beta chain of the transgenic TCR being murinized).

When comparing CRISPR/Cas9 orthotopic single gene replacement and multiple random insertions by retroviral transduction, we found retroviral transduction to be consistently higher. Efficacy of endogenous TCR orthotopic replacement with CHM1^{319}-TCR ranged from 11% to 45%, whereas efficacy of retroviral transduction ranged from 70-90%. Figure 13 depicts the results unspecific (non-engineered), CRISPR/Cas9 and retrovirus (Retrovirus) transduced T cells were derived from the same donor. Retrovirus transduction efficacy was 77% (Figure 13A, right panel Q2 plus Q3), whereas CRISPR/Cas9 transduction efficacy was only 19% (Figure 13A, middle panel Q2 plus Q3). As expected, replacement of the endogenous TCR was more efficient in the CRISPR/Cas9 (Figure 13B, middle panel Q5 plus Q6) as compared to the **Retrovirus (Figure 13B, right panel Q5 plus Q6) group.**

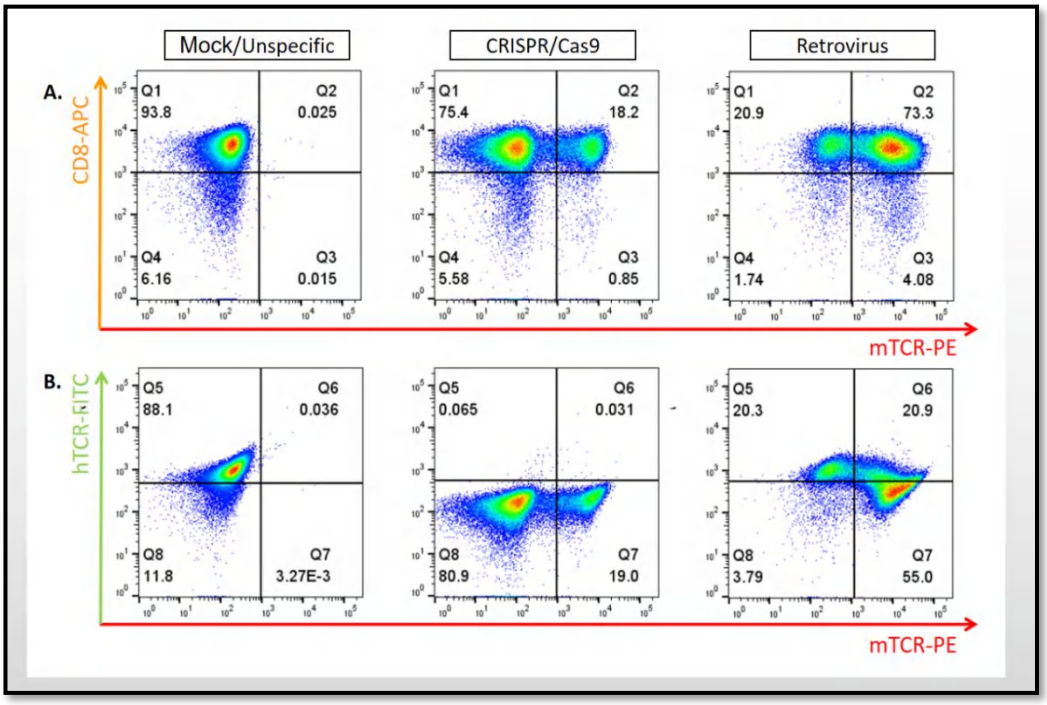

Figure 13. Efficacy of TCR replacement via CRISPR/Cas9 vs. retrovirus-mediated TCR insertion.

(A) T cells were stained with anti-CD8-APC (CD8-APC) and anti-mTCR (mTCR-PE) after culture to assess the efficacy of transduction.
(B) T cells were stained with anti-endogenous TCR (hTCR-FITC) and anti-mTCR (mTCR-PE) after culture to assess the efficacy of transduction, the constant domain of the transgenic TCR beta chain being murinized.
CRISPR/Cas9 and retrovirus (Retrovirus) transduced T cells from the same donor.

7.2.2 PRESERVATION OF A PHYSIOLOGICAL T CELL PHENOTYPE BY CRISPR/CAS9 ENGINEERING

We performed FACS analysis after isolating the transgenic T cells with an anti-mTCR antibody to investigate the phenotype alteration by TCR engineering (Figure 14A, upper panel). There was no difference in the central memory phenotype ($CD62L^+/CD45RO^+$, Q2) between the non-engineered (unspecific) T cells and CRISPR/Cas9 engineered (CRISPR) T cells, whereas retroviral TCR transduction (Retrovirus) induced a central memory phenotype as compared to the other two groups (Figure 14A, lower panel).

The higher percentage of central memory phenotype T cell population after retroviral transduction was also observed over a prolonged period, i.e. at weeks two, three, and four (Figure 14B).

These results suggest that CRISPR/Cas9 engineered T cells resemble more the physiological phenotype of non-engineered T cells, while retroviral TCR transduction skews T cell differentiation towards a central memory phenotype.

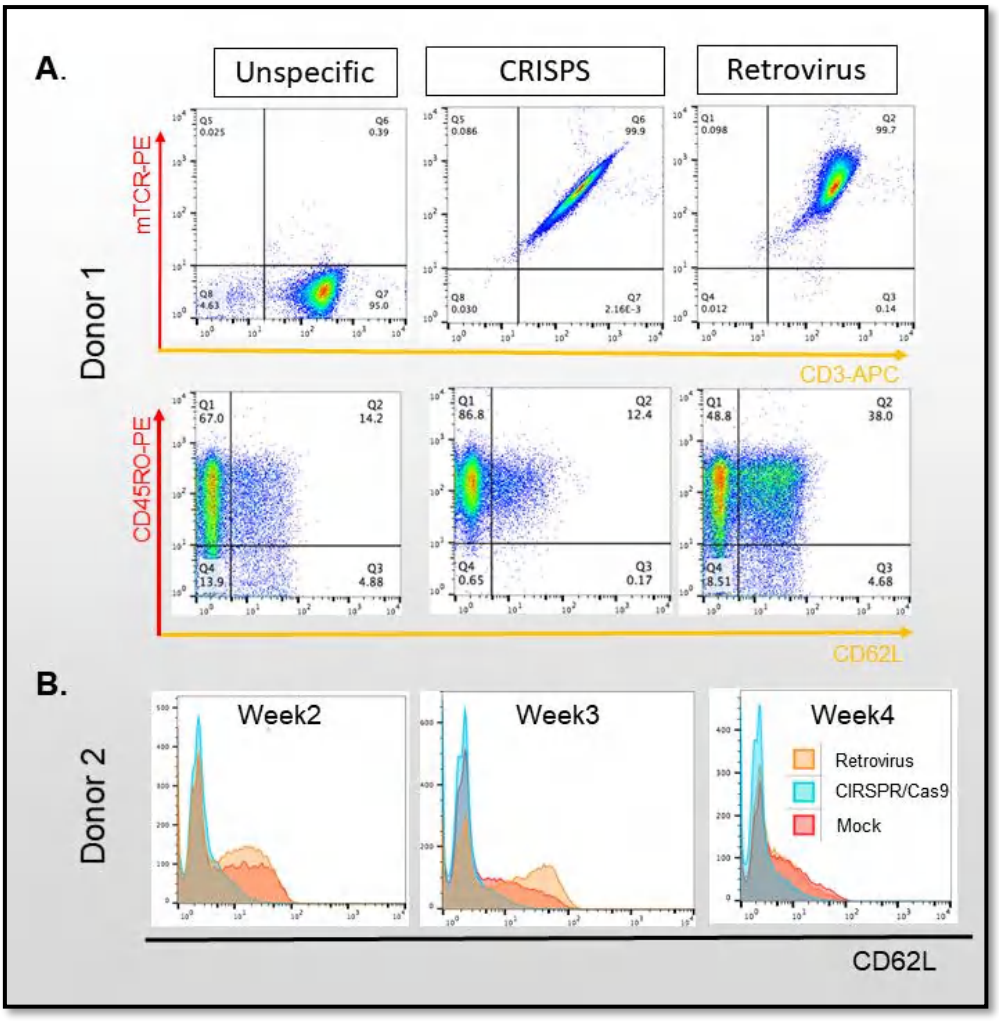

Figure 14. Central memory (CM) phenotype of transgenic T cells after TCR replacement via CRISPR/Cas9 vs. retroviral transduction.

(A) Donor 1: upper panel, the representative of T cells in each group after mTCR antibody isolation, ''Unspecific'' designates non-engineered T cells, "CRISPR" designates T cells with TCR replacement by CRISPR/Cas9 and "Retrovirus" designates T cells with TCR transfer by retrovirus.
Lower panel, CM T cells are characterized by co-expression of CD45RO and CD62L after two weeks.
(B) Donor 2: CD62L expression in T cells at weeks two, three and four after T cells isolation.
Double staining of T cells with anti-CD45RO (CD45RO-PE) and anti-CD62L (CD62L-APC).

7.2.3 REQUIREMENT OF HIGH RETROVIRAL GENE TRANSDUCTION EFFICACY AND HIGH CRISPR/CAS9 KO EFFICACY FOR PREVENTION OF ENDOGENOUS TCR EXPRESSION AND TCR CHAIN MISPAIRING

One of the advantages of orthotopic TCR replacement by CRISPR/Cas9 is that it avoids mispairing of endogenous and exogenous TCR chains and thus averts the generation of promiscuous TCRs recognizing off-target antigens. To gauge this postulated advantage of CRISPR/Cas9 vs. retroviral engineering, we compared the expression of endogenous TCR after CRISPR/Cas9 gene edition vs. retroviral transduction. We found that the decrease of endogenous TCR surface expression in the retrovirus group (Retrovirus) was similar to the expression in the CRISPR group (CRISPR, Figure 15A). After CHM1^{319}-TCR transduction via retrovirus, the transgene positive population (red curve, Figure 15B) shows less endogenous TCR transgene as compared to the negative population (blue curve, Figure 15B).

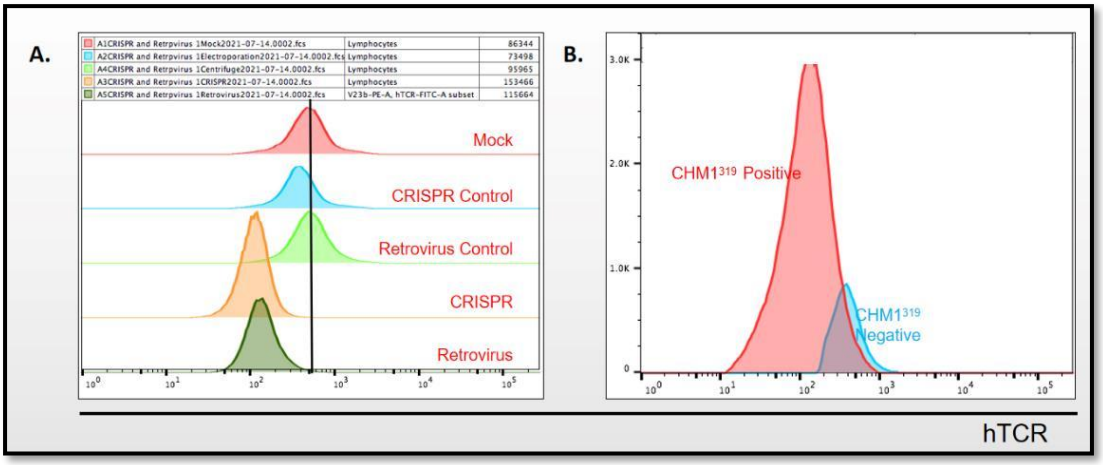

Figure 15. Assessment of endogenous TCR expression after TCR replacement by CRISPR/Cas9 vs. retroviral TCR transduction.

(A) FACS analysis of expression of endogenous TCR expression (hTCR): "Mock" designates a control non-transduced T cells; "CRISPR Control" designates a control containing T cells transduced by electroporation of CRISPR/Cas9 but without guide RNA; "Retrovirus Control" designates a control containing T cells exposed to centrifugation only with no retrovirus added; "CRISPR" designates T cells with TCR replacement by CRISPR/Cas9 and "Retrovirus" designates T cells with TCR transfer by

retrovirus. The “CRISPR” and “Retrovirus” groups were analyzed after isolation with anti-mTCR antibody.
(B) FACS analysis of expression of endogenous TCR expression (hTCR) after retrovirus-mediated TCR transfer (T cells were analyzed before isolation with anti-mTCR antibody).
T cells were stained with anti-mTCR (mTCR-PE) and anti-hTCR (hTCR-FITC).

We also noted that repression of the endogenous receptor after retroviral transduction depends on transduction efficacy (Figure 16). In this experiment, the retroviral transduction efficacy was only 42%. In the setting of this low transduction efficacy, we can identify two distinct subpopulations (Figure 16, left panel): The upper cloud represents a subpopulation with high mTCR expression, i.e. the transduced subpopulation, whereas the lower cloud represents a population with a low mTCR expression. The high mTCR expressing subpopulation has a lower hTCR expression as compared to the subpopulation represented by the lower cloud, which is characterized by low mTCR and higher hTCR expression. This low mTCR/high hTCR subpopulation is comprised of non-transduced cells as indicated by low mTCR expression. Although there is some overlap between both subpopulations, the peaks of transduced and non-transduced subpopulations are distinct (Figure 16, right panel). This finding implicates that a low retroviral transduction efficacy will yield a heterogenous product containing a large subpopulation at risk for mispairing and causing autoimmune side effects.

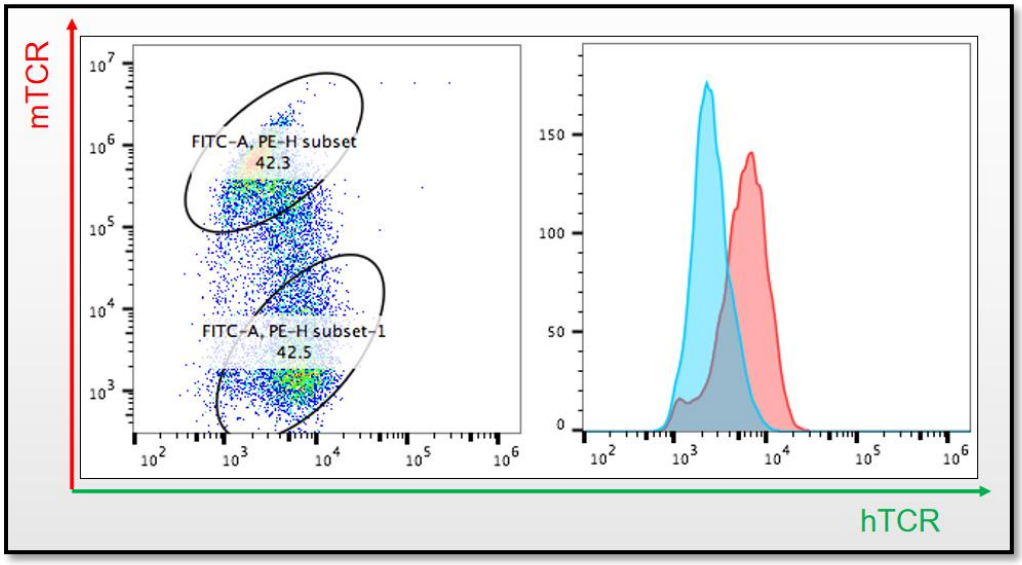

Figure 16. Assessment of endogenous TCR expression on T cell membrane after low retroviral TCR efficiency.

FACS determinates the expression of endogenous TCR expression (hTCR) on cell membrane after retrovirus-mediated TCR transfer with low efficiency ((T cells were analyzed before isolation with mTCR antibody).
T cells were stained with anti-mTCR (mTCR-PE) and anti-hTCR (hTCR-FITC).

For clinical application, we have to ensure the KO both endogenous TCR chains. Failure of β chain KO constitutes a risk of mispairing of the transduced α with the endogenous β chain. The ratio of α to β chain in a single CRISPR/Cas9 engineered cell would be 2:1, since both transgenic chains are expressed from the α locus. When comparing the transduction efficacy of both procedures, in retrovirally transduced T cells the amount of transduced TCRs per cell are by definition and by observation higher (n>1) than the single endogenous TCR (n=1). On the other hand, if CRISPR/Cas9 KO is suboptimal, the risk of mispairing between the exogenous α with the endogenous β chains in a single cell would be X: 1, with X being >1. This implicates, that the risk of mispairing may be higher in CRISPR/Cas9 as compared to retrovirally

transduced T cells (Figure 17).

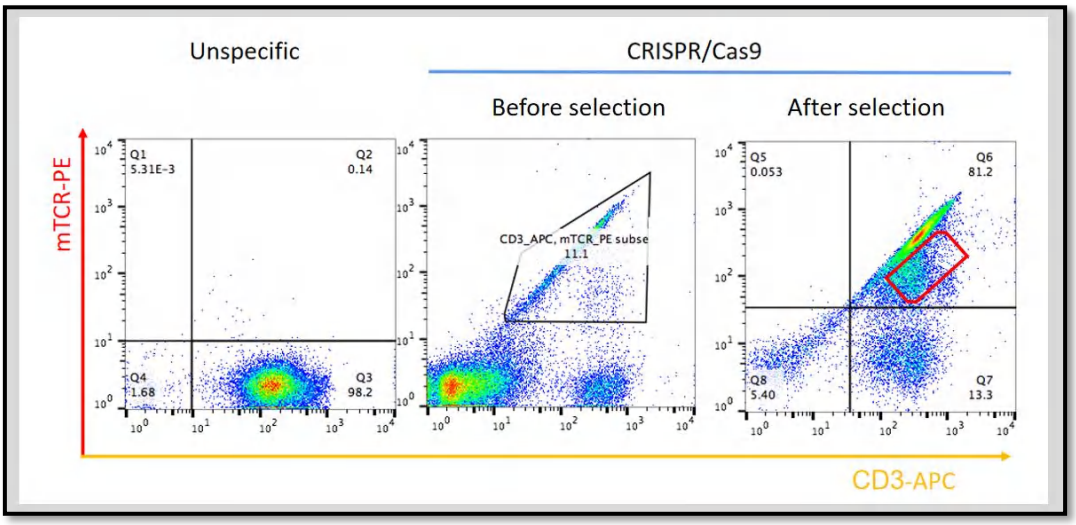

Figure 17. Endogenous β chain mispairing with the transgenic α chain after insufficient CRISPR/Cas9 engineered KI.

CRISPR/Cas9 engineered transgenic T cells from thawed donor: left panel, non-engineered T cells (Unspecific); middle panel: CRISPR/Cas9 engineered transgenic T cells before mTCR selection with an anti-mTCR antibody (CRISPR/Cas9); right panel, CRISPR/Cas9 engineered transgenic T cells after mTCR selection with an anti-mTCR antibody. The red cloud in Q6 indicates the transgenic T cell products with a failure KO of endogenous β chain (CRISPR/Cas9).
T cells were stained with anti-mTCR (mTCR-PE) and anti-CD3 (CD3-APC).

Moreover, retrovirally transduced T cells express more TCR as documented by CD3 expression (Figure 18), due to multiple gene copies.

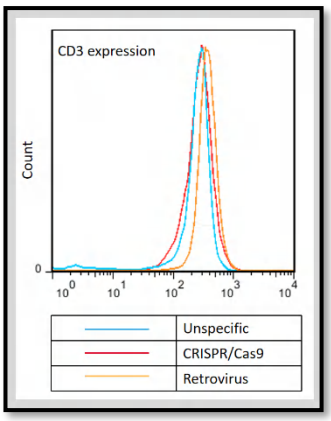

Figure 18. Higher expression of CD3 after retroviral transduction of TCR.

CD3 expression in non-engineered T cells (Unspecific) , CRISPR/Cas9 engineered T cells with orthotopic TCR replacement(CRISPR/Cas9) and retrovirally transduced T cells(Retrovirus).

7.2.4 SPECIFIC TUMOR CELL RECOGNITION AND CYTOTOXICITY *IN VITRO* BY BOTH T CELL PRODUCTS WITH BETTER PROLONGED ACTIVITY OF CRISPR/CAS9 ENGINEERED T CELLS

We next assessed the cytotoxic effects on and specific recognition of EwS cell lines by transgenic T cells obtained with either orthotopic TCR replacement by CRISPR/Cas9 or retroviral transfer. After isolation of the transgenic T cell with mTCR antibody (mTCR-PE), we co-cultured the T cells with HLA-A*02:01^{+}A673. Here we identified an increase in the cl-PARP in A673 after co-culture with both transgenic T cell products. Somewhat more cl-PARP1 was observed with retrovirally transduced T cells compared to CRISPR/Cas9 engineered T cells (Figure 19A).

To assess specific recognition, we co-cultured T cells with T2 cells loaded with either CHM1^{319}-peptide or with control-peptide (FLU) and performed an IFNγ-Elispot on day 35 and day 54 after T cell culture. On day 35, we observed a higher IFNγ release with retrovirally transduced T cells as compared to T cells with orthotopic TCR replacement (Figure 19B). In contrast, a higher IFNγ release was induced by T cells with orthotopic TCR replacement on day 54 (Figure 19C). Of note, we identified similar trends with the control peptide (Figure 19, B and C), albeit with significantly weaker IFNγ signals.

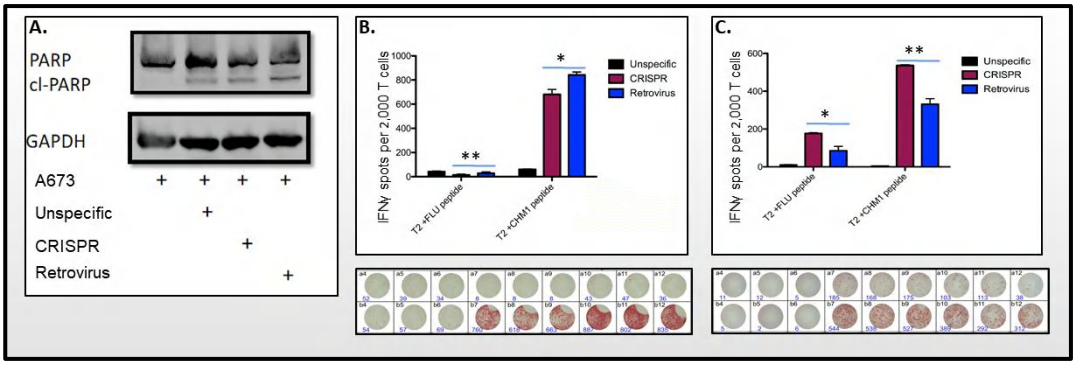

Figure 19. Assessment of PARP cleavage (cl-PARP) by SDS-PAGE and IFNγ release by Elispot to compare the cytotoxic effects targeting A673 Ewing Sarcoma cells and T2 cells loaded with the CHM1 peptide.

(A) Determination of cl-PARP in A673 (HLA-A*02:01^{+}/CHM1^{+}) cells by SDS-PAGE after co-culture of A673 cells with either no T cells, non-engineered T cells (Unspecific), engineered T cells with orthotopic TCR replacement (CRISPR), or retroviral (Retrovirus).

(B, C) Evaluation of activation of T cells by IFNγ-ELISpot assay after co-culture with T2

cells plus CHM1 peptide on 35 days (B) and 54 days (C) after T cell isolation from PBMC. T cells as in panel A. * means $P<0.05$, ** means $P<0.01$.

We next performed xCELLigence assays to compare the cytotoxic effect on EwS cells with transgenic T cells on day 54. T cells with orthotopic TCR replacement targeting CHM1 clearly caused cytotoxicity of HLA-A*02:01$^+$ A673 (sharp decrease of Cell Index, Figure 20A). Of note, there was some marginal detachment on HLA-A*02:01$^-$ SB-KMS-KS again after co-culture with CRISPR/Cas9 engineered T cells (Figure 20B) as previously observed (cf. Figure 10). These findings underline that the xCelligence assay may not represent solely HLA-TCR cognate specific cytotoxicity, at least in our hands.

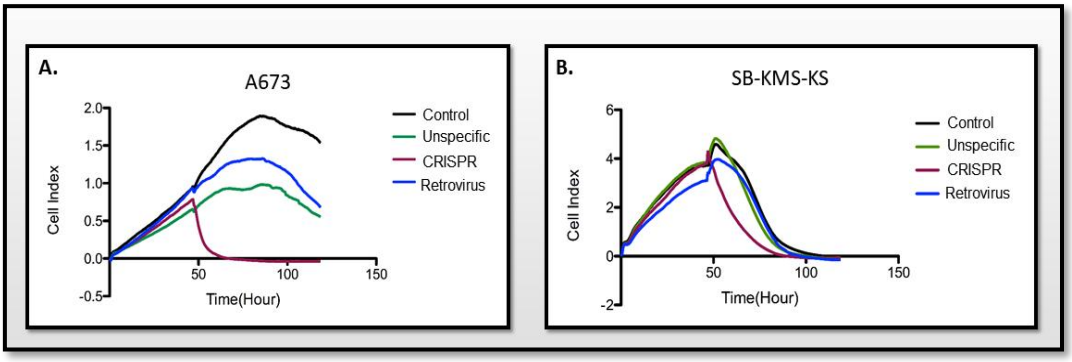

Figure 20. Cytotoxicity of EwS cell lines by real-time xCELLigence assay.

xCELLigence detachment assays were performed to compare the cytotoxic effect of T cells on HLA-A*02:01$^+$/CHM1$^+$ A673 cells (A) and HLA-A*02:01$^+$/CHM1$^-$ SB-KMS-KS (B). Treatment groups include mock control, non-engineered T cells (unspecific), T cells with CRISPR/Cas9 engineered TCR replacement (CRISPR), and T cells with retroviral TCR transduction (Retrovirus).

7.2.5 ADOPTIVE TRANSFER OF BOTH TRANSGENIC T CELL PRODUCTS DECREASES TUMOR GROWTH *IN VIVO*

We expanded the transgenic T cells and non-engineered T (unspecific) cells after isolating the transgenic T cells with an anti-mTCR antibody to obtain

sufficient amounts for *in vivo* experiments. The same amount ($5x10^6$ T cells) of both products and the control was injected into tumor-bearing mice to compare the tumor-control efficiency of both transgenic products. Tumor weight was assessed seventeen days after injection of A673 EwS cells alone (control group, n=3), A673 EwS cells in combination with either unspecific T cells (unspecific group, n=6), CRISPR/Cas9 engineered T cells (CRISPR/Cas9 group, n=6), or retrovirally transduced T cells (retrovirus group, n=6). The mice were sacrificed and analyzed seventeen days after tumor injection. One mouse in the retrovirus group died on day 10.

Before injection to the tumor-bearing mice, we assessed the homogeneity of the engineered T cell products by FACS analysis. The purity of the CRISPR/Cas9 engineered T cell products and retrovirally transduced T cell products were 97.8% and 97.0% respectively (Figure 21,middle and right panel). Engineered T cells products were all CD3 positive (Figure 21, middle and right panel). Non-engineered T cells contained CD3 positive and negative subpopulations (Figure 21 left panel). The higher CD3 purity of the engineered products is due to their enrichment by an anti-mTCR antibody.

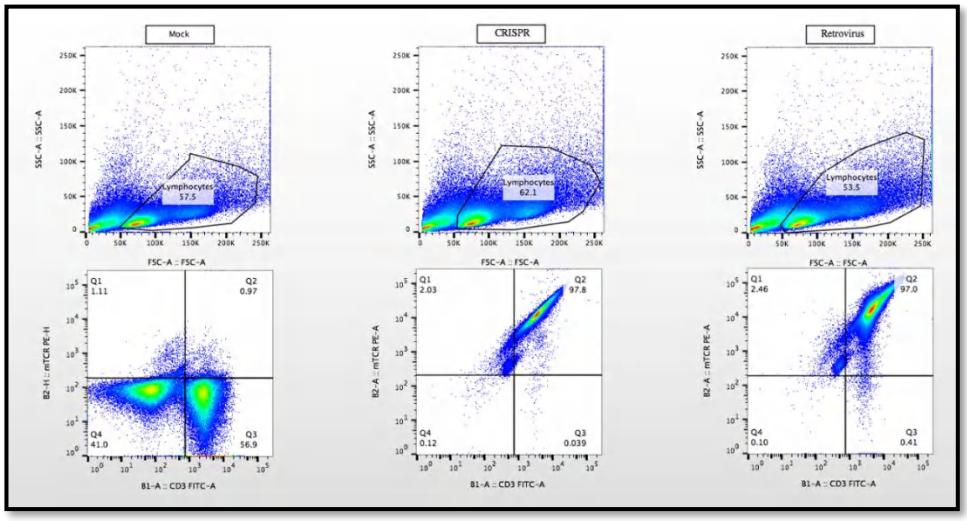

Figure 21. Transgene expression after magnetic beads selection and subsequent expansion* in vitro *at day 27, the first day of* in vivo *experiment.

Sorted and expanded of the non-engineered and transgenic T cells, by either CRISPR/Cas9 (CRISPR) or retroviral transduction after isolation by anti-mTCR antibody. The non-engineered T cells were regarded as Mock.
Cells were stained anti-mTCR (mTCR-PE) and anti-CD3 (CD3-APC) at day 27 of culture, day 4 of the *in vivo* experiment (first day of T cell injection)**.**
T cells were stained with anti-mTCR (mTCR-PE) and anti-CD3 (CD3-FITC).

Last day of the *in vivo* experiments (day 17), we repeated the FACS analysis for further evaluation of the transgenic T cell products as the day before T cell injection (Figrue 22).

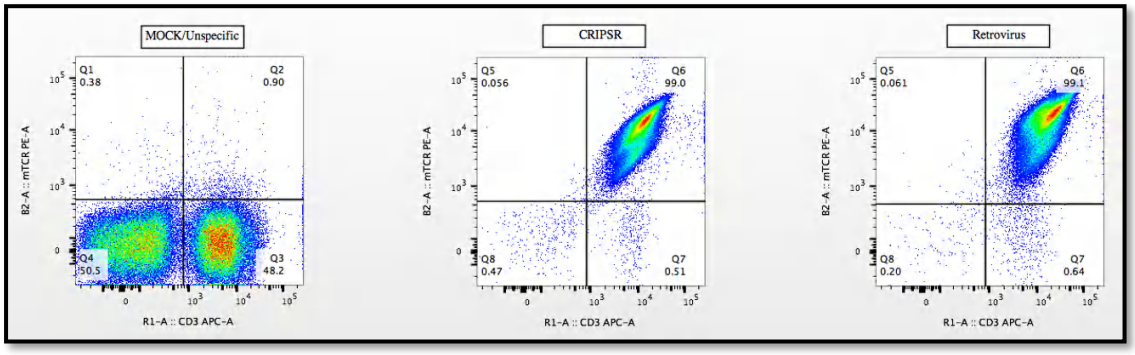

Figure 22. Transgene expression after magnetic beads selection and subsequent expansion* in vitro *at day 54, the last day of* in vivo *experiment.

T cells used as Figure 19 for FACS analysis, but are derived from day 54 of culture (day 17 of in vivo experiments).

To assess tumor control by transgenic T cells, we measured the tumor weight and assessed timuor size after sacrificing the mice. There was a trend to reduction of tumor weight by both transgenic products compared to the non-engineered product (CRISPR/Cas9 p=0.0602, Retrovirus p=0.0152). Of note, no significant difference was observed between the transgenic products and the non-engineered T cells. This lack of difference is probably due to non-specific allo-response activity of the non-engineered cells containing their endogenous HLA TCR, recognizing the tumor HLA- disparate haplotype. Finally, no statistical difference in tumor weight was found between the retroviral and the CRISPR/Cas9 engineered T cells (Figure 23A). Tumor size seemed to be reduced by both engineered products, and somewhat less by non-engineered cells (Figure 23 B). As a note of caution, we would like to explicitly mention that the control group contains here only two mice, because tumor injection in the third mouse failed. However, the tumor size in the two remaining mice was in the range of multiple previous control experiments in our lab (Schirmer et al., 2016; Schober et al., 2020). Transgenic T cells were undetectable in residual tumors (data not shown).

Of note, there was increased cl-PARP generation by transgenic T used for the *in vivo* experiment cells as compared to non-engineered T cells when cultured in parallel *in vitro*. Retroviral T cells induced somewhat more cl-PARP than CRISPR/Cas9 engineered T cells (Figure 23C)

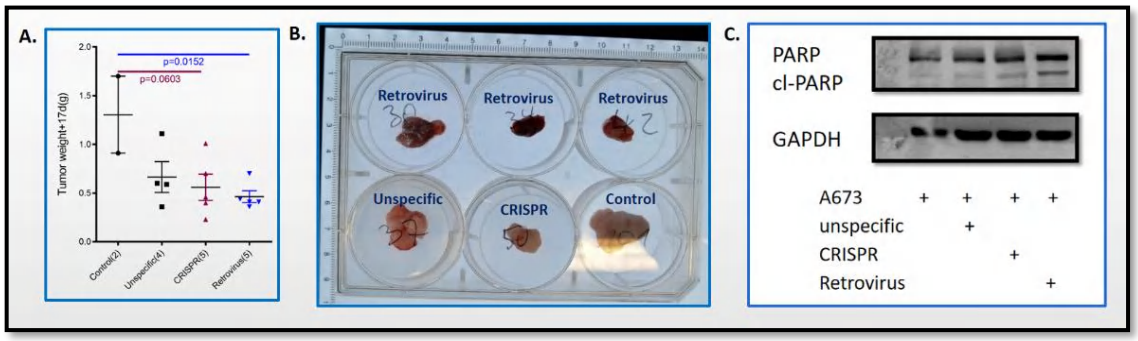

Figure 23.* In Vivo *assessment of effects by transgenic t cells on Tumor volume: Tumor weight and size after T cell therapy in Rag2$^{-/-}\gamma c^{-/-}$ mice.

(A) After injection of $3x10^6$ A673 EwS cells subcutaneously in Rag2-/-γc-/- mice (BALB/c background), four groups were treated with an injection of $5x10^6$ T cells: Group 1 received no T cells (Control); Group 2 received non-engineered T cells (Unspecific); Group 3 received transgenic T cells by orthotopic TCR replacement (CRISPR); Group 4 received T cells by retroviral transduction (Retrovirus).
(B) Representative tumor sizes of each group 17days after tumor injection.
(C) *In vitro* co-culture of A673 with T cells as panel A for 5 hours.

7.2.6 NO REDIRECTION TO OFF-TARGET SITES OF CRISPR/CAS9 ENGINEERED AND NON-ENGINEERED T CELLS IN CONTRAST TO RETROVIRALLY TRANSDUCED T CELLS

Next, we asked whether the marginal significance in reduction of tumor weight was due to the redirection of engineered T cells to off-target sites, i.e. to bone marrow or spleen. To this end, we performed FACS analysis of bone marrow and spleen cells after sacrificing the mice at day 17 after tumor injection. Engineered T cells and non-engineered T cells were detectable at low frequency in both marrow and spleen. There was no significant difference between the transgenic T cell products; however, redirection of retrovirally transduced T cells to the spleen was somewhat more significant than to bone marrow when compared to the control with non-engineered T cells. In contrast, the redirection of CRISPR/Cas9 engineered T cells was not different from non-engineered T cells (Figure 24). Phenotypes were not assessable due to low frequency. These findings may explain at least in part, the limited tumor control by retrovirally transduced T cells but not by CRISPR/Cas9 engineered T cells.

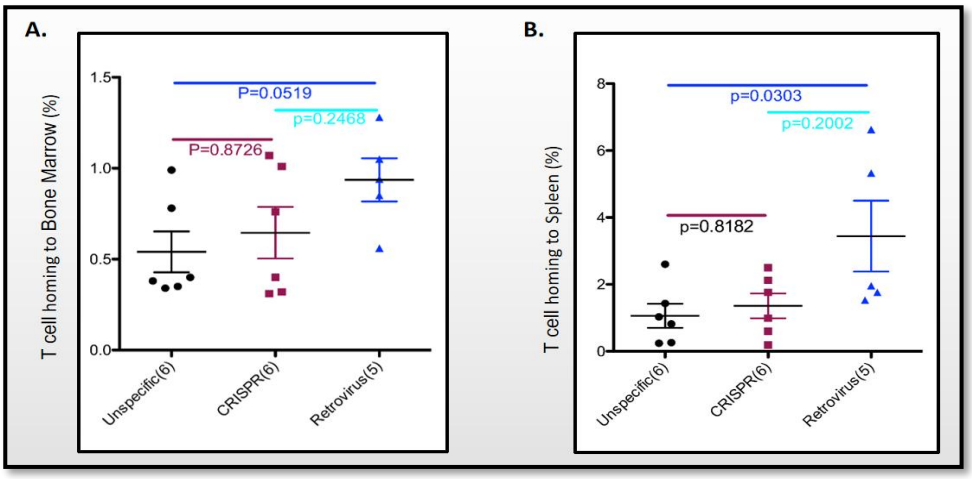

Figure 24.* In Vivo *assessment of T cell homing to bone marrow and spleen after T cell therapy.

(A) T cell homing to bone marrow: Group 1 received non-engineered T cells (Unspecific); Group 2 received transgenic T cells by CRISPR/Cas9 (CRISPR); Group 3 received transgenic T cells by retroviral transduction.
(B) T cell homing to spleen: Group 1 received non-engineered T cells (Unspecific); Group 2 received transgenic T cells by CRISPR/Cas9 (CRISPR); Group 3 received transgenic T cells by retroviral transduction.

7.3 CHM1 AS THE UNIQUE IMMUNOTHERAPY TARGET OF EWS

7.3.1 CHM1 IS A DIRECT TARGET OF EWS-FLI1 SELECTIVELY EXPRESSED IN EWS AND REQUIRED FOR ITS METASTASIS.

As we have previously shown, EWS-FLI1 binds to the (Figure 25) promotor and activates the transcription of CHM1 in EwS. Furthermore, CHM1 sustains the undifferentiated and invasive phenotype of EwS, which promotes lung metastasis of EwS (von Heyking et al., 2017). It is required for metastasis (von Heyking et al., 2017) and serves an EwS-specific antigen (Biele et al., 2021; Blaeschke et al., 2016; Thiel et al., 2017).

We now first analyzed public CHIP-sequence data using the Integrative Genomics View (IGV) browser. CHIP-sequence data confirmed that EWS-FLI1 binds to two promotor sites of CHM1 and induces acetylation of H3K27 (H3K27ac) at both sites, which is associated with the activation of transcription

(Figure 25). Forced expression of EWS-FLI1 in mesenchymal stem cell also enhances H3K27ac at the same sites (Figure 25).

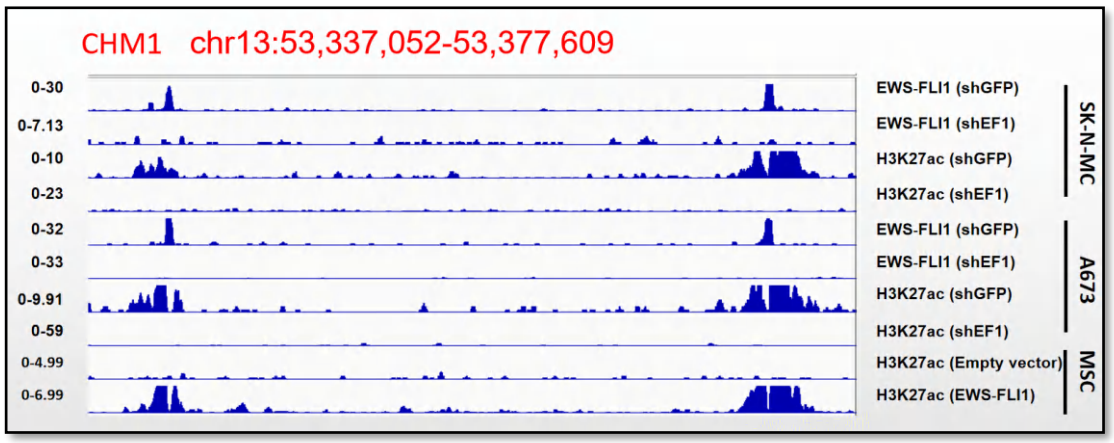

Figure 25. CHIP-sequence analysis revealing CHM1 as a direct target of EWS-FLI1.

Integrative genomics view (hg19) of the CHM1 locus from data of A673, SK-N-MC and mesenchymal stem cell (MSC) cells being transfected with shRNAs targeting either GFP (shGFP; negative control) or EWS-FLI1 (shEF1) or overexpression of EWS-FLI1 in MSC.

We next mined the Cancer Cell Line Encyclopedia (CCLE (Ghandi et al., 2019)). We found CHM1 mRNA is highest expressed in EwS among all tumor cell lines (Figure 26A). Public Gene Expression Omnibus (GEO) database indicates that its expression in EwS tissues is significantly higher than in bone marrow mesenchymal stem cells (Figure 26B). These results are in correspondence to our previous publications (Staege et al., 2004; Thiel, Pirson, et al., 2011; von Heyking et al., 2017). In addition, CHM1 expression does not correlate significantly with recurrence or metastasis (Figure 26C).

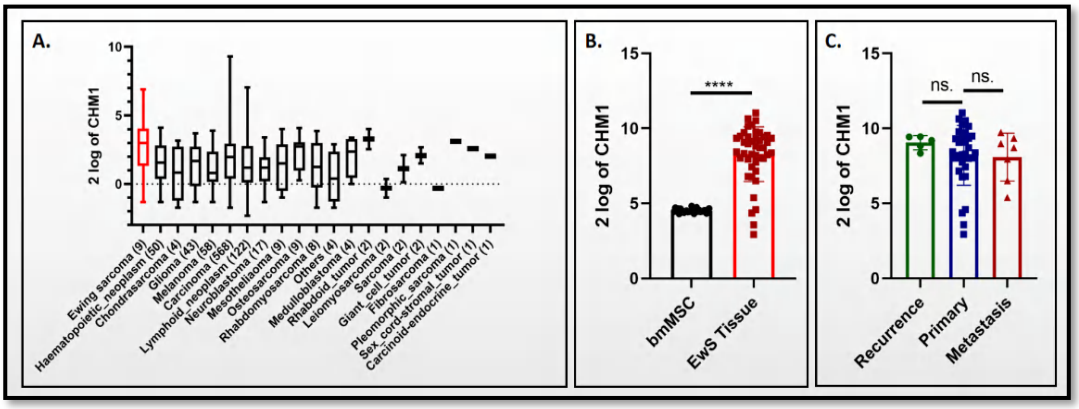

Figure 26. High expression of CHM1 in EwS.

(A) Overexpression of CHM1 in the CCLE database.
(B) High expression of CHM1 in the GEO datasets including normal bone marrow mesenchymal stem cells (GSE 7637) and EwS tissues (GSE 17618).
(C) The correlation of expression level of CHM1 with recurrence and metastasis.
**** means *P*<0.0001.

Finally, we analyzed the expression of CHM1 at the protein level in ProteomicsDB, which is developed by the Chair of Proteomics and Bioanalytics at the Technische Universität München and Cellzome GmbH (Samaras et al., 2020; Schmidt et al., 2018) . We only found a very low expression in vitreous humor, lung, and heart and no expression in other tissues (Figure 27).

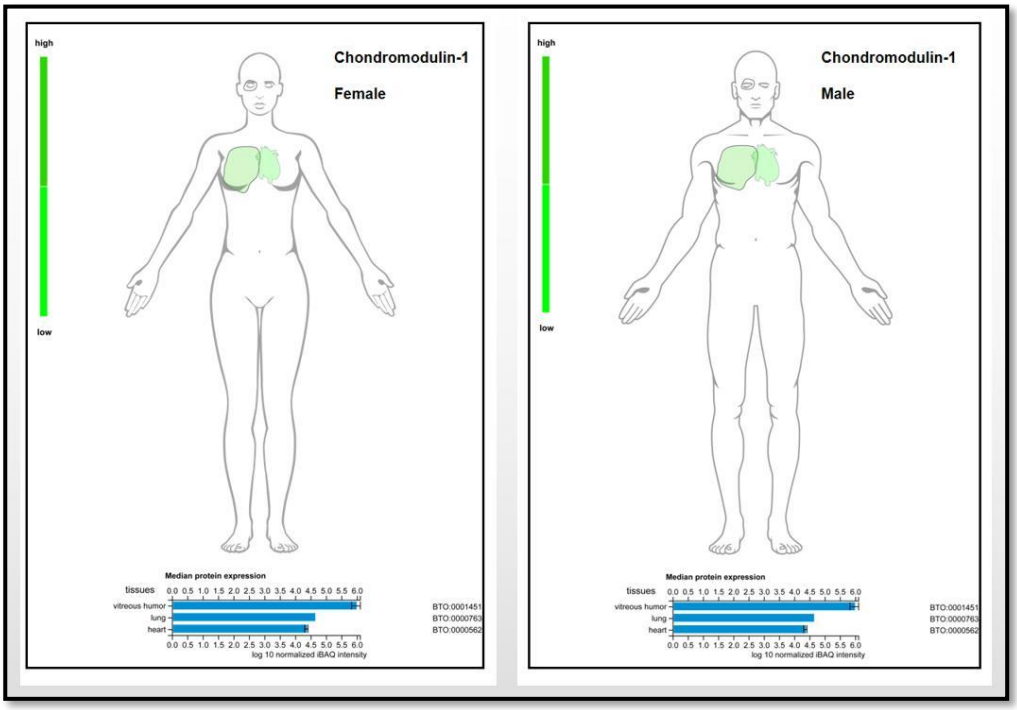

Figure 27. Very low expression of CHM1 protein in human tissue.

ProteomicsDB shows a shallow expression of CHM1 in vitreous humor, lung, and heart. CHM1 is undetectable in other healthy tissues of females (left panel) nor males (right panel).

7.3.2 CHM1 EXPRESSION IS INDUCED BY CHM1 RECOGNIZING TCR TRANSGENIC T CELLS WHILE EWS-FLI1 EXPRESSION FLUCTUATES.

Antigen loss participates in the immune escape after long-term treatment with CAR-T therapy (Majzner & Mackall, 2018), such as CD19 CARs in pediatric B-ALL (Gardner et al., 2016; Sotillo et al., 2015). Our group has a track to identify antigens that are indispensable for the tumor, in particular for its metastatic spread and sought to exclude potential resistance of EwS to CHM1 targeting immunotherapy by antigen loss. We thus analyzed the expression of CHM1 and EWS-FLI1 after co-culture of EwS cells (A673) with CRISPR/Cas9 engineered CHM1 targeting T cells. We found an increased expression of CHM1 (Figure 28 A, B, D, E) in contrast to variable expression of EWS-FLI1 in A673 cells after

co-culture with transgenic T cells with orthotopic TCR replacement targeting CHM1 as compared to non-engineered T cells and other controls (Figure 28 A, C). These data may indicate that CHM1 could serve as a stable therapeutic target in the TCR-based immunotherapy of EwS.

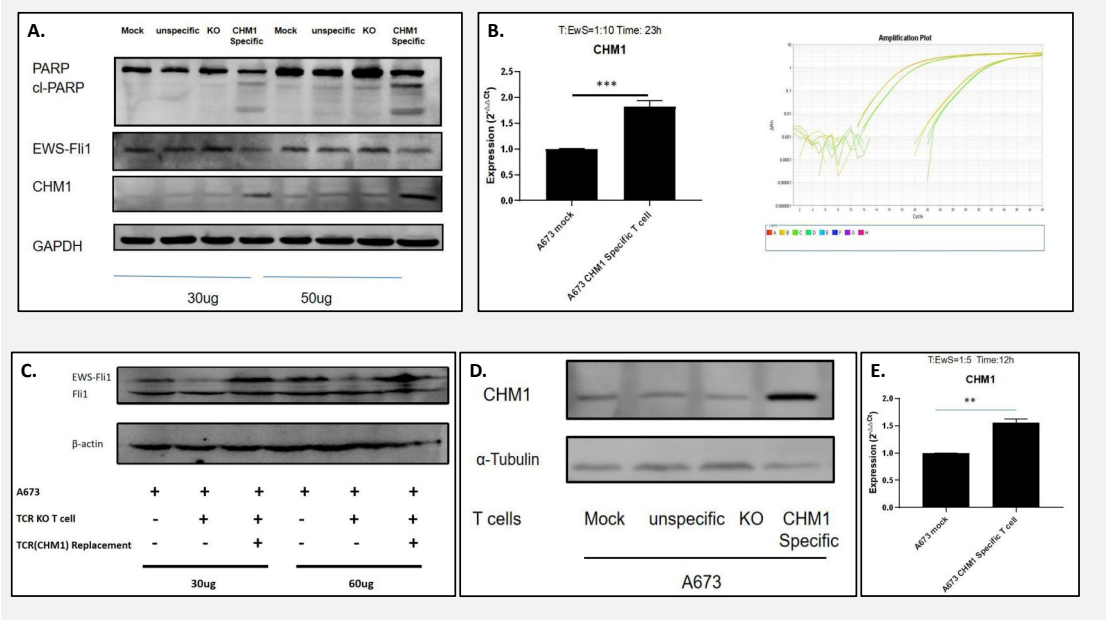

Figure 28. Upregulation of CHM1 after co-culture of A673 with CRISPR/Cas9 engineered CHM1-319 recognizing TCR transgenic T cell.

(A) EWS-FLI1 is downregulated after 23 hours of co-culture of A673 with different group of T cells. However, the expression of CHM1 is increased at the protein level.
(B) Increase of mRNA level of CHM1 after 23 hours co-culture of A673 with CHM1 specific T cells.
(C) EWS-FLI1 is upregulated after 12 hours of co-culture of A673 with different group of T cells.
(D, E) Increase of CHM1 both at the protein and mRNA level after 12 hours of co-culture of A673 with different group of T cells.
Treatment groups including no T cells (Mock), unspecific T cells (mock), T cells with CRISPR/Cas9 engineered TCR KO and replacement, and T cells with CRISPR/Cas9 engineered orthotopic TCR replacement targeting CHM1.
** means $P<0.01$, *** means $P<0.001$.

8 DISCUSSION

8.1 TCR-BASED IMMUNOTHERAPY OF EWING SARCOMA

There is a clear medical need for novel therapies in advanced Ewing sarcoma: High dose therapies with autologous hematopoietic stem-cell rescues has been beneficial only in selected subgroups (Burdach & Jurgens, 2002): AES patients younger than 14 may benefit from treosulfan/melphalan high-dose chemotherapy (TreoMel-HDT) followed by autologous hematopoietic stem-cell transplantation(Koch et al., 2022). Allogeneic hematopoietic stem-cell transplantation from healthy donors has delivered hints for the efficacy of immunotherapy not only in leukemias but also in solid tumors (Copelan, 2006), including advanced Ewing sarcomas (AES) patients (Burdach & Jurgens, 2002; Koch et al., 2022; Thiel et al., 2021). However, no difference in survival with reduced- versus high-intensity conditioning before allo-SCT (Thiel, Wawer, et al., 2011). There is also no difference in survival after HLA mismatched versus HLA matched allo-SCT (Thiel et al., 2021). These findings imply that allogeneic stem cell transplantation is not sufficient for immunotherapy of AES and novel therapeutic strategies are in urgent demand, such as TCR-based immunotherapy (Nicolini et al., 2022). With TCR-based immunotherapy targeting tumor-associated antigens of EwS, such as CHM1 (Blaeschke et al., 2016; Thiel, Pirson, et al., 2011), STEAP1 (Schober et al., 2020) and PAPPA (Kirschner et al., 2017), our group previously achieved efficacious *in vitro* and *in vivo* cytotoxic targeting HLA-A*02:01^{+} EwS. TCR-based immunotherapy even led to partial regression without GvHD in refractory HLA-A2^{+} patients (Thiel et al., 2017).

TCR-based adoptive therapy shows promising anti-sarcoma effects by targeting NY-ESO-1, leading to objective clinical responses (Robbins et al., 2015). More than 600 clinical trials about TCR-based immunotherapy are in processing according to *ClinicalTrials.gov* (*https://clinicaltrials.gov, data accessed on 28.04.2022*).

Retrovirus- and lentivirus-based vectors are commonly used for TCR gene transfer in clinical trials (Manfredi et al., 2020). Both viruses enable stable integration and efficient expression of exogenous TCRs in lymphocytes. However, mispairing of endo- with exogenous TCRs limits the function of the transduced TCR and generates new antigens, which further cause autoreactivity or GvHD (van Loenen et al., 2010). Luckily, there was no the evidence of GvHD in the TCR-based adoptive therapy targeting CHM1 in our treatment trials of EwS, including allogeneic donor lymphocyte infusions (Schober et al., 2019) or allogeneic transgenic T cells (Schober et al., 2019; Thiel et al., 2017). Several strategies, such as murinization of TCR constant regions (Cohen et al., 2006; Sommermeyer & Uckert, 2010), codon optimization(Scholten et al., 2006) and additional cysteine residues (Cohen et al., 2007) have been proposed to prevent mispairing. We used codon optimization and murinization of TCR constant regions. However, these procedures cannot completely eliminate mispairing (Provasi et al., 2012). Random insertion of viruses into the genome also raises safety concerns, such as insertional mutations and tumorigenesis (Howe et al., 2008), albeit tumorigenesis has only been observed after retroviral transfection of hematopoietic stem cells, but not after retroviral transfection of T cells.

8.2 ORTHOTOPIC REPLACEMENT OF TCR WITH CYTOTOXIC FUNCTIONALITY AND PRESERVATION OF A PHYSIOLOGICAL T-CELL PHENOTYPE – THE PROS AND CONS COMPARED TO RETROVIRAL TRANSFER

To address the potential hazards of viral transduction, endogenous TCR KO with simultaneous non-viral orthotopic TCR replacement results in translation of the transduced TCR gene sequence. Activation via the endogenous TCR promoter provides functional results (Eyquem et al., 2017; Muller et al., 2021; Roth et al., 2018; Schober et al., 2019). Non-viral site-specific orthotopic TCR replacement may provide a more physiological T cell function than random

insertion if multiple copies by retroviral transfer.

Our present work showing the feasibility of orthotopic replacement of the endogenous T cell receptor (TCR) with CHM1^{319}-TCR targeting EwS by CRISPR/Cas9 confirms previous publications with different TCRs (Moosmann et al., 2022; Schober et al., 2019). Our CRISPR/Cas9 engineered T cell products demonstrated a strong specific cytotoxic effect towards HLA-A*02:01^{+} EwS cells and preserved a physiological phenotype. Compared to retrovirus transduced T cells, CRISPR/Cas9 prolonged the activity of engineered T cells *in vitro*.

While both engineered products were active in vivo limiting tumor growth, we also observed activity of non-engineered T cells. Their activity may be due to allorecognition of the HLA disparate tumor. The interpretation of this finding is based on the fact that the non-engineered T cells are a heterogenous, i.e. non-specific population retain their endogenous TCRs, rendering them capable of allorecognition. Based on allorecognition these cells carry a great risk of GVHD and are limited value for clinical use. Of note, even TCR KO cells showed some activity in the xCelligence assay as well as marginal cl-PARP induction suggesting non-specific, i.e. TCR independent effects.

Comparing CRISPR/Cas9 with retrovirus transduced T cells, our work indicates that high retroviral transduction efficacy can avoid endogenous TCR expression on the cell membrane, resembling CRISPR/Cas9 engineered T cells. This may indicate that a high efficiency of TCR transduction by the retrovirus is capable to compete with the endogenous TCR to form the heterocomplex with CD3 required for stable TCR membrane expression. This competition may help avoid neo-antigen recognition due to TCR chain mispairing. However, high transduction rates may lead to abundant insertion of vector copy numbers (VCN) (Santeramo et al., 2020). According to the reflection paper on clinical risk management due to insertional mutations from the European Medicines Agency's Committee on Advanced Therapeutics (Aiuti et al., 2013), the risk of

gene-modified cell therapies via insertional oncogenesis should be reduced by restriction of VCN. Also, close-to-random transgene integration via viral transduction further limits the clinical application (Monjezi et al., 2017). In conclusion, there are limitations by both high and low viral transduction rates.

On the other hand, gene editing by CRISPR/Cas9 generates structural defects of the nucleus, chromosomal truncations, micronuclei and chromosome bridges, which initiate a mutational process and cause human congenital disease, even cancer (Cullot et al., 2019; Leibowitz et al., 2021). Rare off-target effects were also identified when using TRAC guide RNA (gRNA) with wild-type Cas9, whereas no off-target effects were detected with the 'enhanced specificity' Cas9 variant eSp.Cas9 (Muller et al., 2021; Slaymaker et al., 2016). We performed our experiments by taking advantage of eSp.Cas9, which potentially avoid off-target, but we did not manage to evaluate the genome-wide editing specificity in the present work. In our work, CRISPR/Cas9 efficacy in thawed T cells is low as compared to fresh cells. For clinical application, we have to ensure the KO both endogenous TCRs. If the KO of β chain fails, there is a possibility of mispairing of the transduced α with the endogenous β chain. The ratio of α to β chain in a single cell would be 2:1, since both transgenic chains are expressed from the α locus.

When we compared the transduction efficacy of both procedures, in retrovirally transduced T cells the amount of transduced TCRs was significantly higher than the endogenous TCR in a single cell, as expected. Thus, the risk of mispairing between exogenous α to endogenous β chains in a single cell would be X:1, with X being >1, depending on the number of transduced gene copies. This implicates, that the risk of inactivation of the therapeutic receptor by mispairing with the endogenous β chain may be higher in CRISPR/Cas9 as compared to retrovirally transduced T cells. In CRISPR/Cas9 transduced T cells, it would be 50% based upon the ratio of α to β chain being 2:1 in a single cell. In retrovirally transduced T cells, the risk of inactivation of the therapeutic depends on the

transduction rate. Assumed that 1,000 gene copies are transduced and given the risk that both exogenous chains may mispair with both endogenous chains the risk would be close to 0.2%. As expected, retrovirally transduced T cells express more TCR on their surface.

8.3 CHALLENGES IN THE *IN VIVO* RECOGNITION AND CYTOTOXICITY OF EWS

Despite the cytotoxic effects targeting HLA-A*02:01^{+}/CHM1^{+} EwS cells *in vitro*, both transgenic T cell products elicited only a partial tumor remission (reduction in tumor size and weight by ≥50%) *in vivo*. Transgenic T cells by retrovirus had slightly better control than T cells engineered by CRISPR/Cas9. This might be due to expression of the alloreactive endogenous TCR which might be essential for the longevity of the response (Stenger et al., 2020). Recent work (Stenger et al., 2020) showed that the endogenous TCR promotes *in vivo* persistence of CD19-CAR-T cells compared to a CRISPR/Cas9-engineered TCR knockout CAR.

Limited *in vivo* tumor control may also be attributed to the induction of an immune suppressive microenvironment (“immune desert”) by EwS (Berghuis et al., 2009; Spurny et al., 2018). We found no T cell infiltration in the tumor. Several causes may contribute to this phenomenon:

1) Regarding “cold tumor” or “immune desert” (Machado et al., 2018; van Erp et al., 2017), HLA class I molecules are essential for antigen presentation. A majority of EwS tissues are characterized by complete or partial absence of HLA class I (Berghuis et al., 2009). In this context, we have previously shown induction of HLA class I on EwS lines by manipulating the environment in vitro (Staege et al., 2003).

2) T cell exhaustion may account for the failure the tumor control *in vivo*. In our hands, a large number of T cells dies after electroporation, especially

CRISPR/Cas9-engineered T cells with orthotopic TCR replacement, probably due to the toxicity of dsDNA. It also requires prolonged culture time to obtain enough T cells for *in vivo* experiments, which might reduce the cytotoxic functionality when targeting the EwS tumor in mice. Meanwhile, retrovirally engineered T cells completely lost the cytotoxic effects on HLA-A*02:01^{+}/CHM1^{+} A673 cells after 54 days, indicating long-time culture *in vitro* leads to the exhaustion of the T cells.

3) A short period of exposure of EwS to the transgenic T cells might be another reason for limited tumor control. We sacrificed the mice two weeks after the injection of T cells for animal protection reasons, which might have limited an adequate response of the tumor to the transgenic T cells. We had to stop the experiment at that time due to excessive tumor volume in the control mice.

Several other limitations were also identified in our work, such as comparatively low transduction efficiency of CRISPR/Cas9, ranging from 10%-45%, due to imponderabilities of cultures or fresh vs. thawed status of the cultured lymphocytes. We could minimize cell death after electroporation especially with TCR KI by directly culturing in Penicillin-Streptomycin (P/S) free T cell medium after electroporation. We think that higher transduction rates with CRISPR/Cas9 engineered TCR KI are possible. While cells with a high transduction rate after electroporation do not tolerate the antibiotics (P/S), an optimization of the protocol could be to culture the cells for 24-48 hours in T cell medium without P/S and change back to standard culture medium afterwards.

Moreover, we excluded redirection to off-target sites of CRISPR/Cas9 engineered and non-engineered T cells whereas retrovirally transduced T cell preferentially were redirected to the spleen and to a lesser degree to bone marrow.

Last not least, we noticed the further induction of CHM1 after co-culture with

CRISPR/Cas9 engineered T cells in addition to its unique high expression in EwS. This counterintuitive finding suggests that the metastatic driver CHM1 is indispensable in EwS and may thus represent an ideal target. In the future, we might take advantage of this surprising finding in the treatment of metastatic disease. At least, the mechanism of CHM1 induction after co-culture with CHM1-TCR engineered T cells warrants further research.

8.4 CONCLUSION AND PERSPECTIVE

In conclusion, T cells engineered with CRISPR/Cas9 to address the metastatic driver CHM1, are feasible for immunotherapy of EwS and may have the advantage of a more physiological T cell phenotype and a more prolonged cytotoxic activity as compared to T cells engineered with retroviral gene transfer. These findings confirm, at least in part our hypothesis. In perspective, these therapeutic cells should be combined with additional approaches to increase the immunogenicity of tumor microenvironment, limit the T cell exhaustion and enhance the T cell contact with their target cells.

9 SUMMARY

Ewing Sarcoma (EwS) is a highly malignant sarcoma of bone and/or soft tissue with early metastatic spread and an age peak in early puberty. The prognosis in advanced stages is still dismal, and the long-term effects of established therapies are severe. Efficacious targeted therapies are urgently needed. Our previous work has provided preliminary safety, and efficacy data of immunotherapy utilizing T cell receptor (TCR) transgenic T cells targeting HLA restricted peptides on the tumor cell membrane derived from metastatic drivers. For these studies, we used retroviral gene transfer. Critics raised concerns about T cells' safety and physiology with random and multiple gene insertions. Thus in this study, we compared T cells engineered with either CRISPR/Cas9 or retroviral gene transfer for immunotherapy of Ewing sarcoma. Firstly, we confirmed the feasibility of orthotopic replacement of the endogenous TCR by CRISPR/Cas9 with a TCR targeting our canonical metastatic driver chondromodulin-1 (CHM1). CRISPR/Cas9 engineered T cell products specifically recognized and killed HLA-A*02:01+ EwS cell lines. Next, we observed a higher efficiency of retroviral transduction compared to CRISPR/Cas9 gene editing. Of note, prevention of endogenous TCR expression was not only achieved by CRISPR/Cas9 mediated knock out of the endogenous TCR chains but also by high retroviral gene transduction efficacy. Nevertheless, CRISPR/Cas9 engineering preserved a physiological T cell phenotype in contrast to retroviral transduction. Finally, both engineered T cell products specifically recognize tumor cells and elicit cytotoxicity in vitro, with CRISPR/Cas9 engineered T cells providing a more prolonged cytotoxic activity. Both T cell products limit *in vivo* tumor growth. Last not least, transgenic T cell products induce an increase in CHM1 expression on the background of high expression of CHM1 driven by EWS-FLI1. This counterintuitive finding suggests that the metastatic driver CHM1 is indispensable in EwS and may thus represent an ideal target. In conclusion, T cells engineered with CRISPR/Cas9

are feasible for immunotherapy of Ewing sarcoma and may have the advantage of a more physiological T cell phenotype and a more prolonged cytotoxic activity as compared to T cells engineered with retroviral gene transfer.

10 SUPPLEMENTARY

SUPPLEMENTARY TABLE 1: 5×SDS LOADING BUFFER

Reagent	Quantity (for 50 mL)	Final concentration
Tris-HCl (1 M, pH 6.8)	12.5 mL	250 mM
SDS (electrophoresis grade)	4 g	8%
Bromophenol blue	50 mg	0.1%
Glycerol (100%, v/v)	15 mL	30% (v/v)

SUPPLEMENTARY TABLE 2: DNA SEQUENCE OF KNOCK-IN CHM1^{319}-TCR

LHA	CTGCCTTTACTCTGCCAGAGTTATATTGCTGGGGTTTTGAAGAAGATCCTATTAA ATAAAAGAATAAGCAGTATTATTAAGTAGCCCTGCATTTCAGGTTTCCTTGAGT GGCAGGCCAGGCCTGGCCGTGAACGTTCACTGAAATCATGGCCTCTTGGCCA AGATTGATAGCTTGTGCCTGTCCCTGAGTCCCAGTCCATCACGAGCAGCTGGTT TCTAAGATGCTATTTCCCGTATAAAGCATGAGACCGTGACTTGCCAGCCCCACA GAGCCCCGCCCTTGTCCATCACTGGCATCTGGACTCCAGCCTGGGTTGGGGCA AAGAGGGAAATGAGATCATGTCCTAACCCTGATCCTCTTGTCCCACAGATATCC AGAACCCTGACCCTGCCGTG
P2A	GGCAGCGGCGCCACCAACTTCAGCCTGCTGAAGCAGGCCGGCGACGTGG AAGAGAACCCCGGGCCC
VDJβ	ATGCTGTCTCCAGATCTGCCTGACAGCGCCTGGAACACCCGGCTGCTGTGC AGAGTGATGCTGTGCCTGCTGGGAGCCGGATCTGTGGCTGCTGGCGTGAT CCAGAGCCCCAGACACCTGATCAAAGAGAAGAGAGAGACAGCCACCCTG AAGTGCTACCCCATCCCCAGGCACGACACCGTGTACTGGTATCAGCAGGG CCCAGGCCAGGACCCCCAGTTCCTGATCAGCTTCTACGAGAAGATGCAGA GCGAC
TRBC with additional cysteine bridges	AAGGGCAGCATCCCCGACAGATTCAGCGCCCAGCAGTTCAGCGACTACCA CAGCGAGCTGAACATGAGCAGCCTGGAACTGGGCGACAGCGCCCTGTAC TTCTGCGCCTCTAGCTTCCTGGGCGAGAAAACCGAGGCATTCTTTGGGCA GGGCACCAGACTGACCGTGGTGGAGGATCTGAGAAATGTGACTCCACCC AAGGTCTCCTTGTTTGAGCCATCAAAAGCAGAGATTGCAAACAAACAAAA GGCTACCCTCGTGTGCTTGGCCAGGGGCTTCTTCCCTGACCACGTGGAGC TGAGCTGGTGGGTGAATGGCAAGGAGGTCCACAGTGGGGTCTGCACGGA CCCTCAGGCCTACAAGGAGAGCAATTATAGCTACTGCCTGAGCAGCCGCCT GAGGGTCTCTGCTACCTTCTGGCACAATCCTCGAAACCACTTCCGCTGCCA AGTGCAGTTCCATGGGCTTTCAGAGGAGGACAAGTGGCCAGAGGGCTCA CCCAAACCTGTCACACAGAACATCAGTGCAGAGGCCTGGGGCCGAGCAG ACTGTGGAATCACTTCAGCATCCTATCATCAGGGGGTTCTGTCTGCAACCAT CCTCTATGAGATCCTACTGGGGAAGGCCACCCTATATGCTGTGCTGGTCAG TGGCCTGGTGCTGATGGCCATGGTCAAGAAAAAAAATTCC

T2A	GGCAGCGGCGAGGGCAGAGGAAGTCTGCTAACATGCGGTGACGTCGAG GAGAATCCTGGACCT
VJα	ATGACCAGCATCCGGGCCGTGTTCATCTTCCTGTGGCTGCAGCTGGACCTC GTGAACGGCGAGAACGTGGAACAGCACCCCAGCACCCTGAGCGTGCAGG AAGGCGATAGCGCCGTGATCAAGTGCACCTACAGCGACTCCGCCAGCAAC TACTTCCCCTGGTACAAGCAGGAACTGGGAAAGCGGCCCCAGCTGATCAT CGACATCCGGTCCAACGTGGGAGAGAAGAAGGACCAGCGGATCGCCGTG ACCCTG
TRAC with additional cysteine bridges	AACAAGACCGCCAAGCACTTCTCCCTGCACATCACCGAGACACAGCCCGA GGACTCCGCCGTGTACTTTTGTGCCGCTTCTGCCGGCGGATCCCAGGGCA ATCTGATCTTCGGCAAGGGCACCAAGCTGAGCGTGAAGCCCAACATCCAG AACCCAGAACCTGCTGTGTACCAGTTAAAAGATCCTCGGTCTCAGGACAG CACCCTCTGCCTGTTCACCGACTTTGACTCCCAAATCAATGTGCCGAAAAC CATGGAATCTGGAACGTTCATCACTGACAAATGCGTGCTGGACATGAAAGC TATGGATTCCAAGAGCAATGGGGCCATTGCCTGGAGCAACCAGACAAGCT TCACCTGCCAAGATATCTTCAAAGAGACCAACGCCACCTACCCCAGTTCAG ACGTTCCCTGTGATGCCACGTTGACTGAGAAAAGCTTTGAAACAGATATGA ACCTAAACTTTCAAAACCTGTCAGTTATGGGACTCCGAATCCTCCTGCTGA AAGTAGCCGGATTTAACCTGCTCATGACGCTGAGGCTGTGGTCCAGT
Stop	TGA
Poly A	CTAGAGCTCGCTGATCAGCCTCGACTGTGCCTTCTAGTTGCCAGCCATCTG TTGTTTGCCCCTCCCCCGTGCCTTCCTTGACCCTGGAAGGTGCCACTCCCA CTGTCCTTTCCTAATAAAATGAGGAAATTGCATCGCATTGTCTGAGTAGGTG TCATTCTATTCTGGGGGGTGGGGTGGGGCAGGACAGCAAGGGGGAGGAT TGGGAAGAGAATAGCAGGCATGCTGGGGA
RHA	TACCAGCTGAGAGACTCTAAATCCAGTGACAAGTCTGTCTGCCTATTCACC GATTTTGATTCTCAAACAAATGTGTCACAAAGTAAGGATTCTGATGTGTATA TCACAGACAAAACTGTGCTAGACATGAGGTCTATGGACTTCAAGAGCAAC AGTGCTGTGGCCTGGAGCAACAAATCTGACTTTGCATGTGCAAACGCCTTC AACAACAGCATTATTCCAGAAGACACCTTCTTCCCCAGCCCAGGTAAGGG CAGCTTTGGTGCCTTCGCAGGCTGTTTCCTTGCTTCAGGAATGGCCAGGTT CTGCCCAGAGCTCTGGTCAATGATG

SUPPLEMENTARY TABLE 3: PRIMER FOR PCR OF KI FRAGMENT

Primer hTRAC forward	CTGCCTTTACTCTGCCAGAG
Primer hTRAC reverse	CATCATTGACCAGAGCTCTG

11 REFERENCES

Abaan, O. D., Levenson, A., Khan, O., Furth, P. A., Uren, A., & Toretsky, J. A. (2005, Apr 14). PTPL1 is a direct transcriptional target of EWS-FLI1 and modulates Ewing's Sarcoma tumorigenesis. *Oncogene, 24*(16), 2715-2722. https://doi.org/10.1038/sj.onc.1208247

Acuto, O., & Reinherz, E. L. (1985, Apr 25). The human T-cell receptor. Structure and function. *N Engl J Med, 312*(17), 1100-1111. https://doi.org/10.1056/NEJM198504253121706

Agra, N., Cidre, F., Garcia-Garcia, L., de la Parra, J., & Alonso, J. (2013). Lysyl oxidase is downregulated by the EWS/FLI1 oncoprotein and its propeptide domain displays tumor supressor activities in Ewing sarcoma cells. *PLoS One, 8*(6), e66281. https://doi.org/10.1371/journal.pone.0066281

Ahmed, N. S., Harrell, L. M., Wieland, D. R., Lay, M. A., Thompson, V. F., & Schwartz, J. C. (2021, May 25). Fusion protein EWS-FLI1 is incorporated into a protein granule in cells. *RNA*. https://doi.org/10.1261/rna.078827.121

Aiuti, A., Cossu, G., de Felipe, P., Galli, M. C., Narayanan, G., Renner, M., Stahlbom, A., Schneider, C. K., & Voltz-Girolt, C. (2013, Jun). The committee for advanced therapies' of the European Medicines Agency reflection paper on management of clinical risks deriving from insertional mutagenesis. *Hum Gene Ther Clin Dev, 24*(2), 47-54. https://doi.org/10.1089/humc.2013.119

Ambros, I. M., Ambros, P. F., Strehl, S., Kovar, H., Gadner, H., & Salzer-Kuntschik, M. (1991, Apr 1). MIC2 is a specific marker for Ewing's sarcoma and peripheral primitive neuroectodermal tumors. Evidence for a common histogenesis of Ewing's sarcoma and peripheral primitive neuroectodermal tumors from MIC2 expression and specific chromosome aberration. *Cancer, 67*(7), 1886-1893. https://doi.org/10.1002/1097-0142(19910401)67:7<1886::aid-cncr2820670712>3.0.co;2-u

Anderton, J., Moroz, V., Marec-Berard, P., Gaspar, N., Laurence, V., Martin-Broto, J., Sastre, A., Gelderblom, H., Owens, C., Kaiser, S., Fernandez-Pinto, M., Fenwick, N., Evans, A., Strauss, S., Whelan, J., Wheatley, K., & Brennan, B. (2020, Jan 17). International randomised controlled trial for the treatment of newly diagnosed EWING sarcoma family of tumours - EURO EWING 2012 Protocol. *Trials, 21*(1), 96. https://doi.org/10.1186/s13063-019-4026-8

Bacci, G., Ferrari, S., Longhi, A., Rimondini, S., Versari, M., Zanone, A., & Forni, C. (1999, Jul-Aug). Prognostic significance of serum LDH in Ewing's sarcoma of bone. *Oncol Rep, 6*(4), 807-811. https://doi.org/10.3892/or.6.4.807

Bacci, G., Forni, C., Longhi, A., Ferrari, S., Donati, D., De Paolis, M., Barbieri, E., Pignotti, E., Rosito, P., & Versari, M. (2004, Jan). Long-term outcome for patients with non-metastatic Ewing's sarcoma treated with adjuvant and neoadjuvant chemotherapies. 402 patients treated at Rizzoli between 1972 and 1992. *Eur J Cancer, 40*(1), 73-83. https://doi.org/10.1016/j.ejca.2003.08.022

Baird, J. H., Frank, M. J., Craig, J., Patel, S., Spiegel, J. Y., Sahaf, B., Oak, J. S., Younes, S. F., Ozawa, M. G., Yang, E., Natkunam, Y., Tamaresis, J., Ehlinger, Z., Reynolds, W. D., Arai, S., Johnston, L., Lowsky, R., Meyer, E., Negrin, R. S., Rezvani, A. R., Shiraz, P., Sidana, S., Weng, W. K., Davis, K. L., Ramakrishna, S., Schultz, L., Mullins, C., Jacob, A., Kirsch, I., Feldman, S. A., Mackall, C. L., Miklos, D. B., & Muffly, L. (2021, Apr 29). CD22-directed CAR T-cell therapy induces complete remissions in CD19-directed CAR-refractory large B-cell lymphoma. *Blood, 137*(17), 2321-2325. https://doi.org/10.1182/blood.2020009432

Beauchamp, E., Bulut, G., Abaan, O., Chen, K., Merchant, A., Matsui, W., Endo, Y., Rubin, J. S., Toretsky,

J., & Uren, A. (2009, Apr 3). GLI1 is a direct transcriptional target of EWS-FLI1 oncoprotein. *J Biol Chem, 284*(14), 9074-9082. https://doi.org/10.1074/jbc.M806233200

Bendle, G. M., Linnemann, C., Hooijkaas, A. I., Bies, L., de Witte, M. A., Jorritsma, A., Kaiser, A. D., Pouw, N., Debets, R., Kieback, E., Uckert, W., Song, J. Y., Haanen, J. B., & Schumacher, T. N. (2010, May). Lethal graft-versus-host disease in mouse models of T cell receptor gene therapy. *Nat Med, 16*(5), 565-570, 561p following 570. https://doi.org/10.1038/nm.2128

Berghuis, D., de Hooge, A. S., Santos, S. J., Horst, D., Wiertz, E. J., van Eggermond, M. C., van den Elsen, P. J., Taminiau, A. H., Ottaviano, L., Schaefer, K. L., Dirksen, U., Hooijberg, E., Mulder, A., Melief, C. J., Egeler, R. M., Schilham, M. W., Jordanova, E. S., Hogendoorn, P. C., & Lankester, A. C. (2009, Jun). Reduced human leukocyte antigen expression in advanced-stage Ewing sarcoma: implications for immune recognition. *J Pathol, 218*(2), 222-231. https://doi.org/10.1002/path.2537

Bernstein, M., Kovar, H., Paulussen, M., Randall, R. L., Schuck, A., Teot, L. A., & Juergens, H. (2006, May). Ewing's sarcoma family of tumors: current management. *Oncologist, 11*(5), 503-519. https://doi.org/10.1634/theoncologist.11-5-503

Biele, E., Schober, S. J., Prexler, C., Thiede, M., Heyking, K. V., Gassmann, H., Eck, J., Xue, B., Burdach, S., & Thiel, U. (2021, Nov 8). Monocyte Maturation Mediators Upregulate CD83, ICAM-1 and MHC Class 1 Expression on Ewing's Sarcoma, Enhancing T Cell Cytotoxicity. *Cells, 10*(11). https://doi.org/10.3390/cells10113070

Bilke, S., Schwentner, R., Yang, F., Kauer, M., Jug, G., Walker, R. L., Davis, S., Zhu, Y. J., Pineda, M., Meltzer, P. S., & Kovar, H. (2013, Nov). Oncogenic ETS fusions deregulate E2F3 target genes in Ewing sarcoma and prostate cancer. *Genome Res, 23*(11), 1797-1809. https://doi.org/10.1101/gr.151340.112

Biswas, B., Shukla, N. K., Deo, S. V., Agarwala, S., Sharma, D. N., Vishnubhatla, S., & Bakhshi, S. (2014, Nov). Evaluation of outcome and prognostic factors in extraosseous Ewing sarcoma. *Pediatr Blood Cancer, 61*(11), 1925-1931. https://doi.org/10.1002/pbc.25095

Blaeschke, F., Thiel, U., Kirschner, A., Thiede, M., Rubio, R. A., Schirmer, D., Kirchner, T., Richter, G. H. S., Mall, S., Klar, R., Riddell, S., Busch, D. H., Krackhardt, A., Grunewald, T. G., & Burdach, S. (2016, Jul 12). Human HLA-A*02:01/CHM1+ allo-restricted T cell receptor transgenic CD8+ T cells specifically inhibit Ewing sarcoma growth in vitro and in vivo. *Oncotarget, 7*(28), 43267-43280. https://doi.org/10.18632/oncotarget.9218

Boro, A., Pretre, K., Rechfeld, F., Thalhammer, V., Oesch, S., Wachtel, M., Schafer, B. W., & Niggli, F. K. (2012, Nov 1). Small-molecule screen identifies modulators of EWS/FLI1 target gene expression and cell survival in Ewing's sarcoma. *Int J Cancer, 131*(9), 2153-2164. https://doi.org/10.1002/ijc.27472

Boulay, G., Sandoval, G. J., Riggi, N., Iyer, S., Buisson, R., Naigles, B., Awad, M. E., Rengarajan, S., Volorio, A., McBride, M. J., Broye, L. C., Zou, L., Stamenkovic, I., Kadoch, C., & Rivera, M. N. (2017, Sep 21). Cancer-Specific Retargeting of BAF Complexes by a Prion-like Domain. *Cell, 171*(1), 163-178 e119. https://doi.org/10.1016/j.cell.2017.07.036

Buchholz, V. R., Flossdorf, M., Hensel, I., Kretschmer, L., Weissbrich, B., Graf, P., Verschoor, A., Schiemann, M., Hofer, T., & Busch, D. H. (2013, May 3). Disparate individual fates compose robust CD8+ T cell immunity. *Science, 340*(6132), 630-635. https://doi.org/10.1126/science.1235454

Burchill, S. A. (2003, Feb). Ewing's sarcoma: diagnostic, prognostic, and therapeutic implications of molecular abnormalities. *J Clin Pathol, 56*(2), 96-102. https://doi.org/10.1136/jcp.56.2.96

Burdach, S. (2004, Jun). Treatment of advanced Ewing tumors by combined radiochemotherapy and engineered cellular transplants. *Pediatr Transplant, 8 Suppl 5*, 67-82. https://doi.org/10.1111/j.1398-2265.2004.00186.x

Burdach, S., & Jurgens, H. (2002, Feb). High-dose chemoradiotherapy (HDC) in the Ewing family of tumors (EFT). *Crit Rev Oncol Hematol, 41*(2), 169-189. https://doi.org/10.1016/s1040-8428(01)00154-8

Burdach, S., Jurgens, H., Peters, C., Nurnberger, W., Mauz-Korholz, C., Korholz, D., Paulussen, M., Pape, H., Dilloo, D., Koscielniak, E., & et al. (1993, Aug). Myeloablative radiochemotherapy and hematopoietic stem-cell rescue in poor-prognosis Ewing's sarcoma. *J Clin Oncol, 11*(8), 1482-1488. https://doi.org/10.1200/JCO.1993.11.8.1482

Burdach, S., & Kolb, H. J. (2013). The vigor of defense against non-self: potential superiority of allorestricted T cells in immunotherapy of cancer? *Front Oncol, 3*, 100. https://doi.org/10.3389/fonc.2013.00100

Burdach, S., Meyer-Bahlburg, A., Laws, H. J., Haase, R., van Kaik, B., Metzner, B., Wawer, A., Finke, R., Gobel, U., Haerting, J., Pape, H., Gadner, H., Dunst, J., & Juergens, H. (2003, Aug 15). High-dose therapy for patients with primary multifocal and early relapsed Ewing's tumors: results of two consecutive regimens assessing the role of total-body irradiation. *J Clin Oncol, 21*(16), 3072-3078. https://doi.org/10.1200/JCO.2003.12.039

Burdach, S., Thiel, U., Schoniger, M., Haase, R., Wawer, A., Nathrath, M., Kabisch, H., Urban, C., Laws, H. J., Dirksen, U., Steinborn, M., Dunst, J., Jurgens, H., & Meta, E. S. G. (2010, Mar). Total body MRI-governed involved compartment irradiation combined with high-dose chemotherapy and stem cell rescue improves long-term survival in Ewing tumor patients with multiple primary bone metastases. *Bone Marrow Transplant, 45*(3), 483-489. https://doi.org/10.1038/bmt.2009.184

Burdach, S., van Kaick, B., Laws, H. J., Ahrens, S., Haase, R., Korholz, D., Pape, H., Dunst, J., Kahn, T., Willers, R., Engel, B., Dirksen, U., Kramm, C., Nurnberger, W., Heyll, A., Ladenstein, R., Gadner, H., Jurgens, H., & Go el, U. (2000, Nov). Allogeneic and autologous stem-cell transplantation in advanced Ewing tumors. An update after long-term follow-up from two centers of the European Intergroup study EICESS. Stem-Cell Transplant Programs at Dusseldorf University Medical Center, Germany and St. Anna Kinderspital, Vienna, Austria. *Ann Oncol, 11*(11), 1451-1462. https://doi.org/10.1023/a:1026539908115

Castillero-Trejo, Y., Eliazer, S., Xiang, L., Richardson, J. A., & Ilaria, R. L., Jr. (2005, Oct 1). Expression of the EWS/FLI-1 oncogene in murine primary bone-derived cells Results in EWS/FLI-1-dependent, ewing sarcoma-like tumors. *Cancer Res, 65*(19), 8698-8705. https://doi.org/10.1158/0008-5472.CAN-05-1704

Challita-Eid, P. M., Morrison, K., Etessami, S., An, Z., Morrison, K. J., Perez-Villar, J. J., Raitano, A. B., Jia, X. C., Gudas, J. M., Kanner, S. B., & Jakobovits, A. (2007, Jun 15). Monoclonal antibodies to six-transmembrane epithelial antigen of the prostate-1 inhibit intercellular communication in vitro and growth of human tumor xenografts in vivo. *Cancer Res, 67*(12), 5798-5805. https://doi.org/10.1158/0008-5472.CAN-06-3849

Chandran, S. S., & Klebanoff, C. A. (2019, Jul). T cell receptor-based cancer immunotherapy: Emerging efficacy and pathways of resistance. *Immunol Rev, 290*(1), 127-147. https://doi.org/10.1111/imr.12772

Charville, G. W., Wang, W. L., Ingram, D. R., Roy, A., Thomas, D., Patel, R. M., Hornick, J. L., van de Rijn,

M., & Lazar, A. J. (2017, Sep). EWSR1 fusion proteins mediate PAX7 expression in Ewing sarcoma. *Mod Pathol, 30*(9), 1312-1320. https://doi.org/10.1038/modpathol.2017.49

Cheng, L., Xu, Y., Song, H., Huang, H., & Zhuo, D. (2020, Nov 11). A rare entity of Primary Ewing sarcoma in kidney. *BMC Surg, 20*(1), 280. https://doi.org/10.1186/s12893-020-00948-9

Choy, E., Butrynski, J. E., Harmon, D. C., Morgan, J. A., George, S., Wagner, A. J., D'Adamo, D., Cote, G. M., Flamand, Y., Benes, C. H., Haber, D. A., Baselga, J. M., & Demetri, G. D. (2014, Nov 5). Phase II study of olaparib in patients with refractory Ewing sarcoma following failure of standard chemotherapy. *BMC Cancer, 14*, 813. https://doi.org/10.1186/1471-2407-14-813

Cieri, N., Mastaglio, S., Oliveira, G., Casucci, M., Bondanza, A., & Bonini, C. (2014, Jan). Adoptive immunotherapy with genetically modified lymphocytes in allogeneic stem cell transplantation. *Immunol Rev, 257*(1), 165-180. https://doi.org/10.1111/imr.12130

Cironi, L., Riggi, N., Provero, P., Wolf, N., Suva, M. L., Suva, D., Kindler, V., & Stamenkovic, I. (2008, Jul 9). IGF1 is a common target gene of Ewing's sarcoma fusion proteins in mesenchymal progenitor cells. *PLoS One, 3*(7), e2634. https://doi.org/10.1371/journal.pone.0002634

Clapier, C. R., & Cairns, B. R. (2009). The biology of chromatin remodeling complexes. *Annu Rev Biochem, 78*, 273-304. https://doi.org/10.1146/annurev.biochem.77.062706.153223

Cohen, C. J., Li, Y. F., El-Gamil, M., Robbins, P. F., Rosenberg, S. A., & Morgan, R. A. (2007, Apr 15). Enhanced antitumor activity of T cells engineered to express T-cell receptors with a second disulfide bond. *Cancer Res, 67*(8), 3898-3903. https://doi.org/10.1158/0008-5472.CAN-06-3986

Cohen, C. J., Zhao, Y., Zheng, Z., Rosenberg, S. A., & Morgan, R. A. (2006, Sep 1). Enhanced antitumor activity of murine-human hybrid T-cell receptor (TCR) in human lymphocytes is associated with improved pairing and TCR/CD3 stability. *Cancer Res, 66*(17), 8878-8886. https://doi.org/10.1158/0008-5472.CAN-06-1450

Copelan, E. A. (2006, Apr 27). Hematopoietic stem-cell transplantation. *N Engl J Med, 354*(17), 1813-1826. https://doi.org/10.1056/NEJMra052638

Cotterill, S. J., Ahrens, S., Paulussen, M., Jurgens, H. F., Voute, P. A., Gadner, H., & Craft, A. W. (2000, Sep). Prognostic factors in Ewing's tumor of bone: analysis of 975 patients from the European Intergroup Cooperative Ewing's Sarcoma Study Group. *J Clin Oncol, 18*(17), 3108-3114. https://doi.org/10.1200/JCO.2000.18.17.3108

Coulie, P. G., Karanikas, V., Colau, D., Lurquin, C., Landry, C., Marchand, M., Dorval, T., Brichard, V., & Boon, T. (2001, Aug 28). A monoclonal cytolytic T-lymphocyte response observed in a melanoma patient vaccinated with a tumor-specific antigenic peptide encoded by gene MAGE-3. *Proc Natl Acad Sci U S A, 98*(18), 10290-10295. https://doi.org/10.1073/pnas.161260098

Cullot, G., Boutin, J., Toutain, J., Prat, F., Pennamen, P., Rooryck, C., Teichmann, M., Rousseau, E., Lamrissi-Garcia, I., Guyonnet-Duperat, V., Bibeyran, A., Lalanne, M., Prouzet-Mauleon, V., Turcq, B., Ged, C., Blouin, J. M., Richard, E., Dabernat, S., Moreau-Gaudry, F., & Bedel, A. (2019, Mar 8). CRISPR-Cas9 genome editing induces megabase-scale chromosomal truncations. *Nat Commun, 10*(1), 1136. https://doi.org/10.1038/s41467-019-09006-2

Dafni, U., Michielin, O., Lluesma, S. M., Tsourti, Z., Polydoropoulou, V., Karlis, D., Besser, M. J., Haanen, J., Svane, I. M., Ohashi, P. S., Kammula, U. S., Orcurto, A., Zimmermann, S., Trueb, L., Klebanoff, C. A., Lotze, M. T., Kandalaft, L. E., & Coukos, G. (2019, Dec 1). Efficacy of adoptive therapy with tumor-infiltrating lymphocytes and recombinant interleukin-2 in advanced cutaneous

melanoma: a systematic review and meta-analysis. *Ann Oncol, 30*(12), 1902-1913. https://doi.org/10.1093/annonc/mdz398

Davis, M. M., & Bjorkman, P. J. (1988, Aug 4). T-cell antigen receptor genes and T-cell recognition. *Nature, 334*(6181), 395-402. https://doi.org/10.1038/334395a0

Delattre, O., Zucman, J., Plougastel, B., Desmaze, C., Melot, T., Peter, M., Kovar, H., Joubert, I., de Jong, P., Rouleau, G., & et al. (1992, Sep 10). Gene fusion with an ETS DNA-binding domain caused by chromosome translocation in human tumours. *Nature, 359*(6391), 162-165. https://doi.org/10.1038/359162a0

Deneen, B., & Denny, C. T. (2001, Oct 11). Loss of p16 pathways stabilizes EWS/FLI1 expression and complements EWS/FLI1 mediated transformation. *Oncogene, 20*(46), 6731-6741. https://doi.org/10.1038/sj.onc.1204875

Dierick, A. M., Roels, H., & Langlois, M. (1993, Feb). The immunophenotype of Ewing's sarcoma. An immunohistochemical analysis. *Pathol Res Pract, 189*(1), 26-32. https://doi.org/10.1016/S0344-0338(11)80113-5

Dylla, L., Moore, C., & Jedlicka, P. (2013). MicroRNAs in Ewing Sarcoma. *Front Oncol, 3*, 65. https://doi.org/10.3389/fonc.2013.00065

Effern, M., Glodde, N., Braun, M., Liebing, J., Boll, H. N., Yong, M., Bawden, E., Hinze, D., van den Boorn-Konijnenberg, D., Daoud, M., Aymans, P., Landsberg, J., Smyth, M. J., Flatz, L., Tuting, T., Bald, T., Gebhardt, T., & Holzel, M. (2020, Sep 15). Adoptive T Cell Therapy Targeting Different Gene Products Reveals Diverse and Context-Dependent Immune Evasion in Melanoma. *Immunity, 53*(3), 564-580 e569. https://doi.org/10.1016/j.immuni.2020.07.007

Erkizan, H. V., Kong, Y., Merchant, M., Schlottmann, S., Barber-Rotenberg, J. S., Yuan, L., Abaan, O. D., Chou, T. H., Dakshanamurthy, S., Brown, M. L., Uren, A., & Toretsky, J. A. (2009, Jul). A small molecule blocking oncogenic protein EWS-FLI1 interaction with RNA helicase A inhibits growth of Ewing's sarcoma. *Nat Med, 15*(7), 750-756. https://doi.org/10.1038/nm.1983

Erkizan, H. V., Uversky, V. N., & Toretsky, J. A. (2010, Aug 15). Oncogenic partnerships: EWS-FLI1 protein interactions initiate key pathways of Ewing's sarcoma. *Clin Cancer Res, 16*(16), 4077-4083. https://doi.org/10.1158/1078-0432.CCR-09-2261

Ewing, J. (1972, Mar-Apr). Classics in oncology. Diffuse endothelioma of bone. James Ewing. Proceedings of the New York Pathological Society, 1921. *CA Cancer J Clin, 22*(2), 95-98. https://doi.org/10.3322/canjclin.22.2.95

Eyquem, J., Mansilla-Soto, J., Giavridis, T., van der Stegen, S. J., Hamieh, M., Cunanan, K. M., Odak, A., Gonen, M., & Sadelain, M. (2017, Mar 2). Targeting a CAR to the TRAC locus with CRISPR/Cas9 enhances tumour rejection. *Nature, 543*(7643), 113-117. https://doi.org/10.1038/nature21405

Ferrari, S., del Prever, A. B., Palmerini, E., Staals, E., Berta, M., Balladelli, A., Picci, P., Fagioli, F., Bacci, G., & Vanel, D. (2009, May). Response to high-dose ifosfamide in patients with advanced/recurrent Ewing sarcoma. *Pediatr Blood Cancer, 52*(5), 581-584. https://doi.org/10.1002/pbc.21917

Gangwal, K., Close, D., Enriquez, C. A., Hill, C. P., & Lessnick, S. L. (2010, Feb 1). Emergent Properties of EWS/FLI Regulation via GGAA Microsatellites in Ewing's Sarcoma. *Genes Cancer, 1*(2), 177-187. https://doi.org/10.1177/1947601910361495

Gangwal, K., Sankar, S., Hollenhorst, P. C., Kinsey, M., Haroldsen, S. C., Shah, A. A., Boucher, K. M., Watkins, W. S., Jorde, L. B., Graves, B. J., & Lessnick, S. L. (2008, Jul 22). Microsatellites as EWS/FLI response elements in Ewing's sarcoma. *Proc Natl Acad Sci U S A, 105*(29), 10149-

10154. https://doi.org/10.1073/pnas.0801073105

Gardner, L. J., Polski, J. M., Fallon, R., & Dunphy, C. H. (1998, Jul). Identification of CD56 and CD57 by flow cytometry in Ewing's sarcoma or primitive neuroectodermal tumor. *Virchows Arch, 433*(1), 35-40. https://doi.org/10.1007/s004280050213

Gardner, R., Finney, O., Smithers, H., Leger, K. J., Annesley, C. E., Summers, C., Brown, C., Mgebroff, S., Lindgren, C., Spratt, K., Oron, A., Li, D., Bleakley, M., Park, J. R., & Jensen, M. C. (2016). CD19CAR T Cell Products of Defined CD4:CD8 Composition and Transgene Expression Show Prolonged Persistence and Durable MRD-Negative Remission in Pediatric and Young Adult B-Cell ALL. *Blood, 128*(22), 219-219. https://doi.org/10.1182/blood.V128.22.219.219

Garnett, M. J., Edelman, E. J., Heidorn, S. J., Greenman, C. D., Dastur, A., Lau, K. W., Greninger, P., Thompson, I. R., Luo, X., Soares, J., Liu, Q., Iorio, F., Surdez, D., Chen, L., Milano, R. J., Bignell, G. R., Tam, A. T., Davies, H., Stevenson, J. A., Barthorpe, S., Lutz, S. R., Kogera, F., Lawrence, K., McLaren-Douglas, A., Mitropoulos, X., Mironenko, T., Thi, H., Richardson, L., Zhou, W., Jewitt, F., Zhang, T., O'Brien, P., Boisvert, J. L., Price, S., Hur, W., Yang, W., Deng, X., Butler, A., Choi, H. G., Chang, J. W., Baselga, J., Stamenkovic, I., Engelman, J. A., Sharma, S. V., Delattre, O., Saez-Rodriguez, J., Gray, N. S., Settleman, J., Futreal, P. A., Haber, D. A., Stratton, M. R., Ramaswamy, S., McDermott, U., & Benes, C. H. (2012, Mar 28). Systematic identification of genomic markers of drug sensitivity in cancer cells. *Nature, 483*(7391), 570-575. https://doi.org/10.1038/nature11005

Gaspar, N., Hawkins, D. S., Dirksen, U., Lewis, I. J., Ferrari, S., Le Deley, M. C., Kovar, H., Grimer, R., Whelan, J., Claude, L., Delattre, O., Paulussen, M., Picci, P., Sundby Hall, K., van den Berg, H., Ladenstein, R., Michon, J., Hjorth, L., Judson, I., Luksch, R., Bernstein, M. L., Marec-Berard, P., Brennan, B., Craft, A. W., Womer, R. B., Juergens, H., & Oberlin, O. (2015, Sep 20). Ewing Sarcoma: Current Management and Future Approaches Through Collaboration. *J Clin Oncol, 33*(27), 3036-3046. https://doi.org/10.1200/JCO.2014.59.5256

Ghandi, M., Huang, F. W., Jane-Valbuena, J., Kryukov, G. V., Lo, C. C., McDonald, E. R., 3rd, Barretina, J., Gelfand, E. T., Bielski, C. M., Li, H., Hu, K., Andreev-Drakhlin, A. Y., Kim, J., Hess, J. M., Haas, B. J., Aguet, F., Weir, B. A., Rothberg, M. V., Paolella, B. R., Lawrence, M. S., Akbani, R., Lu, Y., Tiv, H. L., Gokhale, P. C., de Weck, A., Mansour, A. A., Oh, C., Shih, J., Hadi, K., Rosen, Y., Bistline, J., Venkatesan, K., Reddy, A., Sonkin, D., Liu, M., Lehar, J., Korn, J. M., Porter, D. A., Jones, M. D., Golji, J., Caponigro, G., Taylor, J. E., Dunning, C. M., Creech, A. L., Warren, A. C., McFarland, J. M., Zamanighomi, M., Kauffmann, A., Stransky, N., Imielinski, M., Maruvka, Y. E., Cherniack, A. D., Tsherniak, A., Vazquez, F., Jaffe, J. D., Lane, A. A., Weinstock, D. M., Johannessen, C. M., Morrissey, M. P., Stegmeier, F., Schlegel, R., Hahn, W. C., Getz, G., Mills, G. B., Boehm, J. S., Golub, T. R., Garraway, L. A., & Sellers, W. R. (2019, May). Next-generation characterization of the Cancer Cell Line Encyclopedia. *Nature, 569*(7757), 503-508. https://doi.org/10.1038/s41586-019-1186-3

Gollavilli, P. N., Pawar, A., Wilder-Romans, K., Natesan, R., Engelke, C. G., Dommeti, V. L., Krishnamurthy, P. M., Nallasivam, A., Apel, I. J., Xu, T., Qin, Z. S., Feng, F. Y., & Asangani, I. A. (2018, Aug 15). EWS/ETS-Driven Ewing Sarcoma Requires BET Bromodomain Proteins. *Cancer Res, 78*(16), 4760-4773. https://doi.org/10.1158/0008-5472.CAN-18-0484

Gorthi, A., & Bishop, A. J. R. (2018). Ewing sarcoma fusion oncogene: At the crossroads of transcription and DNA damage response. *Mol Cell Oncol, 5*(4), e1465014. https://doi.org/10.1080/23723556.2018.1465014

Gorthi, A., Romero, J. C., Loranc, E., Cao, L., Lawrence, L. A., Goodale, E., Iniguez, A. B., Bernard, X., Masamsetti, V. P., Roston, S., Lawlor, E. R., Toretsky, J. A., Stegmaier, K., Lessnick, S. L., Chen, Y., & Bishop, A. J. R. (2018, Mar 15). EWS-FLI1 increases transcription to cause R-loops and block BRCA1 repair in Ewing sarcoma. *Nature, 555*(7696), 387-391. https://doi.org/10.1038/nature25748

Graef, P., Buchholz, V. R., Stemberger, C., Flossdorf, M., Henkel, L., Schiemann, M., Drexler, I., Hofer, T., Riddell, S. R., & Busch, D. H. (2014, Jul 17). Serial transfer of single-cell-derived immunocompetence reveals stemness of CD8(+) central memory T cells. *Immunity, 41*(1), 116-126. https://doi.org/10.1016/j.immuni.2014.05.018

Grobner, S. N., Worst, B. C., Weischenfeldt, J., Buchhalter, I., Kleinheinz, K., Rudneva, V. A., Johann, P. D., Balasubramanian, G. P., Segura-Wang, M., Brabetz, S., Bender, S., Hutter, B., Sturm, D., Pfaff, E., Hubschmann, D., Zipprich, G., Heinold, M., Eils, J., Lawerenz, C., Erkek, S., Lambo, S., Waszak, S., Blattmann, C., Borkhardt, A., Kuhlen, M., Eggert, A., Fulda, S., Gessler, M., Wegert, J., Kappler, R., Baumhoer, D., Burdach, S., Kirschner-Schwabe, R., Kontny, U., Kulozik, A. E., Lohmann, D., Hettmer, S., Eckert, C., Bielack, S., Nathrath, M., Niemeyer, C., Richter, G. H., Schulte, J., Siebert, R., Westermann, F., Molenaar, J. J., Vassal, G., Witt, H., Project, I. P.-S., Project, I. M.-S., Burkhardt, B., Kratz, C. P., Witt, O., van Tilburg, C. M., Kramm, C. M., Fleischhack, G., Dirksen, U., Rutkowski, S., Fruhwald, M., von Hoff, K., Wolf, S., Klingebiel, T., Koscielniak, E., Landgraf, P., Koster, J., Resnick, A. C., Zhang, J., Liu, Y., Zhou, X., Waanders, A. J., Zwijnenburg, D. A., Raman, P., Brors, B., Weber, U. D., Northcott, P. A., Pajtler, K. W., Kool, M., Piro, R. M., Korbel, J. O., Schlesner, M., Eils, R., Jones, D. T. W., Lichter, P., Chavez, L., Zapatka, M., & Pfister, S. M. (2018, Mar 15). The landscape of genomic alterations across childhood cancers. *Nature, 555*(7696), 321-327. https://doi.org/10.1038/nature25480

Grohar, P. J., Woldemichael, G. M., Griffin, L. B., Mendoza, A., Chen, Q. R., Yeung, C., Currier, D. G., Davis, S., Khanna, C., Khan, J., McMahon, J. B., & Helman, L. J. (2011, Jun 22). Identification of an inhibitor of the EWS-FLI1 oncogenic transcription factor by high-throughput screening. *J Natl Cancer Inst, 103*(12), 962-978. https://doi.org/10.1093/jnci/djr156

Grunewald, T. G., Bernard, V., Gilardi-Hebenstreit, P., Raynal, V., Surdez, D., Aynaud, M. M., Mirabeau, O., Cidre-Aranaz, F., Tirode, F., Zaidi, S., Perot, G., Jonker, A. H., Lucchesi, C., Le Deley, M. C., Oberlin, O., Marec-Berard, P., Veron, A. S., Reynaud, S., Lapouble, E., Boeva, V., Rio Frio, T., Alonso, J., Bhatia, S., Pierron, G., Cancel-Tassin, G., Cussenot, O., Cox, D. G., Morton, L. M., Machiela, M. J., Chanock, S. J., Charnay, P., & Delattre, O. (2015, Sep). Chimeric EWSR1-FLI1 regulates the Ewing sarcoma susceptibility gene EGR2 via a GGAA microsatellite. *Nat Genet, 47*(9), 1073-1078. https://doi.org/10.1038/ng.3363

Grunewald, T. G., Diebold, I., Esposito, I., Plehm, S., Hauer, K., Thiel, U., da Silva-Buttkus, P., Neff, F., Unland, R., Muller-Tidow, C., Zobywalski, C., Lohrig, K., Lewandrowski, U., Sickmann, A., Prazeres da Costa, O., Gorlach, A., Cossarizza, A., Butt, E., Richter, G. H., & Burdach, S. (2012, Jan). STEAP1 is associated with the invasive and oxidative stress phenotype of Ewing tumors. *Mol Cancer Res, 10*(1), 52-65. https://doi.org/10.1158/1541-7786.MCR-11-0524

Grunewald, T. G. P., Cidre-Aranaz, F., Surdez, D., Tomazou, E. M., de Alava, E., Kovar, H., Sorensen, P. H., Delattre, O., & Dirksen, U. (2018, Jul 5). Ewing sarcoma. *Nat Rev Dis Primers, 4*(1), 5. https://doi.org/10.1038/s41572-018-0003-x

Guillon, N., Tirode, F., Boeva, V., Zynovyev, A., Barillot, E., & Delattre, O. (2009). The oncogenic EWS-FLI1 protein binds in vivo GGAA microsatellite sequences with potential transcriptional activation

function. *PLoS One, 4*(3), e4932. https://doi.org/10.1371/journal.pone.0004932

Hanssens, H., Meeus, F., De Veirman, K., Breckpot, K., & Devoogdt, N. (2022, Jan). The antigen-binding moiety in the driver's seat of CARs. *Med Res Rev, 42*(1), 306-342. https://doi.org/10.1002/med.21818

Harlow, M. L., Chasse, M. H., Boguslawski, E. A., Sorensen, K. M., Gedminas, J. M., Kitchen-Goosen, S. M., Rothbart, S. B., Taslim, C., Lessnick, S. L., Peck, A. S., Madaj, Z. B., Bowman, M. J., & Grohar, P. J. (2019, Jun 1). Trabectedin Inhibits EWS-FLI1 and Evicts SWI/SNF from Chromatin in a Schedule-dependent Manner. *Clin Cancer Res, 25*(11), 3417-3429. https://doi.org/10.1158/1078-0432.CCR-18-3511

He, S., Huang, Q., Hu, J., Li, L., Xiao, Y., Yu, H., Han, Z., Wang, T., Zhou, W., Wei, H., & Xiao, J. (2019, Nov). EWS-FLI1-mediated tenascin-C expression promotes tumour progression by targeting MALAT1 through integrin alpha5beta1-mediated YAP activation in Ewing sarcoma. *Br J Cancer, 121*(11), 922-933. https://doi.org/10.1038/s41416-019-0608-1

Hinrichs, C. S., & Rosenberg, S. A. (2014, Jan). Exploiting the curative potential of adoptive T-cell therapy for cancer. *Immunol Rev, 257*(1), 56-71. https://doi.org/10.1111/imr.12132

Hong, S. H., Youbi, S. E., Hong, S. P., Kallakury, B., Monroe, P., Erkizan, H. V., Barber-Rotenberg, J. S., Houghton, P., Uren, A., & Toretsky, J. A. (2014, Jan 30). Pharmacokinetic modeling optimizes inhibition of the 'undruggable' EWS-FLI1 transcription factor in Ewing Sarcoma. *Oncotarget, 5*(2), 338-350. https://doi.org/10.18632/oncotarget.1495

Horowitz, M. M., Gale, R. P., Sondel, P. M., Goldman, J. M., Kersey, J., Kolb, H. J., Rimm, A. A., Ringden, O., Rozman, C., Speck, B., & et al. (1990, Feb 1). Graft-versus-leukemia reactions after bone marrow transplantation. *Blood, 75*(3), 555-562. https://www.ncbi.nlm.nih.gov/pubmed/2297567

Howe, S. J., Mansour, M. R., Schwarzwaelder, K., Bartholomae, C., Hubank, M., Kempski, H., Brugman, M. H., Pike-Overzet, K., Chatters, S. J., de Ridder, D., Gilmour, K. C., Adams, S., Thornhill, S. I., Parsley, K. L., Staal, F. J., Gale, R. E., Linch, D. C., Bayford, J., Brown, L., Quaye, M., Kinnon, C., Ancliff, P., Webb, D. K., Schmidt, M., von Kalle, C., Gaspar, H. B., & Thrasher, A. J. (2008, Sep). Insertional mutagenesis combined with acquired somatic mutations causes leukemogenesis following gene therapy of SCID-X1 patients. *J Clin Invest, 118*(9), 3143-3150. https://doi.org/10.1172/JCI35798

Huang, X., Park, H., Greene, J., Pao, J., Mulvey, E., Zhou, S. X., Albert, C. M., Moy, F., Sachdev, D., Yee, D., Rader, C., Hamby, C. V., Loeb, D. M., Cairo, M. S., & Zhou, X. (2015). IGF1R- and ROR1-Specific CAR T Cells as a Potential Therapy for High Risk Sarcomas. *PLoS One, 10*(7), e0133152. https://doi.org/10.1371/journal.pone.0133152

Iniguez, A. B., Stolte, B., Wang, E. J., Conway, A. S., Alexe, G., Dharia, N. V., Kwiatkowski, N., Zhang, T., Abraham, B. J., Mora, J., Kalev, P., Leggett, A., Chowdhury, D., Benes, C. H., Young, R. A., Gray, N. S., & Stegmaier, K. (2018, Feb 12). EWS/FLI Confers Tumor Cell Synthetic Lethality to CDK12 Inhibition in Ewing Sarcoma. *Cancer Cell, 33*(2), 202-216 e206. https://doi.org/10.1016/j.ccell.2017.12.009

Ito, R., Inamoto, Y., Inoue, Y., Ito, A., Tanaka, T., Fuji, S., Okinaka, K., Kurosawa, S., Kim, S. W., Yamashita, T., & Fukuda, T. (2019, Feb). Characterization of Late Acute and Chronic Graft-Versus-Host Disease according to the 2014 National Institutes of Health Consensus Criteria in Japanese Patients. *Biol Blood Marrow Transplant, 25*(2), 293-300. https://doi.org/10.1016/j.bbmt.2018.09.014

Jahanseir, K., Folpe, A. L., Graham, R. P., Giannini, C., Robinson, S. I., Sukov, W., & Fritchie, K. (2020, Jun). Ewing Sarcoma in Older Adults: A Clinicopathologic Study of 50 Cases Occurring in Patients Aged >/=40 Years, With Emphasis on Histologic Mimics. *Int J Surg Pathol, 28*(4), 352-360. https://doi.org/10.1177/1066896919893073

Jena, B., Dotti, G., & Cooper, L. J. (2010, Aug 19). Redirecting T-cell specificity by introducing a tumor-specific chimeric antigen receptor. *Blood, 116*(7), 1035-1044. https://doi.org/10.1182/blood-2010-01-043737

Jones, H. F., Molvi, Z., Klatt, M. G., Dao, T., & Scheinberg, D. A. (2020). Empirical and Rational Design of T Cell Receptor-Based Immunotherapies. *Front Immunol, 11*, 585385. https://doi.org/10.3389/fimmu.2020.585385

Juergens, C., Weston, C., Lewis, I., Whelan, J., Paulussen, M., Oberlin, O., Michon, J., Zoubek, A., Juergens, H., & Craft, A. (2006, Jul). Safety assessment of intensive induction with vincristine, ifosfamide, doxorubicin, and etoposide (VIDE) in the treatment of Ewing tumors in the EURO-E.W.I.N.G. 99 clinical trial. *Pediatr Blood Cancer, 47*(1), 22-29. https://doi.org/10.1002/pbc.20820

Juergens, H., Daw, N. C., Geoerger, B., Ferrari, S., Villarroel, M., Aerts, I., Whelan, J., Dirksen, U., Hixon, M. L., Yin, D., Wang, T., Green, S., Paccagnella, L., & Gualberto, A. (2011, Dec 1). Preliminary efficacy of the anti-insulin-like growth factor type 1 receptor antibody figitumumab in patients with refractory Ewing sarcoma. *J Clin Oncol, 29*(34), 4534-4540. https://doi.org/10.1200/JCO.2010.33.0670

Kailayangiri, S., Altvater, B., Lesch, S., Balbach, S., Gottlich, C., Kuhnemundt, J., Mikesch, J. H., Schelhaas, S., Jamitzky, S., Meltzer, J., Farwick, N., Greune, L., Fluegge, M., Kerl, K., Lode, H. N., Siebert, N., Muller, I., Walles, H., Hartmann, W., & Rossig, C. (2019, May 8). EZH2 Inhibition in Ewing Sarcoma Upregulates GD2 Expression for Targeting with Gene-Modified T Cells. *Mol Ther, 27*(5), 933-946. https://doi.org/10.1016/j.ymthe.2019.02.014

Kaliki, S., Rathi, S. G., & Palkonda, V. A. R. (2018, Mar). Primary orbital Ewing sarcoma family of tumors: a study of 12 cases. *Eye (Lond), 32*(3), 615-621. https://doi.org/10.1038/eye.2017.278

Kaneko, S., Mastaglio, S., Bondanza, A., Ponzoni, M., Sanvito, F., Aldrighetti, L., Radrizzani, M., La Seta-Catamancio, S., Provasi, E., Mondino, A., Nagasawa, T., Fleischhauer, K., Russo, V., Traversari, C., Ciceri, F., Bordignon, C., & Bonini, C. (2009, Jan 29). IL-7 and IL-15 allow the generation of suicide gene-modified alloreactive self-renewing central memory human T lymphocytes. *Blood, 113*(5), 1006-1015. https://doi.org/10.1182/blood-2008-05-156059

Katschnig, A. M., Kauer, M. O., Schwentner, R., Tomazou, E. M., Mutz, C. N., Linder, M., Sibilia, M., Alonso, J., Aryee, D. N. T., & Kovar, H. (2017, Oct 26). EWS-FLI1 perturbs MRTFB/YAP-1/TEAD target gene regulation inhibiting cytoskeletal autoregulatory feedback in Ewing sarcoma. *Oncogene, 36*(43), 5995-6005. https://doi.org/10.1038/onc.2017.202

Kinsey, M., Smith, R., & Lessnick, S. L. (2006, Nov). NR0B1 is required for the oncogenic phenotype mediated by EWS/FLI in Ewing's sarcoma. *Mol Cancer Res, 4*(11), 851-859. https://doi.org/10.1158/1541-7786.MCR-06-0090

Kirschner, A., Thiede, M., Grunewald, T. G., Alba Rubio, R., Richter, G. H., Kirchner, T., Busch, D. H., Burdach, S., & Thiel, U. (2017). Pappalysin-1 T cell receptor transgenic allo-restricted T cells kill Ewing sarcoma in vitro and in vivo. *Oncoimmunology, 6*(2), e1273301. https://doi.org/10.1080/2162402X.2016.1273301

Knoop, L. L., & Baker, S. J. (2000, Aug 11). The splicing factor U1C represses EWS/FLI-mediated transactivation. *J Biol Chem, 275*(32), 24865-24871. https://doi.org/10.1074/jbc.M001661200

Koch, R., Gelderblom, H., Haveman, L., Brichard, B., Jurgens, H., Cyprova, S., van den Berg, H., Hassenpflug, W., Raciborska, A., Ek, T., Baumhoer, D., Egerer, G., Eich, H. T., Renard, M., Hauser, P., Burdach, S., Bovee, J., Bonar, F., Reichardt, P., Kruseova, J., Hardes, J., Kuhne, T., Kessler, T., Collaud, S., Bernkopf, M., Butterfass-Bahloul, T., Dhooge, C., Bauer, S., Kiss, J., Paulussen, M., Hong, A., Ranft, A., Timmermann, B., Rascon, J., Vieth, V., Kanerva, J., Faldum, A., Metzler, M., Hartmann, W., Hjorth, L., Bhadri, V., & Dirksen, U. (2022, Apr 15). High-Dose Treosulfan and Melphalan as Consolidation Therapy Versus Standard Therapy for High-Risk (Metastatic) Ewing Sarcoma. *J Clin Oncol*, JCO2101942. https://doi.org/10.1200/JCO.21.01942

Kochenderfer, J. N., Wilson, W. H., Janik, J. E., Dudley, M. E., Stetler-Stevenson, M., Feldman, S. A., Maric, I., Raffeld, M., Nathan, D. A., Lanier, B. J., Morgan, R. A., & Rosenberg, S. A. (2010, Nov 18). Eradication of B-lineage cells and regression of lymphoma in a patient treated with autologous T cells genetically engineered to recognize CD19. *Blood, 116*(20), 4099-4102. https://doi.org/10.1182/blood-2010-04-281931

Kolb, H. J. (2008, Dec 1). Graft-versus-leukemia effects of transplantation and donor lymphocytes. *Blood, 112*(12), 4371-4383. https://doi.org/10.1182/blood-2008-03-077974

Koscielniak, E., Gross-Wieltsch, U., Treuner, J., Winkler, P., Klingebiel, T., Lang, P., Bader, P., Niethammer, D., & Handgretinger, R. (2005, Jan 1). Graft-versus-Ewing sarcoma effect and long-term remission induced by haploidentical stem-cell transplantation in a patient with relapse of metastatic disease. *J Clin Oncol, 23*(1), 242-244. https://doi.org/10.1200/JCO.2005.05.940

Kovar, H., Aryee, D. N., Jug, G., Henockl, C., Schemper, M., Delattre, O., Thomas, G., & Gadner, H. (1996, Apr). EWS/FLI-1 antagonists induce growth inhibition of Ewing tumor cells in vitro. *Cell Growth Differ, 7*(4), 429-437. https://www.ncbi.nlm.nih.gov/pubmed/9052984

Ladenstein, R., Potschger, U., Le Deley, M. C., Whelan, J., Paulussen, M., Oberlin, O., van den Berg, H., Dirksen, U., Hjorth, L., Michon, J., Lewis, I., Craft, A., & Jurgens, H. (2010, Jul 10). Primary disseminated multifocal Ewing sarcoma: results of the Euro-EWING 99 trial. *J Clin Oncol, 28*(20), 3284-3291. https://doi.org/10.1200/JCO.2009.22.9864

Lai, A. Y., & Wade, P. A. (2011, Jul 7). Cancer biology and NuRD: a multifaceted chromatin remodelling complex. *Nat Rev Cancer, 11*(8), 588-596. https://doi.org/10.1038/nrc3091

Lamhamedi-Cherradi, S. E., Menegaz, B. A., Ramamoorthy, V., Aiyer, R. A., Maywald, R. L., Buford, A. S., Doolittle, D. K., Culotta, K. S., O'Dorisio, J. E., & Ludwig, J. A. (2015, Jul). An Oral Formulation of YK-4-279: Preclinical Efficacy and Acquired Resistance Patterns in Ewing Sarcoma. *Mol Cancer Ther, 14*(7), 1591-1604. https://doi.org/10.1158/1535-7163.MCT-14-0334

Larson, R. C., & Maus, M. V. (2021, Mar). Recent advances and discoveries in the mechanisms and functions of CAR T cells. *Nat Rev Cancer, 21*(3), 145-161. https://doi.org/10.1038/s41568-020-00323-z

Leibowitz, M. L., Papathanasiou, S., Doerfler, P. A., Blaine, L. J., Sun, L., Yao, Y., Zhang, C. Z., Weiss, M. J., & Pellman, D. (2021, Jun). Chromothripsis as an on-target consequence of CRISPR-Cas9 genome editing. *Nat Genet, 53*(6), 895-905. https://doi.org/10.1038/s41588-021-00838-7

Lessnick, S. L., Dacwag, C. S., & Golub, T. R. (2002, May). The Ewing's sarcoma oncoprotein EWS/FLI induces a p53-dependent growth arrest in primary human fibroblasts. *Cancer Cell, 1*(4), 393-401. https://doi.org/10.1016/s1535-6108(02)00056-9

Li, J., Ohmura, S., Marchetto, A., Orth, M. F., Imle, R., Dallmayer, M., Musa, J., Knott, M. M. L., Holting, T. L. B., Stein, S., Funk, C. M., Sastre, A., Alonso, J., Bestvater, F., Kasan, M., Romero-Perez, L., Hartmann, W., Ranft, A., Banito, A., Dirksen, U., Kirchner, T., Cidre-Aranaz, F., & Grunewald, T.

G. P. (2021, Sep 16). Therapeutic targeting of the PLK1-PRC1-axis triggers cell death in genomically silent childhood cancer. *Nat Commun, 12*(1), 5356. https://doi.org/10.1038/s41467-021-25553-z

Lin, L., Huang, M., Shi, X., Mayakonda, A., Hu, K., Jiang, Y. Y., Guo, X., Chen, L., Pang, B., Doan, N., Said, J. W., Xie, J., Gery, S., Cheng, X., Lin, Z., Li, J., Berman, B. P., Yin, D., Lin, D. C., & Koeffler, H. P. (2019, Feb 20). Super-enhancer-associated MEIS1 promotes transcriptional dysregulation in Ewing sarcoma in co-operation with EWS-FLI1. *Nucleic Acids Res, 47*(3), 1255-1267. https://doi.org/10.1093/nar/gky1207

Lissat, A., Joerschke, M., Shinde, D. A., Braunschweig, T., Meier, A., Makowska, A., Bortnick, R., Henneke, P., Herget, G., Gorr, T. A., & Kontny, U. (2015, Jul 28). IL6 secreted by Ewing sarcoma tumor microenvironment confers anti-apoptotic and cell-disseminating paracrine responses in Ewing sarcoma cells. *BMC Cancer, 15*, 552. https://doi.org/10.1186/s12885-015-1564-7

Liu, S., Galat, V., Galat, Y., Lee, Y. K. A., Wainwright, D., & Wu, J. (2021, Jan 6). NK cell-based cancer immunotherapy: from basic biology to clinical development. *J Hematol Oncol, 14*(1), 7. https://doi.org/10.1186/s13045-020-01014-w

Luo, W., Gangwal, K., Sankar, S., Boucher, K. M., Thomas, D., & Lessnick, S. L. (2009, Nov 19). GSTM4 is a microsatellite-containing EWS/FLI target involved in Ewing's sarcoma oncogenesis and therapeutic resistance. *Oncogene, 28*(46), 4126-4132. https://doi.org/10.1038/onc.2009.262

Luo, W., Xu, C., Ayello, J., Dela Cruz, F., Rosenblum, J. M., Lessnick, S. L., & Cairo, M. S. (2018, Feb 8). Protein phosphatase 1 regulatory subunit 1A in ewing sarcoma tumorigenesis and metastasis. *Oncogene, 37*(6), 798-809. https://doi.org/10.1038/onc.2017.378

Ma, Y., Baltezor, M., Rajewski, L., Crow, J., Samuel, G., Staggs, V. S., Chastain, K. M., Toretsky, J. A., Weir, S. J., & Godwin, A. K. (2019, Jul). Targeted inhibition of histone deacetylase leads to suppression of Ewing sarcoma tumor growth through an unappreciated EWS-FLI1/HDAC3/HSP90 signaling axis. *J Mol Med (Berl), 97*(7), 957-972. https://doi.org/10.1007/s00109-019-01782-0

Machado, I., Lopez-Guerrero, J. A., Scotlandi, K., Picci, P., & Llombart-Bosch, A. (2018, May). Immunohistochemical analysis and prognostic significance of PD-L1, PD-1, and CD8+ tumor-infiltrating lymphocytes in Ewing's sarcoma family of tumors (ESFT). *Virchows Arch, 472*(5), 815-824. https://doi.org/10.1007/s00428-018-2316-2

Mahlendorf, D. E., & Staege, M. S. (2013, Mar). Characterization of Ewing sarcoma associated cancer/testis antigens. *Cancer Biol Ther, 14*(3), 254-261. https://doi.org/10.4161/cbt.23298

Majzner, R. G., & Mackall, C. L. (2018, Oct). Tumor Antigen Escape from CAR T-cell Therapy. *Cancer Discov, 8*(10), 1219-1226. https://doi.org/10.1158/2159-8290.CD-18-0442

Manfredi, F., Cianciotti, B. C., Potenza, A., Tassi, E., Noviello, M., Biondi, A., Ciceri, F., Bonini, C., & Ruggiero, E. (2020). TCR Redirected T Cells for Cancer Treatment: Achievements, Hurdles, and Goals. *Front Immunol, 11*, 1689. https://doi.org/10.3389/fimmu.2020.01689

Marmont, A. M., Horowitz, M. M., Gale, R. P., Sobocinski, K., Ash, R. C., van Bekkum, D. W., Champlin, R. E., Dicke, K. A., Goldman, J. M., Good, R. A., & et al. (1991, Oct 15). T-cell depletion of HLA-identical transplants in leukemia. *Blood, 78*(8), 2120-2130. https://www.ncbi.nlm.nih.gov/pubmed/1912589

Martinelli, M., Parra, A., Scapoli, L., De Sanctis, P., Chiadini, V., Hattinger, C., Picci, P., Zucchini, C., & Scotlandi, K. (2016, Nov 22). CD99 polymorphisms significantly influence the probability to develop Ewing sarcoma in earlier age and patient disease progression. *Oncotarget, 7*(47), 77958-77967. https://doi.org/10.18632/oncotarget.12862

McDonald, G. B., Tabellini, L., Storer, B. E., Lawler, R. L., Martin, P. J., & Hansen, J. A. (2015, Jul 2). Plasma biomarkers of acute GVHD and nonrelapse mortality: predictive value of measurements before GVHD onset and treatment. *Blood, 126*(1), 113-120. https://doi.org/10.1182/blood-2015-03-636753

Mertens, F., Antonescu, C. R., & Mitelman, F. (2016, Apr). Gene fusions in soft tissue tumors: Recurrent and overlapping pathogenetic themes. *Genes Chromosomes Cancer, 55*(4), 291-310. https://doi.org/10.1002/gcc.22335

Monjezi, R., Miskey, C., Gogishvili, T., Schleef, M., Schmeer, M., Einsele, H., Ivics, Z., & Hudecek, M. (2017, Jan). Enhanced CAR T-cell engineering using non-viral Sleeping Beauty transposition from minicircle vectors. *Leukemia, 31*(1), 186-194. https://doi.org/10.1038/leu.2016.180

Monument, M. J., Johnson, K. M., McIlvaine, E., Abegglen, L., Watkins, W. S., Jorde, L. B., Womer, R. B., Beeler, N., Monovich, L., Lawlor, E. R., Bridge, J. A., Schiffman, J. D., Krailo, M. D., Randall, R. L., & Lessnick, S. L. (2014). Clinical and biochemical function of polymorphic NR0B1 GGAA-microsatellites in Ewing sarcoma: a report from the Children's Oncology Group. *PLoS One, 9*(8), e104378. https://doi.org/10.1371/journal.pone.0104378

Moosmann, C., Muller, T. R., Busch, D. H., & Schober, K. (2022, Mar 18). Orthotopic T-cell receptor replacement in primary human T cells using CRISPR-Cas9-mediated homology-directed repair. *STAR Protoc, 3*(1), 101031. https://doi.org/10.1016/j.xpro.2021.101031

Muller, T. R., Jarosch, S., Hammel, M., Leube, J., Grassmann, S., Bernard, B., Effenberger, M., Andra, I., Chaudhry, M. Z., Kauferle, T., Malo, A., Cicin-Sain, L., Steinberger, P., Feuchtinger, T., Protzer, U., Schumann, K., Neuenhahn, M., Schober, K., & Busch, D. H. (2021, Aug 17). Targeted T cell receptor gene editing provides predictable T cell product function for immunotherapy. *Cell Rep Med, 2*(8), 100374. https://doi.org/10.1016/j.xcrm.2021.100374

MÜNCHEN, C. (2017). Knochentumoren und Weichteilsarkome [book].

Myers, R. M., Taraseviciute, A., Steinberg, S. M., Lamble, A. J., Sheppard, J., Yates, B., Kovach, A. E., Wood, B., Borowitz, M. J., Stetler-Stevenson, M., Yuan, C. M., Pillai, V., Foley, T., Chung, P., Chen, L., Lee, D. W., Annesley, C., DiNofia, A., Grupp, S. A., John, S., Bhojwani, D., Brown, P. A., Laetsch, T. W., Gore, L., Gardner, R. A., Rheingold, S. R., Pulsipher, M. A., & Shah, N. N. (2022, Mar 20). Blinatumomab Nonresponse and High-Disease Burden Are Associated With Inferior Outcomes After CD19-CAR for B-ALL. *J Clin Oncol, 40*(9), 932-944. https://doi.org/10.1200/JCO.21.01405

Neckles, C., Boer, R. E., Aboreden, N., Cross, A. M., Walker, R. L., Kim, B. H., Kim, S., Schneekloth, J. S., Jr., & Caplen, N. J. (2019, Dec). HNRNPH1-dependent splicing of a fusion oncogene reveals a targetable RNA G-quadruplex interaction. *RNA, 25*(12), 1731-1750. https://doi.org/10.1261/rna.072454.119

Nicholson, E., Ghorashian, S., & Stauss, H. (2012). Improving TCR Gene Therapy for Treatment of Haematological Malignancies. *Adv Hematol, 2012*, 404081. https://doi.org/10.1155/2012/404081

Nicolini, A., Rossi, G., Ferrari, P., & Carpi, A. (2022, Feb). Minimal residual disease in advanced or metastatic solid cancers: The G0-G1 state and immunotherapy are key to unwinding cancer complexity. *Semin Cancer Biol, 79*, 68-82. https://doi.org/10.1016/j.semcancer.2020.03.009

Niedan, S., Kauer, M., Aryee, D. N., Kofler, R., Schwentner, R., Meier, A., Potschger, U., Kontny, U., & Kovar, H. (2014, Jul 24). Suppression of FOXO1 is responsible for a growth regulatory repressive transcriptional sub-signature of EWS-FLI1 in Ewing sarcoma. *Oncogene, 33*(30), 3927-3938. https://doi.org/10.1038/onc.2013.361

Olmos, D., Postel-Vinay, S., Molife, L. R., Okuno, S. H., Schuetze, S. M., Paccagnella, M. L., Batzel, G. N., Yin, D., Pritchard-Jones, K., Judson, I., Worden, F. P., Gualberto, A., Scurr, M., de Bono, J. S., & Haluska, P. (2010, Feb). Safety, pharmacokinetics, and preliminary activity of the anti-IGF-1R antibody figitumumab (CP-751,871) in patients with sarcoma and Ewing's sarcoma: a phase 1 expansion cohort study. *Lancet Oncol, 11*(2), 129-135. https://doi.org/10.1016/S1470-2045(09)70354-7

Pappo, A. S., & Dirksen, U. (2018, Jan 10). Rhabdomyosarcoma, Ewing Sarcoma, and Other Round Cell Sarcomas. *J Clin Oncol, 36*(2), 168-179. https://doi.org/10.1200/JCO.2017.74.7402

Paronetto, M. P., Minana, B., & Valcarcel, J. (2011, Aug 5). The Ewing sarcoma protein regulates DNA damage-induced alternative splicing. *Mol Cell, 43*(3), 353-368. https://doi.org/10.1016/j.molcel.2011.05.035

Paulussen, M., Ahrens, S., Burdach, S., Craft, A., Dockhorn-Dworniczak, B., Dunst, J., Frohlich, B., Winkelmann, W., Zoubek, A., & Jurgens, H. (1998, Mar). Primary metastatic (stage IV) Ewing tumor: survival analysis of 171 patients from the EICESS studies. European Intergroup Cooperative Ewing Sarcoma Studies. *Ann Oncol, 9*(3), 275-281. https://doi.org/10.1023/a:1008208511815

Paulussen, M., Braun-Munzinger, G., Burdach, S., Deneke, S., Dunst, J., Fellinger, E., Gobel, U., Mittler, U., Treuner, J., Voute, P. A., & et al. (1993, Jul-Aug). [Results of treatment of primary exclusively pulmonary metastatic Ewing sarcoma. A retrospective analysis of 41 patients]. *Klin Padiatr, 205*(4), 210-216. https://doi.org/10.1055/s-2007-1025229 (Behandlungsergebnisse beim primar ausschliesslich pulmonal metastasierten Ewingsarkom. Eine retrospektive Analyse von 41 Patienten.)

Perlman, E. J., Dickman, P. S., Askin, F. B., Grier, H. E., Miser, J. S., & Link, M. P. (1994, Mar). Ewing's sarcoma--routine diagnostic utilization of MIC2 analysis: a Pediatric Oncology Group/Children's Cancer Group Intergroup Study. *Hum Pathol, 25*(3), 304-307. https://doi.org/10.1016/0046-8177(94)90203-8

Petermann, R., Mossier, B. M., Aryee, D. N., Khazak, V., Golemis, E. A., & Kovar, H. (1998, Aug 6). Oncogenic EWS-Fli1 interacts with hsRPB7, a subunit of human RNA polymerase II. *Oncogene, 17*(5), 603-610. https://doi.org/10.1038/sj.onc.1201964

Pishas, K. I., Drenberg, C. D., Taslim, C., Theisen, E. R., Johnson, K. M., Saund, R. S., Pop, I. L., Crompton, B. D., Lawlor, E. R., Tirode, F., Mora, J., Delattre, O., Beckerle, M. C., Callen, D. F., Sharma, S., & Lessnick, S. L. (2018, Sep). Therapeutic Targeting of KDM1A/LSD1 in Ewing Sarcoma with SP-2509 Engages the Endoplasmic Reticulum Stress Response. *Mol Cancer Ther, 17*(9), 1902-1916. https://doi.org/10.1158/1535-7163.MCT-18-0373

Prieur, A., Tirode, F., Cohen, P., & Delattre, O. (2004, Aug). EWS/FLI-1 silencing and gene profiling of Ewing cells reveal downstream oncogenic pathways and a crucial role for repression of insulin-like growth factor binding protein 3. *Mol Cell Biol, 24*(16), 7275-7283. https://doi.org/10.1128/MCB.24.16.7275-7283.2004

Provasi, E., Genovese, P., Lombardo, A., Magnani, Z., Liu, P. Q., Reik, A., Chu, V., Paschon, D. E., Zhang, L., Kuball, J., Camisa, B., Bondanza, A., Casorati, G., Ponzoni, M., Ciceri, F., Bordignon, C., Greenberg, P. D., Holmes, M. C., Gregory, P. D., Naldini, L., & Bonini, C. (2012, May). Editing T cell specificity towards leukemia by zinc finger nucleases and lentiviral gene transfer. *Nat Med, 18*(5), 807-815. https://doi.org/10.1038/nm.2700

Ramakrishnan, R., Fujimura, Y., Zou, J. P., Liu, F., Lee, L., Rao, V. N., & Reddy, E. S. (2004, Sep 16). Role of

protein-protein interactions in the antiapoptotic function of EWS-Fli-1. *Oncogene, 23*(42), 7087-7094. https://doi.org/10.1038/sj.onc.1207927

Retel, V. P., Steuten, L. M. G., Geukes Foppen, M. H., Mewes, J. C., Lindenberg, M. A., Haanen, J., & van Harten, W. H. (2018, Sep 15). Early cost-effectiveness of tumor infiltrating lymphocytes (TIL) for second line treatment in advanced melanoma: a model-based economic evaluation. *BMC Cancer, 18*(1), 895. https://doi.org/10.1186/s12885-018-4788-5

Richter, G. H., Fasan, A., Hauer, K., Grunewald, T. G., Berns, C., Rossler, S., Naumann, I., Staege, M. S., Fulda, S., Esposito, I., & Burdach, S. (2013, May). G-Protein coupled receptor 64 promotes invasiveness and metastasis in Ewing sarcomas through PGF and MMP1. *J Pathol, 230*(1), 70-81. https://doi.org/10.1002/path.4170

Richter, G. H., Plehm, S., Fasan, A., Rossler, S., Unland, R., Bennani-Baiti, I. M., Hotfilder, M., Lowel, D., von Luettichau, I., Mossbrugger, I., Quintanilla-Martinez, L., Kovar, H., Staege, M. S., Muller-Tidow, C., & Burdach, S. (2009, Mar 31). EZH2 is a mediator of EWS/FLI1 driven tumor growth and metastasis blocking endothelial and neuro-ectodermal differentiation. *Proc Natl Acad Sci U S A, 106*(13), 5324-5329. https://doi.org/10.1073/pnas.0810759106

Riggi, N., Cironi, L., Provero, P., Suva, M. L., Kaloulis, K., Garcia-Echeverria, C., Hoffmann, F., Trumpp, A., & Stamenkovic, I. (2005, Dec 15). Development of Ewing's sarcoma from primary bone marrow-derived mesenchymal progenitor cells. *Cancer Res, 65*(24), 11459-11468. https://doi.org/10.1158/0008-5472.CAN-05-1696

Riggi, N., Knoechel, B., Gillespie, S. M., Rheinbay, E., Boulay, G., Suva, M. L., Rossetti, N. E., Boonseng, W. E., Oksuz, O., Cook, E. B., Formey, A., Patel, A., Gymrek, M., Thapar, V., Deshpande, V., Ting, D. T., Hornicek, F. J., Nielsen, G. P., Stamenkovic, I., Aryee, M. J., Bernstein, B. E., & Rivera, M. N. (2014, Nov 10). EWS-FLI1 utilizes divergent chromatin remodeling mechanisms to directly activate or repress enhancer elements in Ewing sarcoma. *Cancer Cell, 26*(5), 668-681. https://doi.org/10.1016/j.ccell.2014.10.004

Riggi, N., & Stamenkovic, I. (2007, Aug 28). The Biology of Ewing sarcoma. *Cancer Lett, 254*(1), 1-10. https://doi.org/10.1016/j.canlet.2006.12.009

Riggi, N., Suva, M. L., De Vito, C., Provero, P., Stehle, J. C., Baumer, K., Cironi, L., Janiszewska, M., Petricevic, T., Suva, D., Tercier, S., Joseph, J. M., Guillou, L., & Stamenkovic, I. (2010, May). EWS-FLI-1 modulates miRNA145 and SOX2 expression to initiate mesenchymal stem cell reprogramming toward Ewing sarcoma cancer stem cells. *Genes Dev, 24*(9), 916-932. https://doi.org/10.1101/gad.1899710

Riggi, N., Suva, M. L., & Stamenkovic, I. (2021, Jan 14). Ewing's Sarcoma. *N Engl J Med, 384*(2), 154-164. https://doi.org/10.1056/NEJMra2028910

Robbins, P. F., Kassim, S. H., Tran, T. L., Crystal, J. S., Morgan, R. A., Feldman, S. A., Yang, J. C., Dudley, M. E., Wunderlich, J. R., Sherry, R. M., Kammula, U. S., Hughes, M. S., Restifo, N. P., Raffeld, M., Lee, C. C., Li, Y. F., El-Gamil, M., & Rosenberg, S. A. (2015, Mar 1). A pilot trial using lymphocytes genetically engineered with an NY-ESO-1-reactive T-cell receptor: long-term follow-up and correlates with response. *Clin Cancer Res, 21*(5), 1019-1027. https://doi.org/10.1158/1078-0432.CCR-14-2708

Robin, T. P., Smith, A., McKinsey, E., Reaves, L., Jedlicka, P., & Ford, H. L. (2012, Aug). EWS/FLI1 regulates EYA3 in Ewing sarcoma via modulation of miRNA-708, resulting in increased cell survival and chemoresistance. *Mol Cancer Res, 10*(8), 1098-1108. https://doi.org/10.1158/1541-7786.MCR-12-0086

Robinson, J. T., Thorvaldsdottir, H., Wenger, A. M., Zehir, A., & Mesirov, J. P. (2017, Nov 1). Variant Review with the Integrative Genomics Viewer. *Cancer Res, 77*(21), e31-e34. https://doi.org/10.1158/0008-5472.CAN-17-0337

Rodeberg, D. A., Nuss, R. A., Elsawa, S. F., & Celis, E. (2005, Jun 15). Recognition of six-transmembrane epithelial antigen of the prostate-expressing tumor cells by peptide antigen-induced cytotoxic T lymphocytes. *Clin Cancer Res, 11*(12), 4545-4552. https://doi.org/10.1158/1078-0432.CCR-04-2235

Rodeberg, D. A., Nuss, R. A., Elsawa, S. F., Erskine, C. L., & Celis, E. (2006, Jul 1). Generation of tumoricidal PAX3 peptide antigen specific cytotoxic T lymphocytes. *Int J Cancer, 119*(1), 126-132. https://doi.org/10.1002/ijc.21817

Rosenberg, S. A., Spiess, P., & Lafreniere, R. (1986, Sep 19). A new approach to the adoptive immunotherapy of cancer with tumor-infiltrating lymphocytes. *Science, 233*(4770), 1318-1321. https://doi.org/10.1126/science.3489291

Roth, T. L., Puig-Saus, C., Yu, R., Shifrut, E., Carnevale, J., Li, P. J., Hiatt, J., Saco, J., Krystofinski, P., Li, H., Tobin, V., Nguyen, D. N., Lee, M. R., Putnam, A. L., Ferris, A. L., Chen, J. W., Schickel, J. N., Pellerin, L., Carmody, D., Alkorta-Aranburu, G., Del Gaudio, D., Matsumoto, H., Morell, M., Mao, Y., Cho, M., Quadros, R. M., Gurumurthy, C. B., Smith, B., Haugwitz, M., Hughes, S. H., Weissman, J. S., Schumann, K., Esensten, J. H., May, A. P., Ashworth, A., Kupfer, G. M., Greeley, S. A. W., Bacchetta, R., Meffre, E., Roncarolo, M. G., Romberg, N., Herold, K. C., Ribas, A., Leonetti, M. D., & Marson, A. (2018, Jul). Reprogramming human T cell function and specificity with non-viral genome targeting. *Nature, 559*(7714), 405-409. https://doi.org/10.1038/s41586-018-0326-5

Rudolph, M. G., Stanfield, R. L., & Wilson, I. A. (2006). How TCRs bind MHCs, peptides, and coreceptors. *Annu Rev Immunol, 24*, 419-466. https://doi.org/10.1146/annurev.immunol.23.021704.115658

Samaras, P., Schmidt, T., Frejno, M., Gessulat, S., Reinecke, M., Jarzab, A., Zecha, J., Mergner, J., Giansanti, P., Ehrlich, H. C., Aiche, S., Rank, J., Kienegger, H., Krcmar, H., Kuster, B., & Wilhelm, M. (2020, Jan 8). ProteomicsDB: a multi-omics and multi-organism resource for life science research. *Nucleic Acids Res, 48*(D1), D1153-D1163. https://doi.org/10.1093/nar/gkz974

Sanchez-Molina, S., Figuerola-Bou, E., Blanco, E., Sanchez-Jimenez, M., Taboas, P., Gomez, S., Ballare, C., Garcia-Dominguez, D. J., Prada, E., Hontecillas-Prieto, L., A, M. C., Tirado, O. M., Hernandez-Munoz, I., de Alava, E., Lavarino, C., Di Croce, L., & Mora, J. (2020, Oct). RING1B recruits EWSR1-FLI1 and cooperates in the remodeling of chromatin necessary for Ewing sarcoma tumorigenesis. *Sci Adv, 6*(43). https://doi.org/10.1126/sciadv.aba3058

Sankar, S., Bell, R., Stephens, B., Zhuo, R., Sharma, S., Bearss, D. J., & Lessnick, S. L. (2013, Oct 17). Mechanism and relevance of EWS/FLI-mediated transcriptional repression in Ewing sarcoma. *Oncogene, 32*(42), 5089-5100. https://doi.org/10.1038/onc.2012.525

Sankar, S., Theisen, E. R., Bearss, J., Mulvihill, T., Hoffman, L. M., Sorna, V., Beckerle, M. C., Sharma, S., & Lessnick, S. L. (2014, Sep 1). Reversible LSD1 inhibition interferes with global EWS/ETS transcriptional activity and impedes Ewing sarcoma tumor growth. *Clin Cancer Res, 20*(17), 4584-4597. https://doi.org/10.1158/1078-0432.CCR-14-0072

Santeramo, I., Bagnati, M., Harvey, E. J., Hassan, E., Surmacz-Cordle, B., Marshall, D., & Di Cerbo, V. (2020, Jun 12). Vector Copy Distribution at a Single-Cell Level Enhances Analytical Characterization of Gene-Modified Cell Therapies. *Mol Ther Methods Clin Dev, 17*, 944-956.

https://doi.org/10.1016/j.omtm.2020.04.016

Sarukhan, A., Garcia, C., Lanoue, A., & von Boehmer, H. (1998, May). Allelic inclusion of T cell receptor alpha genes poses an autoimmune hazard due to low-level expression of autospecific receptors. *Immunity, 8*(5), 563-570. https://doi.org/10.1016/s1074-7613(00)80561-0

Schirmer, D., Grunewald, T. G., Klar, R., Schmidt, O., Wohlleber, D., Rubio, R. A., Uckert, W., Thiel, U., Bohne, F., Busch, D. H., Krackhardt, A. M., Burdach, S., & Richter, G. H. (2016, Jun). Transgenic antigen-specific, HLA-A*02:01-allo-restricted cytotoxic T cells recognize tumor-associated target antigen STEAP1 with high specificity. *Oncoimmunology, 5*(6), e1175795. https://doi.org/10.1080/2162402X.2016.1175795

Schirmer, D., Storz, I., Wisskirchen, K., Feederle, R., Schmidt, O., Abken, H., Protzer, U., Burdach, S., & Richter, G. H. S. (2018). Abstract A09: GPR64-specific CAR-transgenic T cells selectively kill Ewing sarcoma in vivo. *Cancer Research, 78*(19_Supplement), A09-A09. https://doi.org/10.1158/1538-7445.Pedca17-a09

Schmidt, D., Harms, D., & Burdach, S. (1985). Malignant peripheral neuroectodermal tumours of childhood and adolescence. *Virchows Arch A Pathol Anat Histopathol, 406*(3), 351-365. https://doi.org/10.1007/BF00704304

Schmidt, T., Samaras, P., Frejno, M., Gessulat, S., Barnert, M., Kienegger, H., Krcmar, H., Schlegl, J., Ehrlich, H. C., Aiche, S., Kuster, B., & Wilhelm, M. (2018, Jan 4). ProteomicsDB. *Nucleic Acids Res, 46*(D1), D1271-D1281. https://doi.org/10.1093/nar/gkx1029

Schober, K., Muller, T. R., Gokmen, F., Grassmann, S., Effenberger, M., Poltorak, M., Stemberger, C., Schumann, K., Roth, T. L., Marson, A., & Busch, D. H. (2019, Dec). Orthotopic replacement of T-cell receptor alpha- and beta-chains with preservation of near-physiological T-cell function. *Nat Biomed Eng, 3*(12), 974-984. https://doi.org/10.1038/s41551-019-0409-0

Schober, S. J., Thiede, M., Gassmann, H., Prexler, C., Xue, B., Schirmer, D., Wohlleber, D., Stein, S., Grunewald, T. G. P., Busch, D. H., Richter, G. H. S., Burdach, S. E. G., & Thiel, U. (2020, Jun 29). MHC Class I-Restricted TCR-Transgenic CD4(+) T Cells Against STEAP1 Mediate Local Tumor Control of Ewing Sarcoma In Vivo. *Cells, 9*(7). https://doi.org/10.3390/cells9071581

Scholten, K. B., Kramer, D., Kueter, E. W., Graf, M., Schoedl, T., Meijer, C. J., Schreurs, M. W., & Hooijberg, E. (2006, May). Codon modification of T cell receptors allows enhanced functional expression in transgenic human T cells. *Clin Immunol, 119*(2), 135-145. https://doi.org/10.1016/j.clim.2005.12.009

Schreiber, R. D., Old, L. J., & Smyth, M. J. (2011, Mar 25). Cancer immunoediting: integrating immunity's roles in cancer suppression and promotion. *Science, 331*(6024), 1565-1570. https://doi.org/10.1126/science.1203486

Schuck, A., Ahrens, S., Paulussen, M., Kuhlen, M., Konemann, S., Rube, C., Winkelmann, W., Kotz, R., Dunst, J., Willich, N., & Jurgens, H. (2003, Jan 1). Local therapy in localized Ewing tumors: results of 1058 patients treated in the CESS 81, CESS 86, and EICESS 92 trials. *Int J Radiat Oncol Biol Phys, 55*(1), 168-177. https://doi.org/10.1016/s0360-3016(02)03797-5

Schuck, A., Rube, C., Konemann, S., Rube, C. E., Ahrens, S., Paulussen, M., Dunst, J., Jurgens, H., & Willich, N. (2002, Jan). Postoperative radiotherapy in the treatment of Ewing tumors: influence of the interval between surgery and radiotherapy. *Strahlenther Onkol, 178*(1), 25-31. https://doi.org/10.1007/s00066-002-0883-1

Schwentner, R., Papamarkou, T., Kauer, M. O., Stathopoulos, V., Yang, F., Bilke, S., Meltzer, P. S., Girolami, M., & Kovar, H. (2015, Mar 11). EWS-FLI1 employs an E2F switch to drive target gene expression.

Nucleic Acids Res, 43(5), 2780-2789. https://doi.org/10.1093/nar/gkv123

Selvanathan, S. P., Graham, G. T., Grego, A. R., Baker, T. M., Hogg, J. R., Simpson, M., Batish, M., Crompton, B., Stegmaier, K., Tomazou, E. M., Kovar, H., Uren, A., & Toretsky, J. A. (2019, Oct 10). EWS-FLI1 modulated alternative splicing of ARID1A reveals novel oncogenic function through the BAF complex. *Nucleic Acids Res, 47*(18), 9619-9636. https://doi.org/10.1093/nar/gkz699

Slaymaker, I. M., Gao, L., Zetsche, B., Scott, D. A., Yan, W. X., & Zhang, F. (2016, Jan 1). Rationally engineered Cas9 nucleases with improved specificity. *Science, 351*(6268), 84-88. https://doi.org/10.1126/science.aad5227

Smith, R., Owen, L. A., Trem, D. J., Wong, J. S., Whangbo, J. S., Golub, T. R., & Lessnick, S. L. (2006, May). Expression profiling of EWS/FLI identifies NKX2.2 as a critical target gene in Ewing's sarcoma. *Cancer Cell, 9*(5), 405-416. https://doi.org/10.1016/j.ccr.2006.04.004

Smyth, M. J., Hayakawa, Y., Takeda, K., & Yagita, H. (2002, Nov). New aspects of natural-killer-cell surveillance and therapy of cancer. *Nat Rev Cancer, 2*(11), 850-861. https://doi.org/10.1038/nrc928

Sommermeyer, D., & Uckert, W. (2010, Jun 1). Minimal amino acid exchange in human TCR constant regions fosters improved function of TCR gene-modified T cells. *J Immunol, 184*(11), 6223-6231. https://doi.org/10.4049/jimmunol.0902055

Sorensen, P. H., Lessnick, S. L., Lopez-Terrada, D., Liu, X. F., Triche, T. J., & Denny, C. T. (1994, Feb). A second Ewing's sarcoma translocation, t(21;22), fuses the EWS gene to another ETS-family transcription factor, ERG. *Nat Genet, 6*(2), 146-151. https://doi.org/10.1038/ng0294-146

Sotillo, E., Barrett, D. M., Black, K. L., Bagashev, A., Oldridge, D., Wu, G., Sussman, R., Lanauze, C., Ruella, M., Gazzara, M. R., Martinez, N. M., Harrington, C. T., Chung, E. Y., Perazzelli, J., Hofmann, T. J., Maude, S. L., Raman, P., Barrera, A., Gill, S., Lacey, S. F., Melenhorst, J. J., Allman, D., Jacoby, E., Fry, T., Mackall, C., Barash, Y., Lynch, K. W., Maris, J. M., Grupp, S. A., & Thomas-Tikhonenko, A. (2015). Convergence of Acquired Mutations and Alternative Splicing of CD19 Enables Resistance to CART-19 Immunotherapy. *Cancer Discovery, 5*(12), 1282-1295. https://doi.org/10.1158/2159-8290.Cd-15-1020

Spurny, C., Kailayangiri, S., Altvater, B., Jamitzky, S., Hartmann, W., Wardelmann, E., Ranft, A., Dirksen, U., Amler, S., Hardes, J., Fluegge, M., Meltzer, J., Farwick, N., Greune, L., & Rossig, C. (2018, Jan 19). T cell infiltration into Ewing sarcomas is associated with local expression of immune-inhibitory HLA-G. *Oncotarget, 9*(5), 6536-6549. https://doi.org/10.18632/oncotarget.23815

Staege, M. S., Gorelov, V., Bulankin, A., Fischer, U., Dumon, K., Hohndorf, L., Hattenhorst, U., Kramm, C., & Burdach, S. (2003, Mar). Stable transgenic expression of IL-2 and HSV1-tk by single and fusion tumor cell lines bearing EWS/FLI-1 chimeric genes. *Pediatr Hematol Oncol, 20*(2), 119-140. https://doi.org/10.1080/0880010390158612

Staege, M. S., Hutter, C., Neumann, I., Foja, S., Hattenhorst, U. E., Hansen, G., Afar, D., & Burdach, S. E. (2004, Nov 15). DNA microarrays reveal relationship of Ewing family tumors to both endothelial and fetal neural crest-derived cells and define novel targets. *Cancer Res, 64*(22), 8213-8221. https://doi.org/10.1158/0008-5472.CAN-03-4059

Stenger, D., Stief, T. A., Kaeuferle, T., Willier, S., Rataj, F., Schober, K., Vick, B., Lotfi, R., Wagner, B., Grunewald, T. G. P., Kobold, S., Busch, D. H., Jeremias, I., Blaeschke, F., & Feuchtinger, T. (2020, Sep 17). Endogenous TCR promotes in vivo persistence of CD19-CAR-T cells compared to a CRISPR/Cas9-mediated TCR knockout CAR. *Blood, 136*(12), 1407-1418. https://doi.org/10.1182/blood.2020005185

Tang, S. W., Bilke, S., Cao, L., Murai, J., Sousa, F. G., Yamade, M., Rajapakse, V., Varma, S., Helman, L. J., Khan, J., Meltzer, P. S., & Pommier, Y. (2015, Sep 15). SLFN11 Is a Transcriptional Target of EWS-FLI1 and a Determinant of Drug Response in Ewing Sarcoma. *Clin Cancer Res, 21*(18), 4184-4193. https://doi.org/10.1158/1078-0432.CCR-14-2112

Thacker, M. M., Temple, H. T., & Scully, S. P. (2005, Apr). Current treatment for Ewing's sarcoma. *Expert Rev Anticancer Ther, 5*(2), 319-331. https://doi.org/10.1586/14737140.5.2.319

Theisen, E. R., Pishas, K. I., Saund, R. S., & Lessnick, S. L. (2016, Apr 5). Therapeutic opportunities in Ewing sarcoma: EWS-FLI inhibition via LSD1 targeting. *Oncotarget, 7*(14), 17616-17630. https://doi.org/10.18632/oncotarget.7124

Thiel, U., Pirson, S., Muller-Spahn, C., Conrad, H., Busch, D. H., Bernhard, H., Burdach, S., & Richter, G. H. (2011, Mar 15). Specific recognition and inhibition of Ewing tumour growth by antigen-specific allo-restricted cytotoxic T cells. *Br J Cancer, 104*(6), 948-956. https://doi.org/10.1038/bjc.2011.54

Thiel, U., Schober, S. J., Einspieler, I., Kirschner, A., Thiede, M., Schirmer, D., Gall, K., Blaeschke, F., Schmidt, O., Jabar, S., Ranft, A., Alba Rubio, R., Dirksen, U., Grunewald, T. G. P., Sorensen, P. H., Richter, G. H. S., von Luttichau, I. T., Busch, D. H., & Burdach, S. E. G. (2017). Ewing sarcoma partial regression without GvHD by chondromodulin-I/HLA-A*02:01-specific allorestricted T cell receptor transgenic T cells. *Oncoimmunology, 6*(5), e1312239. https://doi.org/10.1080/2162402X.2017.1312239

Thiel, U., Schober, S. J., Ranft, A., Gassmann, H., Jabar, S., Gall, K., von Luttichau, I., Wawer, A., Koscielniak, E., Diaz, M. A., Ussowicz, M., Kazantsev, I., Afanasyev, B., Merker, M., Klingebiel, T., Prete, A., Gruhn, B., Bader, P., Jurgens, H., Dirksen, U., Handgretinger, R., Burdach, S., & Lang, P. (2021, Jul). No difference in survival after HLA mismatched versus HLA matched allogeneic stem cell transplantation in Ewing sarcoma patients with advanced disease. *Bone Marrow Transplant, 56*(7), 1550-1557. https://doi.org/10.1038/s41409-020-01200-x

Thiel, U., Wawer, A., von Luettichau, I., Bender, H. U., Blaeschke, F., Grunewald, T. G., Steinborn, M., Roper, B., Bonig, H., Klingebiel, T., Bader, P., Koscielniak, E., Paulussen, M., Dirksen, U., Juergens, H., Kolb, H. J., & Burdach, S. E. (2016, Oct 25). Bone marrow involvement identifies a subgroup of advanced Ewing sarcoma patients with fatal outcome irrespective of therapy in contrast to curable patients with multiple bone metastases but unaffected marrow. *Oncotarget, 7*(43), 70959-70968. https://doi.org/10.18632/oncotarget.10938

Thiel, U., Wawer, A., Wolf, P., Badoglio, M., Santucci, A., Klingebiel, T., Basu, O., Borkhardt, A., Laws, H. J., Kodera, Y., Yoshimi, A., Peters, C., Ladenstein, R., Pession, A., Prete, A., Urban, E. C., Schwinger, W., Bordigoni, P., Salmon, A., Diaz, M. A., Afanasyev, B., Lisukov, I., Morozova, E., Toren, A., Bielorai, B., Korsakas, J., Fagioli, F., Caselli, D., Ehninger, G., Gruhn, B., Dirksen, U., Abdel-Rahman, F., Aglietta, M., Mastrodicasa, E., Torrent, M., Corradini, P., Demeocq, F., Dini, G., Dreger, P., Eyrich, M., Gozdzik, J., Guilhot, F., Holler, E., Koscielniak, E., Messina, C., Nachbaur, D., Sabbatini, R., Oldani, E., Ottinger, H., Ozsahin, H., Schots, R., Siena, S., Stein, J., Sufliarska, S., Unal, A., Ussowicz, M., Schneider, P., Woessmann, W., Jurgens, H., Bregni, M., Burdach, S., Solid Tumor Working, P., the Pediatric Disease Working Party of the European Group for, B., Marrow, T., Asia Pacific, B., Marrow, T., Pediatric Registry for Stem Cell, T., & the Meta, E. S. G. (2011, Jul). No improvement of survival with reduced- versus high-intensity conditioning for allogeneic stem cell transplants in Ewing tumor patients. *Ann Oncol, 22*(7), 1614-1621. https://doi.org/10.1093/annonc/mdq703

Tomazou, E. M., Sheffield, N. C., Schmidl, C., Schuster, M., Schonegger, A., Datlinger, P., Kubicek, S., Bock, C., & Kovar, H. (2015, Feb 24). Epigenome mapping reveals distinct modes of gene regulation and widespread enhancer reprogramming by the oncogenic fusion protein EWS-FLI1. *Cell Rep, 10*(7), 1082-1095. https://doi.org/10.1016/j.celrep.2015.01.042

Tran, K. Q., Zhou, J., Durflinger, K. H., Langhan, M. M., Shelton, T. E., Wunderlich, J. R., Robbins, P. F., Rosenberg, S. A., & Dudley, M. E. (2008, Oct). Minimally cultured tumor-infiltrating lymphocytes display optimal characteristics for adoptive cell therapy. *J Immunother, 31*(8), 742-751. https://doi.org/10.1097/CJI.0b013e31818403d5

van Erp, A. E. M., Versleijen-Jonkers, Y. M. H., Hillebrandt-Roeffen, M. H. S., van Houdt, L., Gorris, M. A. J., van Dam, L. S., Mentzel, T., Weidema, M. E., Savci-Heijink, C. D., Desar, I. M. E., Merks, H. H. M., van Noesel, M. M., Shipley, J., van der Graaf, W. T. A., Flucke, U. E., & Meyer-Wentrup, F. A. G. (2017, Sep 19). Expression and clinical association of programmed cell death-1, programmed death-ligand-1 and CD8(+) lymphocytes in primary sarcomas is subtype dependent. *Oncotarget, 8*(41), 71371-71384. https://doi.org/10.18632/oncotarget.19071

van Loenen, M. M., de Boer, R., Amir, A. L., Hagedoorn, R. S., Volbeda, G. L., Willemze, R., van Rood, J. J., Falkenburg, J. H., & Heemskerk, M. H. (2010, Jun 15). Mixed T cell receptor dimers harbor potentially harmful neoreactivity. *Proc Natl Acad Sci U S A, 107*(24), 10972-10977. https://doi.org/10.1073/pnas.1005802107

von Heyking, K., Calzada-Wack, J., Gollner, S., Neff, F., Schmidt, O., Hensel, T., Schirmer, D., Fasan, A., Esposito, I., Muller-Tidow, C., Sorensen, P. H., Burdach, S., & Richter, G. H. S. (2017, Sep). The endochondral bone protein CHM1 sustains an undifferentiated, invasive phenotype, promoting lung metastasis in Ewing sarcoma. *Mol Oncol, 11*(9), 1288-1301. https://doi.org/10.1002/1878-0261.12057

von Levetzow, C., Jiang, X., Gwye, Y., von Levetzow, G., Hung, L., Cooper, A., Hsu, J. H., & Lawlor, E. R. (2011, Apr 29). Modeling initiation of Ewing sarcoma in human neural crest cells. *PLoS One, 6*(4), e19305. https://doi.org/10.1371/journal.pone.0019305

Whelan, J., Le Deley, M. C., Dirksen, U., Le Teuff, G., Brennan, B., Gaspar, N., Hawkins, D. S., Amler, S., Bauer, S., Bielack, S., Blay, J. Y., Burdach, S., Castex, M. P., Dilloo, D., Eggert, A., Gelderblom, H., Gentet, J. C., Hartmann, W., Hassenpflug, W. A., Hjorth, L., Jimenez, M., Klingebiel, T., Kontny, U., Kruseova, J., Ladenstein, R., Laurence, V., Lervat, C., Marec-Berard, P., Marreaud, S., Michon, J., Morland, B., Paulussen, M., Ranft, A., Reichardt, P., van den Berg, H., Wheatley, K., Judson, I., Lewis, I., Craft, A., Juergens, H., Oberlin, O., Euro, E. W. I. N. G., & Investigators, E.-. (2018, Sep 6). High-Dose Chemotherapy and Blood Autologous Stem-Cell Rescue Compared With Standard Chemotherapy in Localized High-Risk Ewing Sarcoma: Results of Euro-E.W.I.N.G.99 and Ewing-2008. *J Clin Oncol*, JCO2018782516. https://doi.org/10.1200/JCO.2018.78.2516

Widhe, B., & Widhe, T. (2000, May). Initial symptoms and clinical features in osteosarcoma and Ewing sarcoma. *J Bone Joint Surg Am, 82*(5), 667-674. https://doi.org/10.2106/00004623-200005000-00007

Wiles, E. T., Lui-Sargent, B., Bell, R., & Lessnick, S. L. (2013). BCL11B is up-regulated by EWS/FLI and contributes to the transformed phenotype in Ewing sarcoma. *PLoS One, 8*(3), e59369. https://doi.org/10.1371/journal.pone.0059369

Womer, R. B., West, D. C., Krailo, M. D., Dickman, P. S., Pawel, B. R., Grier, H. E., Marcus, K., Sailer, S., Healey, J. H., Dormans, J. P., & Weiss, A. R. (2012, Nov 20). Randomized controlled trial of interval-compressed chemotherapy for the treatment of localized Ewing sarcoma: a report

from the Children's Oncology Group. *J Clin Oncol, 30*(33), 4148-4154. https://doi.org/10.1200/JCO.2011.41.5703

Worch, J., Ranft, A., DuBois, S. G., Paulussen, M., Juergens, H., & Dirksen, U. (2018, Sep). Age dependency of primary tumor sites and metastases in patients with Ewing sarcoma. *Pediatr Blood Cancer, 65*(9), e27251. https://doi.org/10.1002/pbc.27251

Yang, L., Chansky, H. A., & Hickstein, D. D. (2000, Dec 1). EWS.Fli-1 fusion protein interacts with hyperphosphorylated RNA polymerase II and interferes with serine-arginine protein-mediated RNA splicing. *J Biol Chem, 275*(48), 37612-37618. https://doi.org/10.1074/jbc.M005739200

Yee, C. (2018, Apr). Adoptive T cell therapy: points to consider. *Curr Opin Immunol, 51*, 197-203. https://doi.org/10.1016/j.coi.2018.04.007

Zhang, H. F., Hughes, C. S., Li, W., He, J. Z., Surdez, D., El-Naggar, A. M., Cheng, H., Prudova, A., Delaidelli, A., Negri, G. L., Li, X., Orum-Madsen, M. S., Lizardo, M. M., Oo, H. Z., Colborne, S., Shyp, T., Scopim-Ribeiro, R., Hammond, C. A., Dhez, A. C., Langman, S., Lim, J. K. M., Kung, S. H. Y., Li, A., Steino, A., Daugaard, M., Parker, S. J., Geltink, R. I. K., Orentas, R. J., Xu, L. Y., Morin, G. B., Delattre, O., Dimitrov, D. S., & Sorensen, P. H. (2021, Nov). Proteomic Screens for Suppressors of Anoikis Identify IL1RAP as a Promising Surface Target in Ewing Sarcoma. *Cancer Discov, 11*(11), 2884-2903. https://doi.org/10.1158/2159-8290.CD-20-1690

Zhou, H., & Lee, K. A. (2001, Mar 22). An hsRPB4/7-dependent yeast assay for trans-activation by the EWS oncogene. *Oncogene, 20*(12), 1519-1524. https://doi.org/10.1038/sj.onc.1204135

Zhou, Z., Yu, L., & Kleinerman, E. S. (2014, Feb 15). EWS-FLI-1 regulates the neuronal repressor gene REST, which controls Ewing sarcoma growth and vascular morphology. *Cancer, 120*(4), 579-588. https://doi.org/10.1002/cncr.28555

12 APPENDIX

12.1 LIST OF FIGURES

12.2 LIST OF SUPPLEMENTARY TABLES

13 PUBLICATIONS

13.1 PUBLICATIONS DURING THE DOCTOR THESIS WORK:

1. **Xue, B**.; von Heyking, K.; Gassmann, H.; Poorebrahim, M.; Thiede, M.; Schober, K.; Mautner, J.; Hauer, J.; Ruland, J.; Busch, D.H.; Thiel, U.; Burdach, S.E.G. T Cells Directed against the Metastatic Driver Chondromodulin-1 in Ewing Sarcoma: Comparative Engineering with CRISPR/Cas9 vs. Retroviral Gene Transfer for Adoptive Transfer. Cancers 2022, 14, 5485. https://doi.org/10.3390/cancers14225485

2. Sipol A, Hameister E, **Xue B**, Hofstetter J, Barenboim M, Öllinger R, Jain G, Prexler C, Rubio RA, Baldauf MC, Franchina DG, Petry A, Schmäh J, Thiel U, Görlach A, Cario G, Brenner D, Richter GHS, Grünewald TGP, Rad R, Wolf E, Ruland J, Sorensen PH, Burdach SEG. MondoA drives malignancy in B-ALL through enhanced adaptation to metabolic stress. Blood. 2022 Feb 24; 139 (8):1184-1197. doi: 10.1182/blood.2020007932. PMID: 33908607.

3. Schober SJ, Thiede M, Gassmann H, Prexler C, **Xue B**, Schirmer D, Wohlleber D, Stein S, Grünewald TGP, Busch DH, Richter GHS, Burdach SEG, Thiel U. MHC Class I-Restricted TCR-Transgenic $CD4^+$ T Cells Against STEAP1 Mediate Local Tumor Control of Ewing Sarcoma In Vivo. Cells. 2020 Jun 29;9(7):1581. doi: 10.3390/cells9071581 . PMID: 32610710 ; PMCID: PMC7408051.

4. Gassmann H, Schneider K, Evdokimova V, Ruzanov P, Schober SJ, **Xue B**, von Heyking K, Thiede M, Richter GHS, Pfaffl MW, Noessner E, Stein LD, Sorensen PH, Burdach SEG, Thiel U. Ewing Sarcoma-Derived Extracellular Vesicles Impair Dendritic Cell Maturation and Function. Cells. 2021 Aug 13;10 (8):2081. doi: 10.3390/cells10082081. PMID: 34440851; PMCID: PMC8391167.

5. Biele E, Schober SJ, Prexler C, Thiede M, Heyking KV, Gassmann H, Eck J,

Xue B, Burdach S, Thiel U. Monocyte Maturation Mediators Upregulate CD83, ICAM-1 and MHC Class 1 Expression on Ewing's Sarcoma, Enhancing T Cell Cytotoxicity. Cells. 2021 Nov 8;10 (11):3070. doi: 10.3390/cells10113070. PMID: 34831294; PMCID: PMC8624504.

6. Kong L, Liu P, Zheng M, **Xue B**, Liang K, Tan X. Multi-omics analysis based on integrated genomics, epigenomics and transcriptomics in pancreatic cancer. Epigenomics. 2020 Mar;12(6):507-524. doi: 10.2217/epi-2019-0374. Epub 2020 Feb 12. PMID: 32048534.

13.2 PUBLICATIONS IN PREPARATION:

1. **Busheng Xue**, et al. & Poul H. Sorensen, Stefan E.G. Burdach, Yan Li. Identification and targeting of UHRF1, a critical partner of EWS-FLI1 in Ewing sarcoma (Original article).

14 ACKNOWLEDGEMENTS

Finally, I would like to thank everyone who contributed to the success of this doctoral thesis, especially my mentor and thesis advisor Prof. Dr. Stefan Burdach. In addition, I would like to thank his previous team at the Children's Cancer Research Center (CCRC), Department of Pediatrics including Dr. Uwe Thiel, Kristina von Heyking, Sebastian J. Schober, Hendrik Gassmann, Melanie Thiede, Nadine Kliese and not excluding others. Moreover, I specifically thank PD Dr. Josef Mautner for his committee advice and mentorship as well as Prof. Dr. Julia Hauer for her encouragement and support during the last part of my work at CCRC.

I am also most grateful to PD Dr. Kilian Schober and Prof. Dr. Dirk H. Busch for sharing the knowledge of their CRISPR/Cas9 protocol as well as to the China Scholarship Council and the Cura Placida Children's Cancer Research Foundation for their grant support.

Vielen Dank für Ihre Hilfe!

Thank you so much for your help!

非常感谢你们的帮助!